PERFORMANCE OF REINFORCED COLLAPSIBLE SOILS

Sherif Soliman

A Dissertation

In the Department of

Building, Civil and Environmental Engineering

Presented in partial fulfillment of the requirements for the degree of

DOCTOR OF PHILOSOPHY

Concordia University

Montreal, Quebec, Canada

Your file Votre référence
ISBN: 978-0-494-67359-1
Our file Notre référence
ISBN: 978-0-494-67359-1

ABSTRACT

Geotechnical engineers face serious problems when construction sites contain collapsible soils, which are known by their strength when dry and experience sudden and excessive settlement when inundated. The amount of soil collapse depends on the extent of the wetting zone and the degree of saturation reached when the surface water is the source of inundation. On the other hand, full saturation of the collapsible soil and accordingly, the maximum collapse are expected when the source of inundation is the rise of groundwater table.

In this thesis, experimental investigation was carried out on prototype set-up to simulate the case of a surface rigid strip footing resting on collapsible soils. The objective of this research has been to evaluate the collapse settlement of the footing when the collapsible soils are subjected to full inundation due to the rise of ground water table. The case of footings on homogeneous collapsible soils having various collapse potentials, heights and applied stresses were first examined. Then, the case of footing resting on partially replaced collapsible soils by compacted sand was tested to establish the optimum thickness of the soil replaced on the collapse settlement of these footings. In addition, tests were carried out on these footings where geosynthetic layers were placed at the interface between the replaced and the collapsible soil layers and within the replaced soil layer.

Analytical and empirical models were developed to predict the collapse settlement of these footings for a given soil / replacement layer / geotextile layer conditions. Design procedures and charts were provided for practicing use.

ACKNOWLEDGEMENTS

I would like to express my sincere gratitude to Professor Dr. Adel Hanna, Professor of Building, Civil and Environmental Engineering, Concordia University for his continuous guidance, valuable suggestions and the time he gave generously and patiently. His comprehensive knowledge was most helpful throughout the research program.

My special thanks to Dr. Tahar Ayadat of the department of Building, Civil and Environmental Engineering for his assistance and fruitful discussions throughout my research.

I would like to thank my colleagues in the foundation lab Gustavo Guedez and Ibrahim Mashhour for the friendly and supportive environment in the lab. Also, I would like to thank technicians and staff in the department of Building, Civil and Environmental Engineering for their help specially Joseph Herb, Danny Roy, Rocco Lombardi, Ngoc Lang Vo and Luc Demers. From the Academic and Information Technology Services I would like to thank Francois Carriere and Sylvain Belanger for their assistance. From the department of Mechanical Engineering I would like to thank Gilles Huard for his advice.

I would like to express my sincere gratitude to my parents and all family members for their continuous support and love. Special thanks to Dr. Fayek S. Guirguis (Ph.D.) for his encouragement, care and moral support.

I would like also to extend my sincere gratitude to my dear Victoria for her support and patience.

Table of Contents

LIST OF FIGURES

LIST OF TABLES

LIST OF SYMBOLS

(Δ) collapse settlement of partially replaced collapsible soils with / without reinforcements.

(B) footing width

(C_p) soil collapse potential measured at $\bar{\sigma}$ equals to 200 kPa

(CSRF) collpse settlement reduction factor

(d_c) collapsible soil depth

(d_s) compacted sand layer thickness

(d_t) total soil depth

(L) geotextile deformed length

(RF) Reduction factor and equals $(1 - CSRF)$

(δ) elongation of geotextile

(Δ_h) collapse settlement for homogeneous collapsible soil

(Δ_h) collapse settlement of homogeneous collapsible soils

(ε_c) collapse strain = Δ_h / d_c,

(θ) geotextile deformation angle

(σ) stress acting on the footing in kPa

(ε_t) strain developed in the geotextile

$a_1, a_2 \ldots\ldots a_5$, b, c, d, e, k = Constants

E_t modulus of elasticity for the geotextile material in kPa

CHAPTER 1

INTRODUCTION

Due to the increase of land development all over the world, the need to deal with difficult soils became essential, collapsible soil is no exception. Collapsible soil is known to experience reduction in strength, excessive and sudden settlement when it becomes wet leading to failure of the structure.

Collapsible soil also known as loess can be found in many countries, such as, the former Soviet Union, China, the United States, Brazil, Australia, and many countries in Eastern Europe. Collapsible soil is also found in arid regions around the globe (Houston et al. 2001). Construction on such a type of soil remains one of the outstanding problems in geotechnical engineering. It could be difficult, costly or sometimes even impossible to modify the designs of railway tracks, highways or power supply lines in order to avoid the area covered with collapsible soils.

The cost of repair at a cement plant in central Utah, which was built on collapsible soil, was more than $ 20,000,000 US (Hepworth and Langfelder 1988). North of Santa Fe, N. M., damage to homes built on collapsible soils was so dramatic that the governor declared it as a disaster area (Shaw and Johnpeer 1985). Lawton et al. (1992) reported the case of two-story, wood-frame structures supported on continuous footing over compacted fill. They reported that the total costs from damage and litigation associated with this project were estimated at $ 36,000,000 US.

In the literature, several treatment methods are suggested to deal with collapsible soil, to include:

1. Totally or partially removing the collapsible soil and replacing it with well compacted cohesionless soil, which could be expensive in some cases. Therefore, this method is limited to shallow depths of collapsible soil.
2. Chemical treatment of the collapsible soil was used in Eastern Europe; nevertheless, the rest of the world didn't implement it due to the high cost and unpredictable future.
3. Pile foundation to penetrate the collapsible soil layer to a much stronger layer. However, this technique is not applicable for cases such as highways or railway tracks.
4. Stone columns encapsulated in geofabrics, which require special techniques and skilled workers to install columns.

This research project is directed to establish a new method in dealing with collapsible soil, which is economical and efficient utilizing the combined effect of soil replacement and soil reinforcements. Experimental investigation is carried out to examine the behavior of shallow, rigid strip footing under axial load and subjected to inundation resulting from the rise of the groundwater table reaching full saturation status for the cases of homogeneous collapsible soils and partially replaced collapsible soils with or without geosynthetics reinforcement. Analytical and empirical models are developed to predict collapse settlement of shallow strip footing, strain developed in the geotextile and deformed shape at collapse. The outcome of this research will lead to significant increase in the safety conditions of highways and railways beside the reduction of maintenance cost.

CHAPTER 2

LITERATURE REVIEW

2.1. GENERAL

Collapsible soil is a type of soil that experiences excessive, sudden settlement and loss in strength when it becomes wet. Engineers have been constantly searching for economical and practical alternatives to improve this type of soils. Some of these techniques are compaction, preloading, pre-wetting and partial replacement of collapsible soils. However, each of these methods has its limitations on applications and results.

In the literature researchers have carried out the studies using soil reinforcement or partially replacing the collapsible soil layer with granular soil. Nevertheless, these methods have not been validated by sufficient laboratory or field tests and further, no theory was developed to predict such behavior.

In this chapter, the literature will be reviewed under the following headings:

1. Literature pertinent to collapsible soil.
2. Literature pertinent to soil reinforcement.
3. Discussion of the literature review.

2.2. LITERATURE PERTINENT TO COLLAPSIBLE SOIL

2.2.1. Definitions, origins and characterization of collapsible soils

Collapsible soils are defined as "an unsaturated soil that goes through a radical rearrangement of particles and great loss of volume upon wetting with or without additional loading" Bara (1976).

Collapsible soils are formed naturally such as in case of wind or volcanic dust deposits and residual soils from the weathering process of parent rocks. Also, engineered compacted fills may experience volume moisture sensitivity. Compaction to low density and dry of optimum produces the greatest susceptibility to densification when wetting (Adnan and Erdil 1992, Ishihara and Harada 1994, Rogers 1995 and Houston et al., 1997 and 2001). Rogers (1995) presented the classification of collapsible soils and the formation of each type as shown in Figure (2-1)

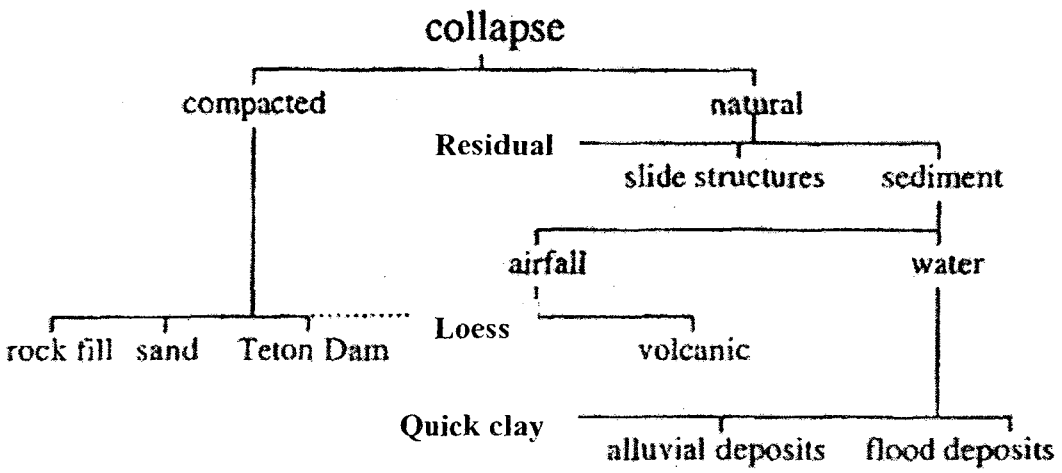

Figure (2-1): Classification of collapsible soils (Rogers 1995).

Jennings and Knight (1975) suggested a procedure to determine the collapse potential of a soil (C_p) by using a sample of an undisturbed soil in the consolidometer ring (Figure 2-2), which is defined as:

$$C_p = \frac{\Delta e_c}{1 + e_\circ} \qquad or \qquad C_p = \frac{\Delta H_\circ}{H_c}$$

Where Δe_c change in void ratio upon wetting, e_o initial void ratio, ΔH_o change in height upon wetting and H_c initial height.

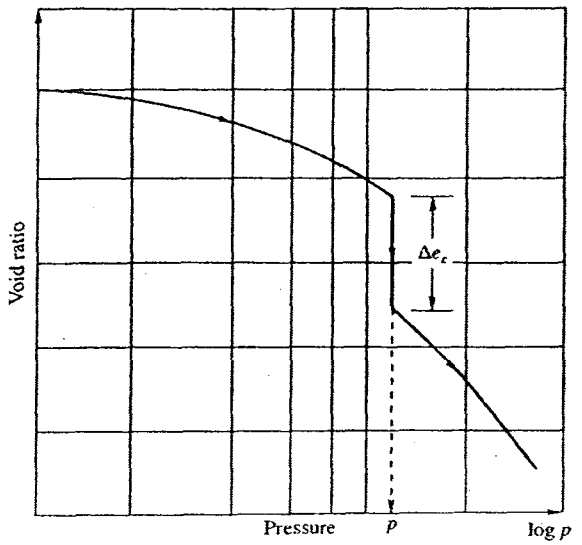

Figure (2-2): Typical collapse potential test results (Jennings and Knight, 1975)

The authors provided range of values for collapse potential that are shown in Table (2-1) and, accordingly, the severity of the problem is characterized.

Table (2-1): Collapse potential values (Jennings and Knight, 1975)

C_p%	Severity of problem
0–1	No problem
1–5	Moderate trouble
3–10	Trouble
10–20	Severe trouble
> 20	Very severe trouble

Adnan and Erdil (1992) studied the effects of various factors on the collapse potential of a collapsible soil. The studied factors were: soil type, compaction water content, initial dry unit weight and applied pressure at wetting. They reported that increasing the sand-

clay percentage, initial dry unit weight or initial water content decreased the collapse potential.

Houston et al. (2002) studied collapsible soil and its effect on highway engineering. They concluded that, site geology and the processes that occurred till the soil was formed should be considered when studying the collapse potential for the soil under consideration. Also, depth of wetting, depth of collapsible layer and degree of saturation were of concern when studying the soil collapse. When wetting was due to rising groundwater table, then full saturation and full collapse would occur.

Ayadat and Hanna (2007) conducted oedometer tests in laboratory prepared collapsible soils. The effects of initial dry unit weight, water content and uniformity coefficient on the induced collapse strain were considered. The authors developed a model that can predict the collapse strain for collapsible soils under various conditions.

2.2.2. Construction on collapsible soils

Chemical stabilization has been used to improve the performance of many types of soils including collapsible soils. Sokolovich and Semkin (1984) carried out laboratory tests on loess soil stabilized by solution of Sodium Silicate and solutions of Ammonia. Semkin and Ermoshin (1986) presented a case study on applying chemical stabilization on loess soil in Uzbekistan by using Silicate injection and showed that it was an effective method to control the settlement of an existing building. Badeev et al. (1987) carried out a study on stabilizing loess soil at the base of bored injection piles. They showed that it was possible to stabilize the soil under the pile foot with the required thickness and strength. Ata and Vipulanandan (1998 and 1999) studied different properties of silicate-

grouted sand and also the effect of sand type and curing period on the grouted sand behavior.

Evstatiev (1988) and Houston and Houston (1989) presented a review for the majority of mitigation methods available to improve the performance and properties of loess soil. These methods included, compaction achieved by different methods, addition of coarser material, stabilization by grouting or mixing by binders and chemical reagents, replacement with other soils, reinforcement and different kinds of wetting such as pre-wetting, controlled wetting and differential wetting.

The effects of partial excavation and wetting of collapsible soils on the reduction of the settlement were examined by many researchers. Romani and Hick (1989) applied this method in a project in Antelope Valley area of Southern California. Rollins and Rogers (1994) conducted six full-scale load tests on 1.5 m square footings built on collapsible soil and suggested different methods to improve the soil till 4.0 m below the footing such as: pre-wetting with water at a 2% sodium silicate solution, partial excavation and replacement with compacted granular fill, dynamic compaction on dry soil and dynamic compaction on pre-wet soil.

Souza et al. (1995) carried out field plate load tests in a site with collapsible soil of more than 10 m in depth in Sao Paulo State – Brazil to study the effect of soil compaction on reducing collapse settlement. Two brick walls, 1.6 m in height, founded on strip footings 0.6 m wide and 3.0 m long, were constructed on natural and compacted soil, loaded by additional surcharge and then wetted, to study the behavior of the footings in both cases. Field tests showed that 87% reduction of collapse settlement and about 110%

increase in the allowable bearing capacity can be achieved due to compaction (Figures 2-3 and 2-4). For the walls on strip footings, soil compaction showed a reduction in settlement of 50%, when applying the surcharge on the walls, while this reduction reached 80% when the soil was wetted.

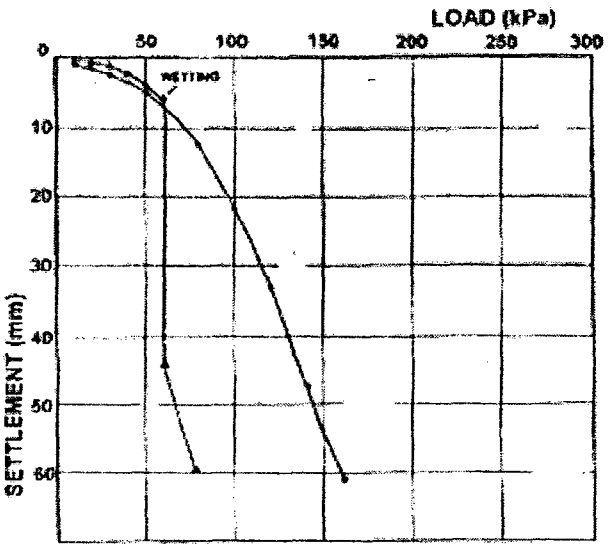

Figure (2-3): Plate load tests on natural and wet soils (Souza et al., 1995)

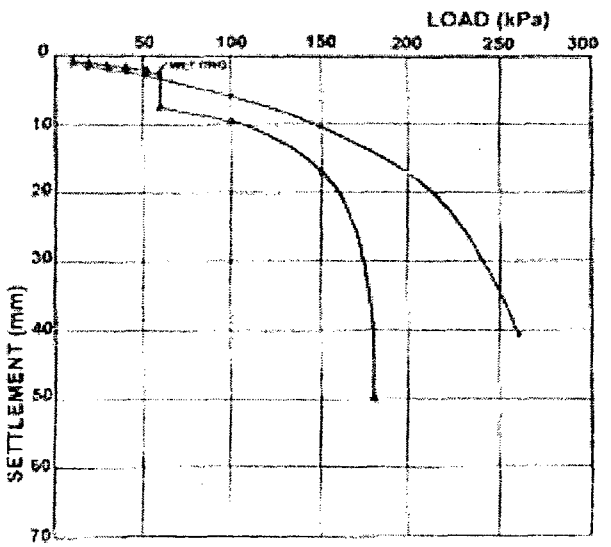

Figure (2-4): Plate load tests on compacted and compacted-wetted soils

(Souza et al., 1995)

Ayadat and Hanna (2005) carried out experimental studies to investigate the performance of sand columns encapsulated in geofabrics, installed in collapsible soil and subjected to inundation. The parameters considered were length of the sand column, degree of inundation and strength of the geofabrics. They concluded that, using geofabrics as reinforcement for the sand columns increases the carrying capacity and decreases the settlement; the level of improvement depends on the stiffness of the geofabrics, Figures (2-5) and (2-6). The authors also developed a theoretical model to predict the carrying capacity and settlement of these columns.

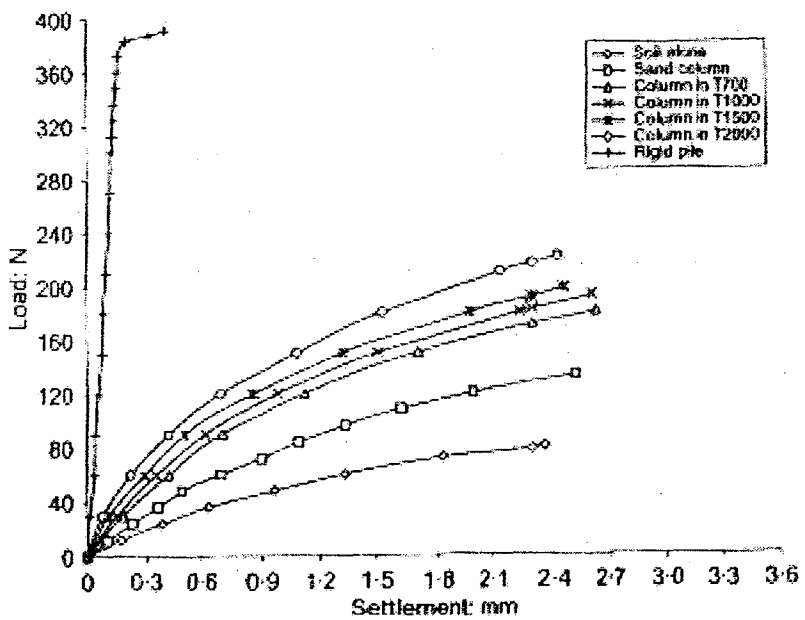

Figure (2-5): Load-settlement curves for various footing supports

(Ayadat and Hanna, 2005)

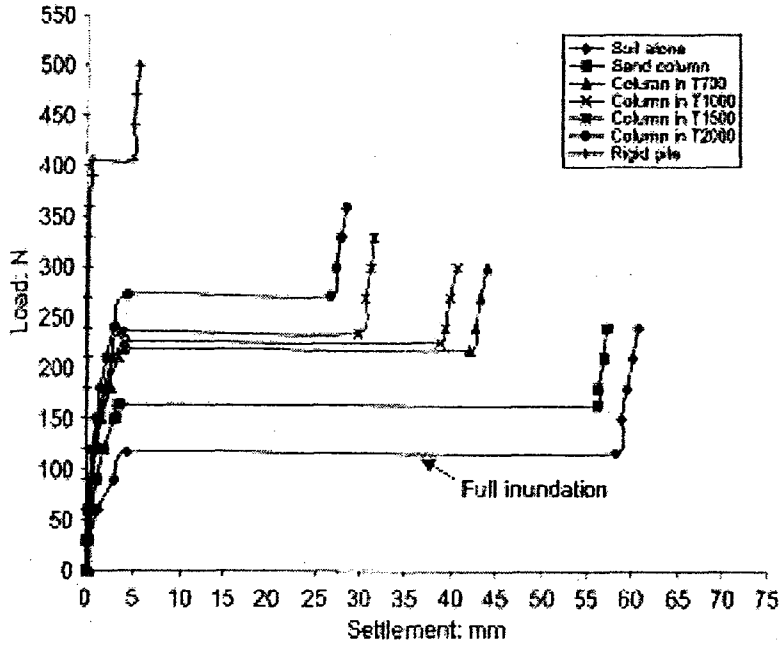

Figure (2-6): Load-settlement curves for various footing supports, of length L = 410 mm, after full inundation under applied load equal to 80% P_u (Ayadat and Hanna, 2005)

Jefferson et al. (2008) reported the use of a variety of cementations materials to enhance the properties of loess soils to mitigate its collapse potential. They stated that in Bulgaria alone some 100 buildings have been successfully built on loess collapsible soils using soil cement cushions (mixed with 3 to 7% Portland cement by weight). They also described a case of using loess-cement cushions, which is a strengthened layer of the soil base situated immediately under the footing, to treat loess collapsible soil effectively and construct a nuclear power plant in Bulgaria.

2.3. LITERATURE PERTINENT TO SOIL REINFORCEMENT

2.3.1. General

Researchers and engineers investigated the effect of using reinforcing materials on both settlement and bearing capacity of shallow footings. Research was carried out on

homogenous soils in addition to layered soil, which is mainly strong layer overlying weaker one. The bearing capacity ratio (BCR), which is equal to the bearing capacity of reinforced soil divided by the bearing capacity of unreinforced soil, was used to measure the improvement in the bearing capacity gained by using reinforcement.

A general review of studies that have been done on homogenous soils is introduced, after which a detailed description and discussion of research on layered soil and collapsible soil are presented.

2.3.2. Literature pertinent to soil reinforcement on homogenous soil

Yang (1972), Binquet and Lee (1975a), Akinmusuru and Akinbolade (1981) and Fragaszy and Lawton (1984) carried out model tests on circular plates, strip, square and rectangular footings respectively to investigate the improvement in bearing capacity and settlement of reinforced sand. Yang (1972) used fiberglass nets as reinforcement material, Binquet and Lee (1975a) used flat metal strips, Akinmusuru and Akinbolade (1981) used flat strips of rope fiber material and Fragaszy and Lawton (1984) used strips cut from rolls of household aluminum foil. The main parameters considered in these investigations were reinforcement configuration.

Observing the failure mechanism in the model tests conducted by Binquet and Lee (1975a), Binquet and Lee (1975b) concluded that, there are three possible bearing capacity failure modes for the isolated strip footing resting on reinforced sand and corresponding to a given settlement, which depend on the strength and the arrangement of the reinforcement. Possible failure modes are shown in Figure (2-7).

The authors proposed an analytical approach for getting the pressure on this footing. They checked the validity of this approach by comparing the obtained results with that from model tests by Binquet and Lee (1975a).

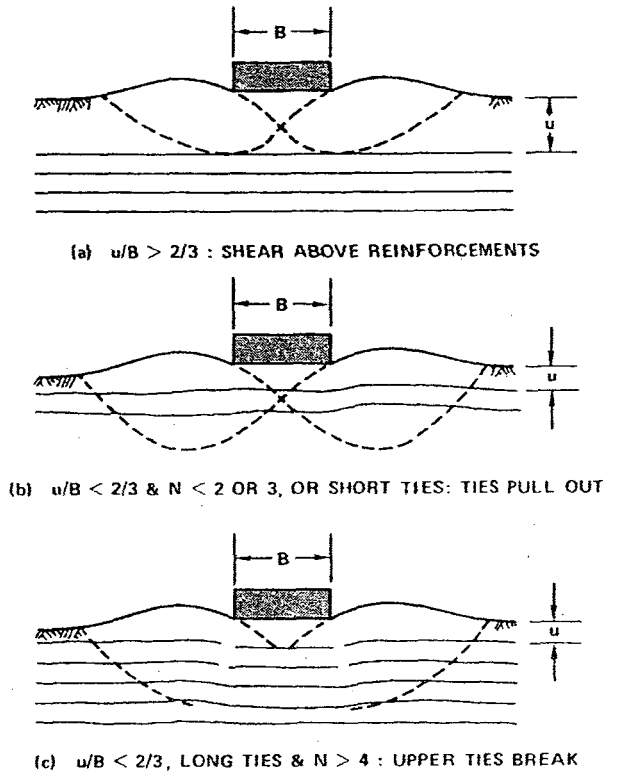

Figure (2-7): Modes of failure (Binquet and Lee, 1975 b)

Guido et al. (1986) performed plate bearing tests on square footing resting on sand reinforced by polymer grid (geogrid) or geotextile. Tests were aimed at studying the bearing capacity of geogrid and geotextile reinforced earth slab by varying the reinforcement configuration (depth, width, spacing, number and tensile strength).

Sakti and Das (1987) carried out experimental investigation on small-scale set-up to study the ultimate bearing capacity and settlement of a model strip footing on saturated

soft clay reinforced with geotextile layers. Tests were conducted under undrained and plane strain conditions while varying the reinforcement configuration (depth, length, spacing and number). Settlement of footings at ultimate load with or without geotextile reinforcement was studied. The ultimate load was determined according to Vesic (1973), which was the point at which the load displacement plot became practically linear.

Sreekantiah (1988) carried out experimental tests on square and strip footings to study the behavior of reinforced earth in improving bearing capacity and settlement resistance of sand. The studied parameters were, ratio of depth of the first reinforcing layer to the footing width (ranged from 0.3 to 0.7), horizontal and vertical spacing between adjacent reinforcing layers and number of reinforcing layers.

Samtani and Sonpal (1989) carried out experimental investigation on strip footings resting on reinforced cohesive soil. The purpose of this investigation was to study the increase in the bearing capacity and to examine the failure profile for such a case. In these tests, metal strips, cut from 0.05 mm thick aluminum foil to a width of 20 mm, were used as reinforcement. The undrained condition and parameters including the length of reinforcement and distance between the strips in the direction of the footing length were considered. Other parameters such as depth of the first layer of the reinforcement, the spacing and the number of reinforcement layers were not a part of the study

Huang and Tatsuoka (1990) performed series of plane-strain model tests to develop a theory to predict bearing capacity of reinforced horizontal sandy ground loaded by rigid, rough, strip footing. The study aimed at obtaining a fundamental understanding of the failure mechanism of reinforced sand loaded with surface footing, studying,

experimentally, the effects of length, number of layers, horizontal spacing, stiffness and rupture strength of reinforcement on bearing capacity and finally developing a method of stability analysis suitable for designing.

Hirao et al. (1992) carried out laboratory tests to study the effects of geotextile properties (tensile strength, frictional force between soil and reinforcement and bending stiffness) in addition to the soft clay layer thickness on the improvement of bearing capacity of soft clay ground. Load settlement curves were drawn and the ultimate bearing capacity was obtained from the intersection point in these curves on arithmetic scale.

Makiuchi and Minegishi (1992) carried out laboratory loading tests on soft layer of remolded Kaolin clay under plane strain condition to examine and modify the ultimate bearing capacity formula proposed by Yamanouchi and Gotoh (1979 a). The effects of tensile force of geotextile, width of loading plate and moisture content of the soil on the load settlement relationships were studied. In this study, the geotextile was put at the ground surface.

Based on Rankine's theory, Soni et al. (1992) presented an analytical model to predict the length of the horizontal reinforcement, which is an effective parameter to increase the bearing capacity. They developed the following formula to calculate the required reinforcement length for any layer.

$$L_i = [\sec^2 (45 + \phi/2) - 2u_i \tan (45 + \phi/2)/ B + 0.5] B$$

The formula indicates that the length of the reinforcement depends on the angle of internal friction of the soil (ϕ), depth of reinforcement layers (u) and width of the footing

(B). The results from this analytical method were compared to the results from the experimental results carried out by Fragaszy et al (1983), Guido et al. (1985), Huang and Tatsuoka (1990) and Mandal and Manjunath (1990), where good agreements were noted except in the case of Fragaszy et al (1983). However, pullout failure of the reinforcement was considered in deriving this formula, which may not necessary, be the general case.

Tanabashi et al. (1992) carried out numerical analysis, using Finite Element Technique, and proposed an analytical procedure to study the effect of using geotextile as reinforcement on the bearing capacity and deformation characteristics of the soft alluvial clay ground. The advantage of this proposed technique was that it modeled the soil, the geotextile and the interaction between soil and geotextile. Soil model was the elasto-viscoplastic model; geotextile model took into consideration the nonlinearity of tensile stress-strain curves. The interaction between soil and geotextile was considered as deformation dependency of the pull-out resistance. The numerical analysis had been done under the combination of the ratio of clay layer thickness to footing width, type of reinforcement and the method of supporting the ends of the geotextile.

Shin et al. (1993) conducted laboratory model tests to study the behavior of a strip footing supported by a saturated clay layer reinforced by layers of geogrid. Various soils with different undrained shear strengths were tested. Depth and width of reinforcement layers and the location of the first layer of reinforcement measured from the bottom of the footing were studied to obtain the maximum possible bearing capacity ratio. The ultimate bearing capacity was determined according to Vesic (1973).

Yetimoglu et al (1994) carried out laboratory tests to investigate the bearing capacity of rectangular footings on sand reinforced with geogrid. The parameters considered were the depth of the first layer of reinforcement, vertical spacing, number, size, width and stiffness of reinforcement layers. An analytical study was also conducted using finite element computer program, DACSAR (deformation analysis considering stress anisotropy and reorientation), which was originally developed by Lizuka and Ohta (1987). The rectangular footing was treated as an equivalent to circular plate of the same footing area. The results from the computer program were validated with laboratory test results, full scale loading tests and field tests. The ultimate bearing was defined at the point in which either the load reaches a maximum value where settlements continued without further increase in the loads or where there was an abrupt change in the load-settlement relationship.

Adams and Collin (1997) performed Large-scale model footing load tests on sand soil to evaluate the performance of geosynthetic reinforced soil footings with respect to bearing capacity and settlement. The studied parameter in the testing program included, number, spacing, area of reinforcement layers, depth to the first reinforcement layer, soil density and type of reinforcement (planar geogrid or geocell).

El-Naggar et al. (1997) carried out triaxial tests to study the effect of reinforced sandy soil with metallic strips on the basic mechanical properties for sand. The authors examined the stress-strain relationships of soil samples reinforced with horizontal metallic strips under different confined pressure. This study showed the improvement on

the soil mechanical properties due to reinforcement and the different failure planes for unreinforced and reinforced samples.

Using a three dimensional, nonlinear soil reinforcement interface friction element with other three dimensional elements, Kurian et al. (1997) presented a three dimensional, nonlinear finite element analysis to study the settlement of reinforced sand footings. In this analysis, individual attention was paid to soil, reinforcement and the interface between them. Laboratory tests were also carried out on square footing on sand reinforced with coir rope 4.3 mm in diameter which was tied to bamboo strips 35 mm x 5 mm and served as anchorage. Results obtained from finite element analysis were compared with that from the laboratory tests.

Using a rigid plastic finite element formulation, which is based on the upper bound theorem of the theory of plasticity, Otani et al. (1998) analyzed the bearing capacity of geosynthetic reinforced footing loaded by flexible uniform strip footing. In the rigid plastic finite element technique, the bearing capacity was obtained as a load factor at the ultimate limit state without specifying the location and shape of the failure mechanism. The studied parameters were depth, length, number of layers, and strength of the geosynthetics.

Based on the failure criteria for homogenized reinforced soils and the application of the slip line method, Zhao (1998) presented theoretical model for the plastic failure region and the ultimate bearing capacity of reinforced soils under strip footings. In this study, perfectly smooth and perfectly rough footing bases were considered and the studied parameters were reinforcement tensile strength, soil friction angle and cohesion.

The effects of these parameters on the bearing capacity of reinforced footing and the plastic failure region were investigated.

Haeri et al. (2000) have conducted laboratory triaxial compression tests to study the effects of number of geotextile layers, type and arrangement of geotextile, confining pressure and the sample size on the mechanical behavior of geotextile reinforced dry beach sand. The study showed that adding reinforcement to the soil sample affected the soil characteristics and also showed that different arrangement for the same reinforcement had an effect on the behavior of the soil sample. The tests were carried on for three different kinds of geotextiles under different values of confining pressure.

Yamamoto and Otani (2002) carried out model loading tests on a ground of aluminum rods 5.0 cm long, 1.6 and 3.0 mm diameter and mixed at a ratio of 3:2 by weight simulating a sandy soil to investigate the bearing capacity and the failure mechanism of reinforced ground below a footing. They also conducted a rigid plastic finite element analysis taking into consideration the effect of geometrical non-linearity to investigate the increase in the bearing capacity and the progress in deformation due to a certain settlement of the loading plate.

Boushehrian and Hataf (2003) carried out experimental tests on model ring and circular footings on reinforced sand to study the effects of number of layers of reinforcement, depth of the first layer of reinforcement and spacing between layers on the bearing capacity of these footings. A numerical model for the case described was carried out using a finite element program (PLAXIS 7.12). The additional parameters considered in this study were the ratio between internal and external diameters for the ring footing

and elastic normal stiffness of the geogrid. The results obtained from the numerical investigation were compared with those from the experimental test.

Michalowski and Shi (2003) performed laboratory load tests on strip footings on granular soil reinforced with one long layer of reinforcement. The purpose of this study was to investigate the failure mechanisms under these footings. After each displacement increment, images were recorded for the deformed sand under footing with a digital camera and the displacements were found by the correlation based digital technique for motion detection. The results presented in this study were according to the authors assumption that the reinforcement was strong and the collapse occurred in the footing was due to the pull out of the reinforcement.

Abdrabbo et al. (2004) conducted laboratory experiments on model square footing to study the effect of adding single reinforcing sheet of woven geotextile on the bearing capacity of sand. The parameters considered were the relative density of sand, reinforcing sheet depth ratio and length ratio. The ultimate load was defined as the load where settlement continued without any further increase of loads. The authors examined the effect of relative densities of the sand on the bearing capacity and determined the critical length ratio and the critical reinforcement embedment ratio in which the maximum benefit from adding reinforcement can be determined.

Michalowski (2004) used the kinematic approach of limit analysis to calculate limit loads on strip footings over soils reinforced with horizontal layers of geosynthetics. Depending on the reinforcement strength and size of footing, two modes of reinforcement failure were considered. The first was where reinforcement layers slip within the soil,

which is commonly seen in small-scale experiments, and the second was where reinforcement ruptures, which is realistic for large-scale footings.

Based on the non-linear constitutive laws of soil, Kumar et al. (2005) proposed an analytical method to draw the pressure-settlement relation of rectangular footing on reinforced sand. This work is considered as an extension to the method proposed by Sharan (1977) and Prakash et al. (1984), which gave the pressure-settlement relation of footing on unreinforced sand. The results obtained from this study were validated with the large-scale test results of Adams and Collin (1997) and also with model test results of Kumar (1997, 2003). Comparing the predicted with the experimental results, it was noted that they match well up to a value equal to two thirds of the ultimate bearing pressure, after that there was a wide discrepancy between the two values. This agreement represents the working pressure, which is normally acceptable in the design of foundations. The study is limited to smooth footing.

Basudhar et al. (2007) studied the load settlement behavior of circular footing resting on geotextile reinforced sand bed. They carried out experimental tests in addition to numerical modeling. Various parameters were considered such as footing size, reinforcement configurations and soil relative density.

Chen et al (2007) studied, experimentally, the effect of geosynthetic inclusion on the bearing capacity and settlement of square footing on clayey soil. The parameters considered were reinforcement configurations and strain distribution along the reinforcement element. Although the model footing was a square, the test box was a

rectangle with width equal to 6 times the footing width, which may lead to boundary effect on the obtained results.

2.3.3. Literature pertinent to soil reinforcement on layered soil

Dembicki et al. (1986) carried out experimental study on rigid strip footing on layered soil (mud covered by sand) reinforced by geotextile at the interface between the two layers. Two types of geotextiles were used, non-woven punched sewn and non-woven punched thermally bonded. The studied parameters were type and length of geotextile, thickness of sand layer, inclination and eccentricity of applied load. The bearing capacity was measured at a settlement equal 0.05 m (ratio of settlement to footing width equal 0.25). From the experimental results it was concluded that for different geotextile types, increasing sand layer thickness increased the bearing capacity ratio (Figure 2-8).

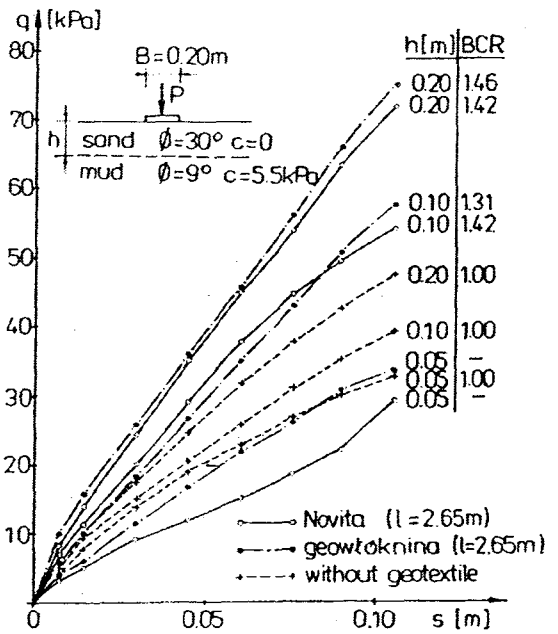

Figure (2-8): Influence of upper layer thickness and type of geotextile on bearing capacity of subsoil (Dembicki et al., 1986)

Also, increasing geotextile length increased the bearing capacity ratio (Figure 2-9).

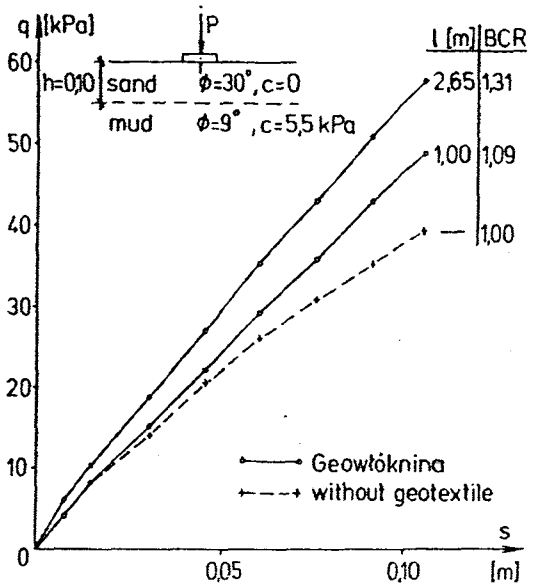

Figure (2-9): Influence of geotextile length on bearing capacity of subsoil

(Dembicki et al., 1986)

Das (1988) performed experimental study on a strip footing on compacted sand over a soft clay layer with and without using geotextile at the interface between the two layers. In the case of not using geotextile the ultimate bearing capacity increased with the increase of the ratio between sand layer thicknesses to the footing width up to a maximum value, which depended on the footing embedment ratio, and then remained constant. In case of using geotextile at the interface between sand and soft clay, Das (1988) concluded that the maximum bearing capacity was obtained at ratio of sand layer thickness to footing depth equal to 0.75 (Figure 2-10). Studying the effect of geotextile width, the ultimate bearing capacity increased increasing geotextile width till it reached 4 times the footing width after that no significant increase in the ultimate bearing capacity was obtained.

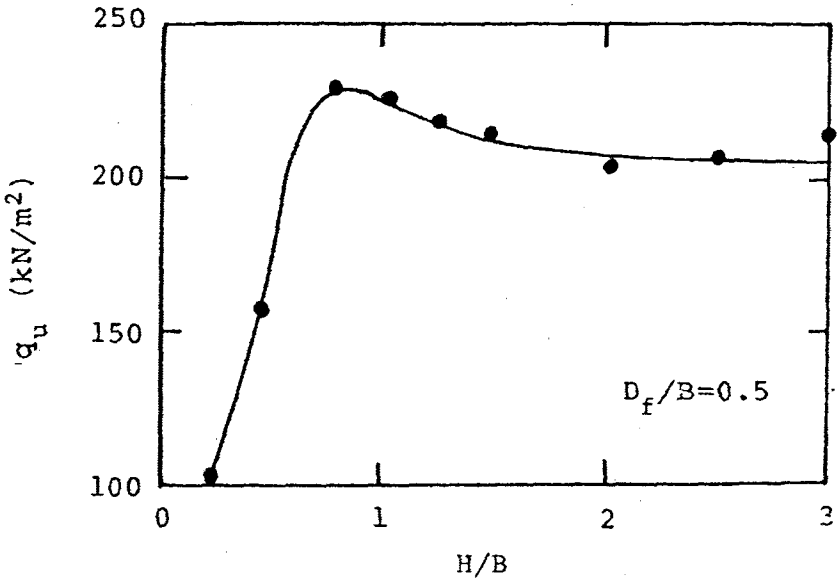

Figure (2-10): Variation of ultimate bearing capacity with sand layer thickness ratio with geotextile at the interface (Das, 1988).

Kim and Cho (1988) carried out laboratory model tests using strip footing on sand overlaying weak clays to study the effect of using geotextile at the interface between the two layers on bearing capacity of the footing, settlement of soil, and sliding length of the geotextile material. The parameters considered were sand layer thickness, embedment depth, and settlement of footing. Tests were carried out under partially drained condition at 50% consolidation. From test results it was concluded that the sand layer thickness ratio that gave the maximum benefit for the geotextile was between 0.5 and 1.0 for settlement ratio less than 1.0. Due to geotextile reinforcement, the failure occurred at high bearing pressure in large deformation mode of circle, while the unreinforced soil failed at low bearing pressure in small deformation mode.

Patel (1988) conducted laboratory model tests on strip footing placed on the surface of covering pad of good frictional sand over virgin weak sand deposit reinforced with

fiberglass woven rowing geotextile placed at the interface between the two layers. The aim was to study the improvement in the bearing capacity of the system. Three series of tests were carried out. The first: for one layer of weak sand and one layer of frictional sand. The second: by varying the thickness of the frictional sand. The third: by introducing the geotextile at the interface between the two layers at different depths (different thickness of frictional sand). From test results, it was concluded that for geotextile depth ratio equal to 1.5, the geotextile gave better effect on the bearing capacity than that for frictional sand alone. Beyond reinforcement depth of 1.65 the footing width, that effect was not so evident.

Som (1988) carried out experimental investigation to study the effect of using geotextile on the bearing capacity of circular footing on Kaolinite clay with and without using a fill layer above it. Different materials with varied thickness were used as filling layers such as loose sand, compacted clay and compacted lime-fly ash. When using geotextile at the interface between the filling layer and the kaolinite clay it was concluded that at the same settlement value the load carrying capacity increases for all cases of tested kaolinite. This increase was more obvious for settlement more than 10% of the footing's diameter. By increasing the thickness of the filling material the bearing capacity of the soil increases. However, for thickness more than 0.7 the footing diameter there was almost no increase in the bearing capacity. The increase in case of dense sand was relatively small as compared to the loose state, and it was greater in case of compacted clay or compacted lime-fly ash. Also, the effect of using geotextile on the bearing capacity was more pronounced when the thickness of the filling material was less than half of the footing diameter (Table 2-2).

Table (2-2): Gain in bearing capacity (Som, 1988)

Base material	Thickness (mm)	Gain in Bearing Capacity	
		With no geo-textile (%)	With Geotextile at Interface (%)
Nc base (Footing placed on subgrade)	-	-	82
Sand	10	21	46
	20	25	46
	30	18	46
Compacted Clay	10	54	82
	20	121	132
	30	125	136
Compacted lime/flyash	10	89	100
	20	125	150
	30	150	160

Khing et al. (1994) carried out laboratory model tests to determine the bearing capacity of strip footing supported by a strong sand layer underlain by weak clay with geogrid reinforcement at the sand clay interface. The studied parameters were, sand layer thickness and width of reinforcing material. From test results, it was concluded that using geogrid, regardless of its type, at the interface between sand and clay increased the ultimate bearing capacity of the strip footing. The maximum effect can be gained at ratio of sand layer thickness to footing width equal to 2/3 and it was negligible for values more than 1.5 times the footing width. Also, increasing the geogrid width increased the (BCR) up to a value of geogrid width equal to 6 times the footing width after which the (BCR) remained almost constant.

Ismail and Raymond (1995) carried out experimental tests to study the influence of reinforcement depth in a uniform weak soil with or without a stronger thin upper layer,

under static and repeated loading, on the bearing capacity and settlement of a surface strip footing. The tests were divided into 3 cases:

- Case (1): applying static load on the soil deposit which consisted of the upper stronger layer with thickness equal to 0.0625 the footing width and a lower weaker layer with thickness equal to the footing width. A single layer of reinforcement at different depths was used.
- Case (2): applying static load on one weak layer with the whole thickness and using two layers of reinforcement, the first at a fixed depth equal to 0.0625 the footing width and the depth of the other was varied.
- Case (3): similar to case (2) except that only one layer of reinforcement was used with varied depth.

For test results under static loading, it was concluded that,

1. For cases (1 and 2) significant increase in ultimate bearing capacity and decrease in settlement could be achieved for ratio of reinforcement depth to footing width between 0.3 and 0.5.

2. When placing the reinforcement on the above-mentioned depths, the ultimate bearing capacity could be at least doubled and the settlement reduced by about 50%.

3. For case (3), increasing the reinforcement depth decreased the ultimate bearing capacity and increased the settlements for the same load.

4. Comparing the values of the ultimate bearing capacity obtained from the three cases, case (2), which was using 2 layers of reinforcement in the whole weak layer, was always the highest.

Das et al., (1998) carried out laboratory model tests on rigid strip surface footing to investigate the effect of using a geogrid layer, at the interface between a granular soil (sand) underlain by soft clay, on the bearing capacity. The studied parameters were sand layer thickness and width of geogrid layer. In case of two soil layers with no reinforcement, the experimental results showed an excellent agreement with the theoretical ones obtained from Meyerhof and Hanna (1978). In case of using geogrid layer at the interface between the sand and the clay, the maximum increase in the bearing capacity was at ratio of sand layer thickness to footing width of 0.67 and it was almost negligible for values more than 1.3. At ratio of sand layer thickness to footing width equal to 0.67, the effective width ratio was found to be equal to 6.0 and the (BCR) became constant after that value.

Lee et al. (1999) carried out small scale model tests to study the bearing capacity and settlement of a rigid strip footing on dense sand overlying thick, homogeneous bed of clay with and without a layer of geotextile at the interface. The studied parameters were thickness of sand layer and width of the geotextile. The ultimate bearing capacity was determined from load settlement curve by drawing tangents from the initial and end points of the curve and the point of intersection was produced back to Y-axis to obtain the ultimate bearing capacity (Figure 2-11). This Figure also shows the effect of sand layer thickness ratios on the footing carrying capacity. Using the finite element program (PLAXIS), a numerical study was also carried out to validate the model test results.

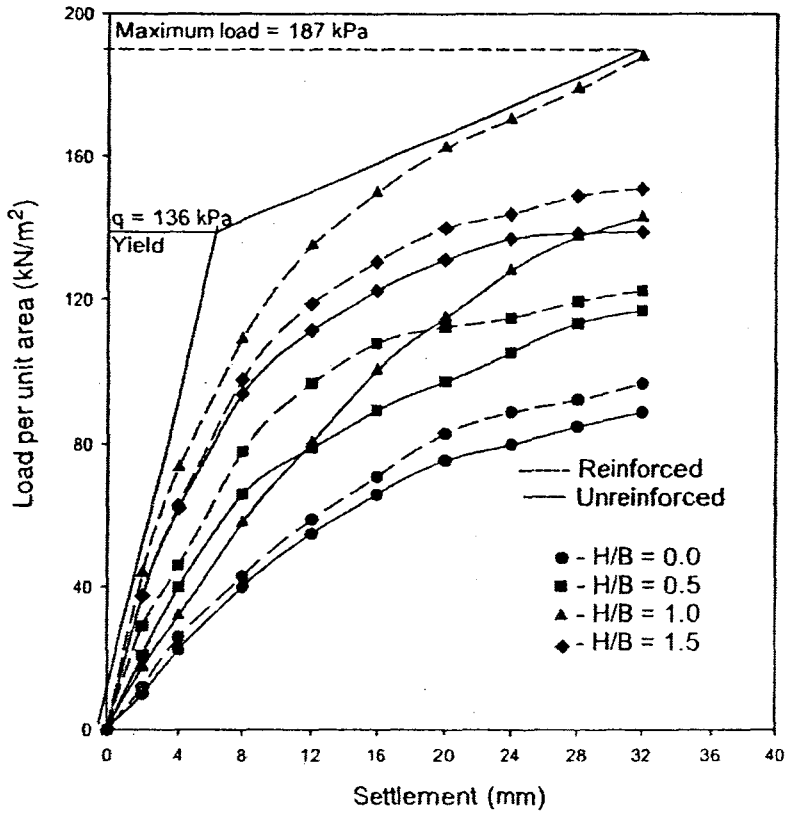

Figure (2-11): Summary of load-settlement curves at different sand layer thickness ratios (model tests) (Lee et al., 1999)

From this study it was concluded that

1. The maximum (BCR_u) for the unreinforced soil was obtained at ratio of sand layer thickness to footing width equal to 1.5 after which the (BCR_u) remained constant. While for the case of reinforced soil, this ratio was equal to 0.8 after which it dropped down till it approached the value of unreinforced soil at a ratio of sand layer thickness to footing width equal to 1.5 (Figure 2-12).

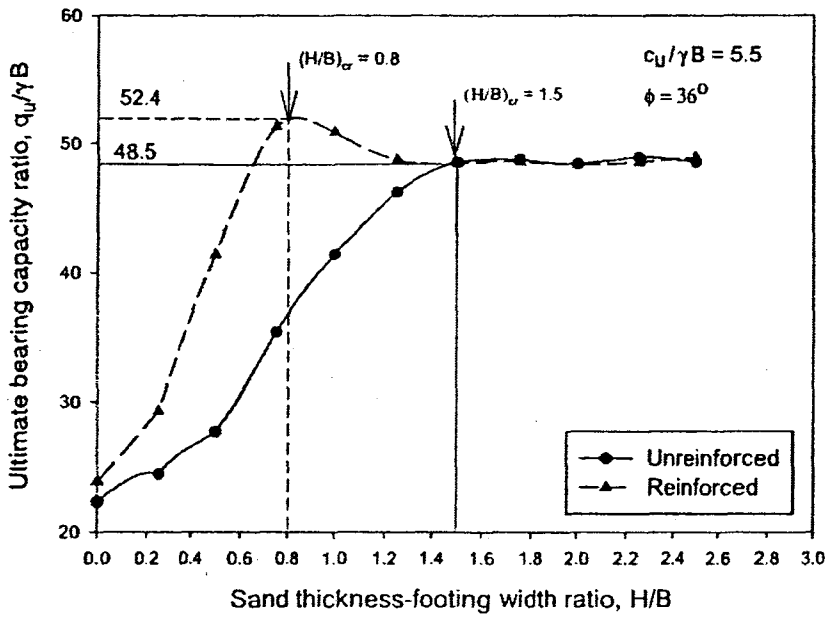

Figure (2-12): Variation of ultimate bearing capacity with sand layer thickness ratio (model tests) (Lee et al., 1999)

2. The ultimate bearing capacity increases due to the increase of the reinforcement width up to a peak value, which takes place at a reinforcement width equal to 5 times the footing width. Extending the reinforcement beyond this value had no effect on the (BCR_u) (Figure 2-13).

3. Although the results from the numerical study were not in exact agreement with the model tests, the two results agreed in the optimum values for the sand layer thickness (Figure 2-14) and reinforcement width (Figure 2-15).

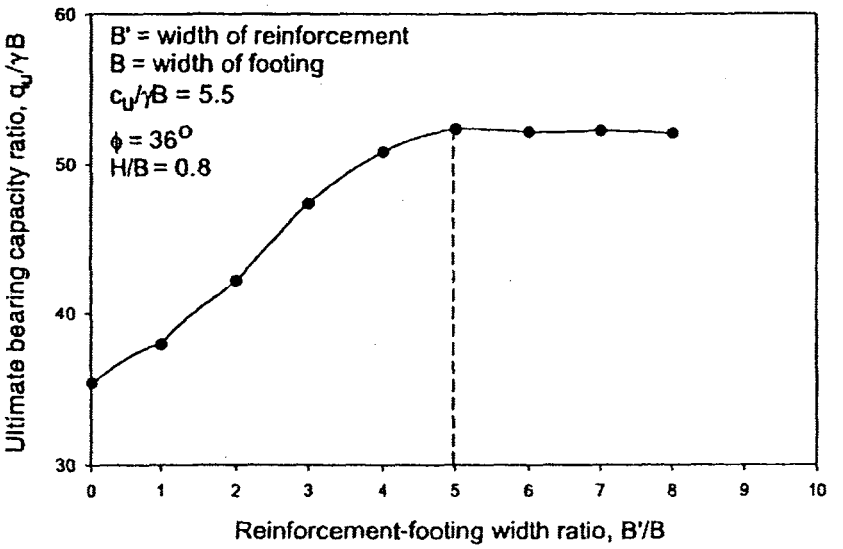

Figure (2-13): Variation of ultimate bearing capacity with reinforcement width ratio (model tests) (Lee et al., 1999)

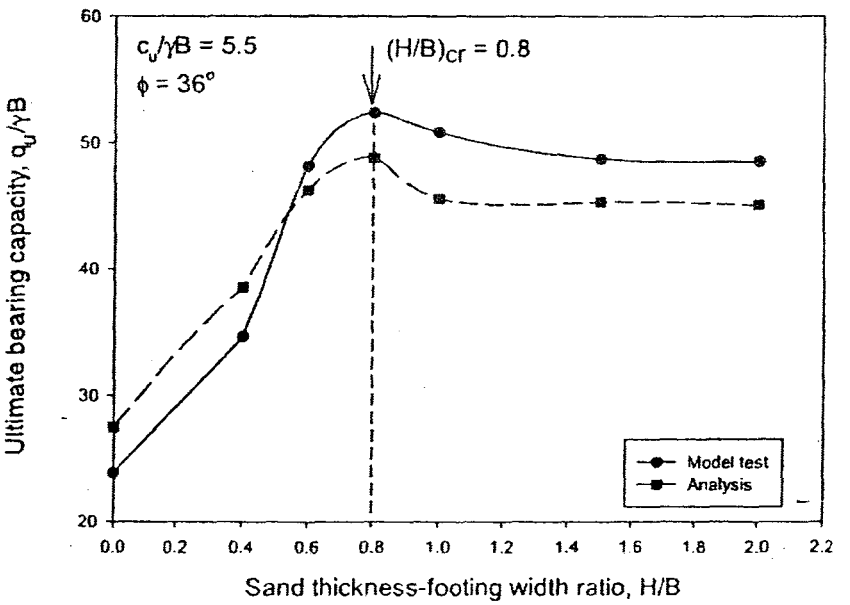

Figure (2-14): Comparison between results for model tests and numerical analysis for sand thickness-footing width ratio (Lee et al., 1999)

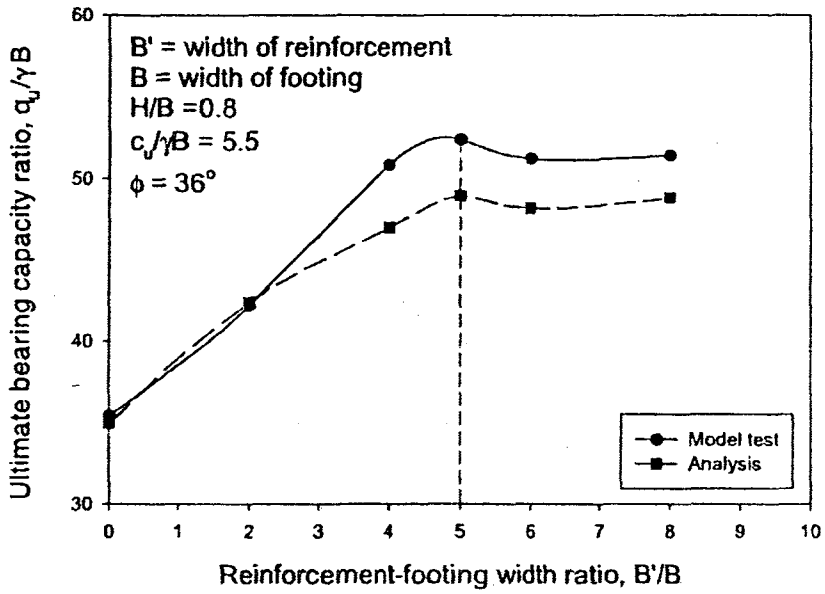

Figure (2-15): Comparison between results for model tests and numerical analysis for reinforcement-footing width ratio (Lee et al., 1999)

A parametric numerical study using (PLAXIS) was carried out to study parameters that were not investigated during the experimental work such as undrained shear strength of the clay, angle of internal friction of the sand, axial stiffness of the geotextile and strength reduction factor at the soil-geotextile interface. Results from this study showed that clay cohesion has almost no effect on the optimum ratio of sand layer thickness in case of reinforced soil. Also, increasing angle of internal friction for the sand layer or axial stiffness of the geotextile increased the ultimate bearing capacity and reduced settlement.

Unnikrishnan et al. (2002) carried out unconsolidated, undrained, triaxial compression tests to study the strength improvement due to providing a sand layer on either side of the reinforcement within reinforced clay soils under both static and cyclic loading. Three different types of reinforcement were used, woven, non-woven geotextiles

and micro-grid. In case of testing under monotonic loading, two sizes of samples were prepared, a small one for tests with one reinforcement layer, and a large one for tests on multiple reinforcement layers. The studied parameters in this case were, sand layer thickness, moisture content, reinforcement type, number of reinforcement layers and confining pressure. From test results, Unnikrishnan et al. (2002) concluded that for a constant confining pressure and for all reinforcement cases, the maximum deviator stress didn't increase significantly after a sand layer thickness of about 10% of the sample length, however in case of lower confining pressure, the maximum deviator stress continued to increase after this value (Figure 2-16), which showed that, the optimum thickness of sand layer depend on the stress range in the soil. In case of two layers of reinforcement in large samples, there were higher strength and stiffness than single layer of reinforcement (Figure 2-17). Also, the influence of introducing the reinforcement and the sand layer is more obvious in case of moisture content of sample on the wet side of the optimum (Table 2-3), where OMC is the optimum moisture content of the soil.

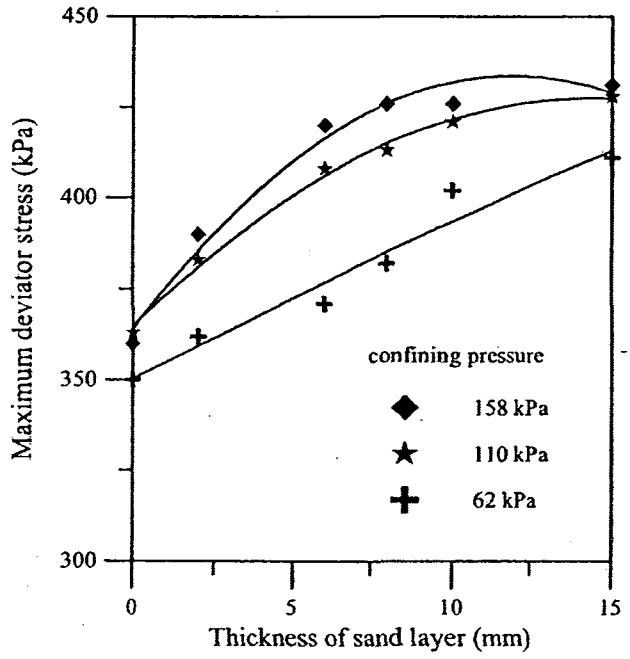

Figure (2-16): Effect of confining pressure on the maximum deviator stress developed

(Unnikrishnan et al., 2002)

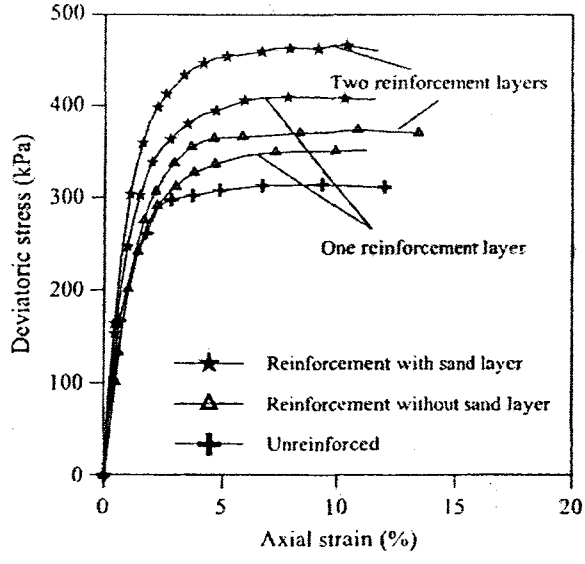

Figure (2-17): Triaxial compression test on 100 mm diameter specimens

(Unnikrishnan et al., 2002)

Table (2-3): Influence of water content on ultimate strengths (Unnikrishnan et al., 2002)

Test sample	Maximum deviator stress (kPa) and % change in strength		
	Dry side of OMC	OMC	Wet side of OMC
Unreinforced soil	425	340	230
Soil + geotextile	445 (4.7%)	360 (+5.6%)	238 (+3.4%)
Soil + geotextile + sandwich layer	460 (8.2%)	380 (+11.8%)	275 (+19.6%)

This study showed that there is no definite value for the sand layer thickness that gives the best performance of the soil as this value depends on the stress level on the sample.

Yetimoglu et al. (2005) carried out laboratory California Bearing Ratio tests to study the effect of fiber reinforcement content on bearing capacity, stiffness and ductility of fiber reinforced sand fill on soft clay subgrade. The test set up in case of fiber-reinforced sand is shown in (Figure 2-18).

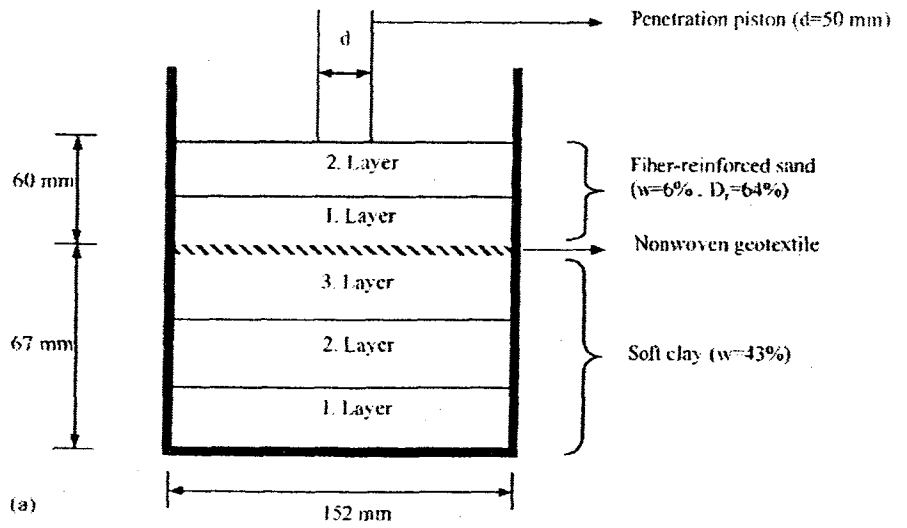

Figure (2-18): Cross section of test setup for fiber reinforced sand with one geotextile layer (Yetimoglu et al., 2005)

Using a second geotextile layer (Figure 2-19), a second group of tests for geotextile reinforced sand were carried out and results were compared to the case of using fiber reinforcement.

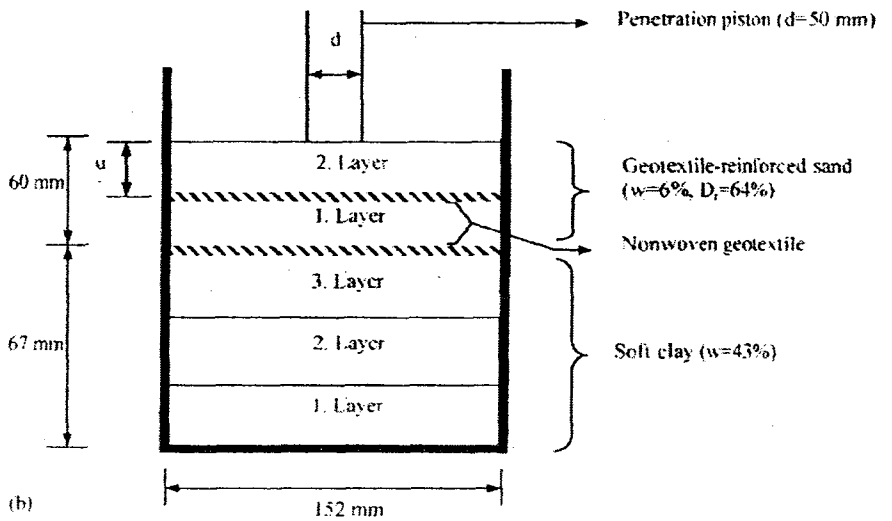

Figure (2-19): Cross section of test setup for geotextile reinforced sand specimens (Yetimoglu et al., 2005)

In these tests, the thickness of both sand and soft clay was kept constant. Some of the difficulties mentioned by the authors related to the use of CBR small test apparatus were limiting the amount of fiber inclusion and that the end effect can affect the results. From test results it was concluded that, increasing the fiber reinforcement content increased the peak load ratio, which is the ratio of the peak load on piston for reinforced sample to the peak load on piston for unreinforced sample, up to 5 times (Figure 2-20). It was also shown that Load penetration behavior for tests carried out by using second geotextile layer was similar to that reinforced randomly with a small amount of fibers i.e. the effect of fiber reinforcement was similar to the geotextile reinforcement.

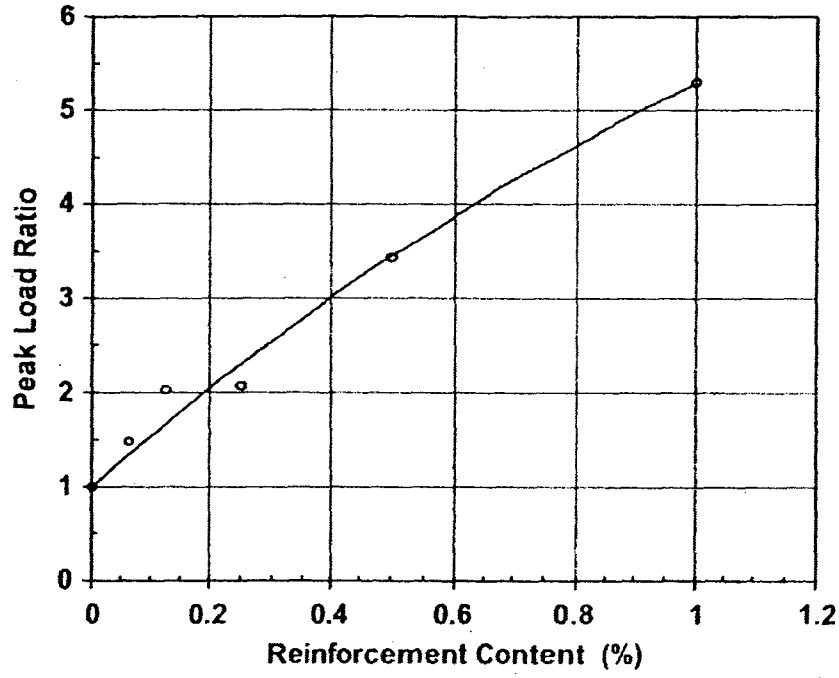

Figure (2-20): Variation of peak load ratio with reinforcement content

(Yetimoglu et al., 2005)

The main shortcoming of this study, as mentioned by the authors, was related to the size of the California Bearing Ratio test apparatus.

Kazimierowicz-Frankowska (2007) analyzed results obtained from different research and studies on the case of granular layer over soft ground reinforced with geosynthetic layer at the interface between the two layers. Also, results from the membrane-action model presented by Burd (1995) were discussed with the main conclusion that researchers still didn't agree on a specific method to estimate the load dispersion angle in the top layer although that minor change in its value significantly affect the calculated settlement that footings experience.

Kumar et al. (2007) carried out experimental study to investigate the effect of partially replacing weak deposit by well graded soil with and without using reinforcement (geogrid) within the top layer on the bearing capacity and settlement of strip footing. It was concluded from this study that up to 3 to 4 times increase in the ultimate bearing capacity of the strip footing can be achieved when replacing the weak soil with well graded sand with thickness equal to the foundation width and reinforcing the sand layer with 2-4 layers of geogrid. It was also observed that at all levels of settlement (2%, 3% and 4%) there is an improvement in the bearing capacity.

Basudhar et al. (2008) studied, numerically, the behavior of a geotextile reinforced sand bed subjected to strip loading. The cases of homogeneous soil, non-homogeneous soil and two-layer system were investigated. Among the authors' conclusions are that the optimum placement depth of the geotextile layer is 0.6 the footing width, also in the two-layerd system, Young's modulus and Poisson's ratio have great influence on the settlement reduction.

2.3.4. Literature pertinent to soil reinforcement on collapsible soil

Limited studies were carried out to investigate the effect of using reinforcement on the collapse settlement of collapsible soils as follows:

Mashhour et al. (1999) carried out model tests to investigate the settlement of strip footing resting on collapsible soil. The effects of soaking pressure and direction of flow on the footing settlement were considered. The authors suggested treatment methods to reduce the footing settlement by replacing the collapsible soil with clean sand with or without the inclusion of geogrid layer at the interface between the two soil layers. Results

showed that settlement of footing on collapsible soil increased with the increase of soaking pressure and that there was some difference in footing settlement caused by downward flow or upward flow (downward flow causes 18% higher settlement). The authors reported significant reductions on the footing settlement when using replacement with sand technique with or without the inclusion of geogrid layer at the interface between the two soil layers.

Alawaji (2001) carried out model load tests on circular plate founded on geogrid reinforced sand over collapsible soil. The objective was to study the effect of geogrid reinforced sand on controlling the wetting induced collapse settlement. The parameters considered in this investigation included width (diameter) and depth of the geogrid layer. The effects of varying these parameters on footing collapse settlement; deformation modulus and bearing capacity were investigated. Other parameters, such as sand soil thickness and collapsible layer thickness were kept constant. From test results, Alawaji concluded that, in general, using geogrid reinforced sand instead of sand alone decreased the settlement and increased the load carrying capacity as shown in Figure (2-21). The geogrid depth corresponding to the minimum settlement was equal to 0.10 the diameter of the loaded plate (Figure 2-22). The optimum value of the geogrid diameter to loading plate diameter was equal to 4.0 and that corresponded to reduction of about 95% in settlement ratio (Figure 2-23).

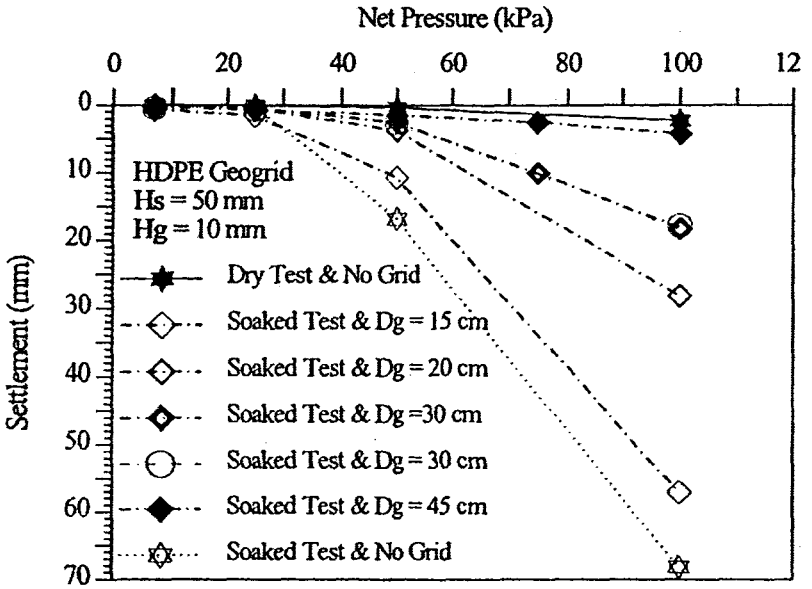

Figure (2-21): Pressure-settlement curves for geogrid reinforced sand over collapsible soils (Alawaji, 2001)

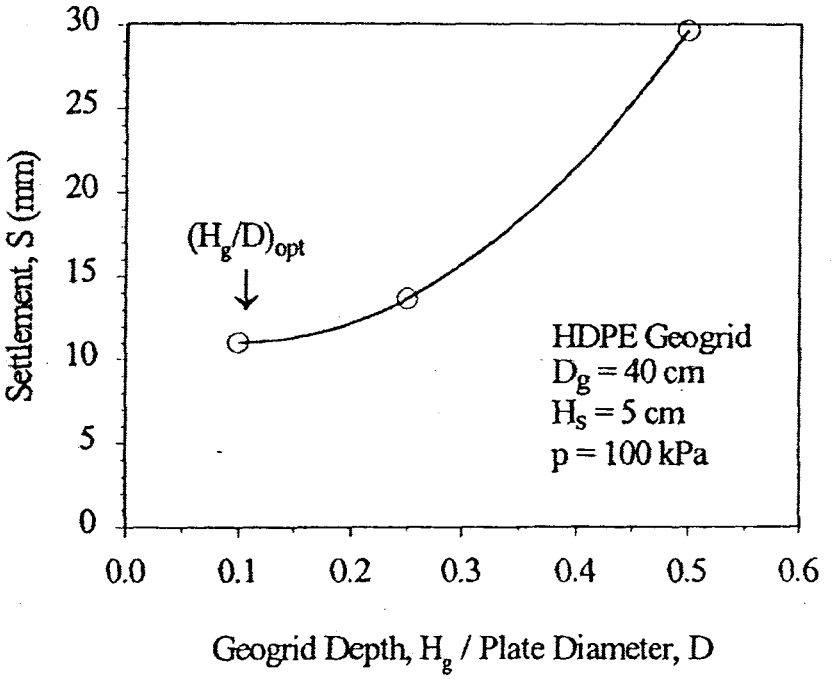

Figure (2-22): Dry then soaked collapse settlement versus geogrid depth / plate diameter for geogrid reinforced sand over collapsible soils (Alawaji 2001)

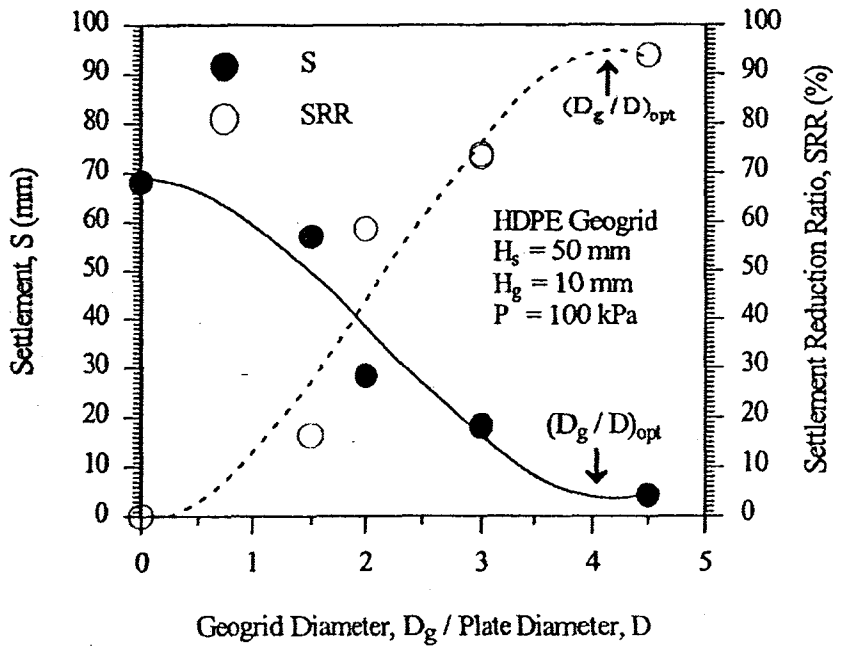

Figure (2-23): Collapse settlement and settlement reduction ratio versus geogrid diameter / plate diameter for geogrid reinforced sand over collapsible soils (Alawaji 2001)

2.4. DISCUSSION

Based on the literature review highlighted in this chapter, it can be stated that,

1. Various improvement techniques for construction on collapsible soils were suggested by researchers such as partial wetting, chemical stabilization and soil reinforcement.
2. No design procedures or formulas were developed to design shallow strip footing on collapsible soils.
3. Soil reinforcement, as one of the soil improvement techniques, helps in reducing the settlement and increasing the bearing capacity of the normally behaving soils. Research has been done in using soil reinforcement in homogeneous soil (sand or clay with different properties) and layered soil (partial replacement of weak soil by granular stronger one).

4. Partial replacement and reinforcement of collapsible soils showed efficiency on reducing collapse settlement. Limited studies were carried out using this technique with parameters such as effects of collapse potential values, soil depth, variation of replacement layer thickness and reinforcement types out of the scope of those studies.

Accordingly, the objectives of this study are:

1. To conduct experimental investigation to examine the behavior of shallow, rigid strip footing under axial load and subjected to inundation resulting from the rise of the groundwater table reaching full saturation status for the case of:
    a. Homogeneous collapsible soils,
    b. Partially replaced collapsible soils.
    c. Partially replaced collapsible soils with geosynthetics reinforcement.

2. To develop analytical and empirical models to predict: collapse settlement of shallow strip footing, strain developed in the geotextile and deformed shape at collapse.

3. To produce design procedures and design charts to assist in design and construction of shallow rigid strip footing on collapsible soil subjected to inundation.

CHAPTER 3

EXPERIMENTAL INVESTIGATION

3.1. GENERAL

An experimental setup was designed and built in the Foundation Engineering laboratory at Concordia University to examine the settlement characteristics of rigid surface strip footings on deep homogeneous collapsible soil and on partially replaced collapsible soil with / without the inclusion of geosynthetics (geotextile and geogrid) during ground inundation. The set-up is equipped to measure the collapse settlement (Δ), collapsible soil depth (d_c), water level changes and load on the footing during inundation.

This chapter describes the design of the experimental setup and its components, the properties of the materials used and includes the preparation of the collapsible soil, replacement soil and geosynthetic materials.

3.2. TEST SETUP

Figure (3-1) presents a sketch for the setup used in this investigation, which consists of testing tank resting on steel frame, loading device supported by the steel frame, elevated water tank with constant water head that supplies the water to the soil in the testing tank through water distribution system. The detailed descriptions and specifications for the setup components are as follows:

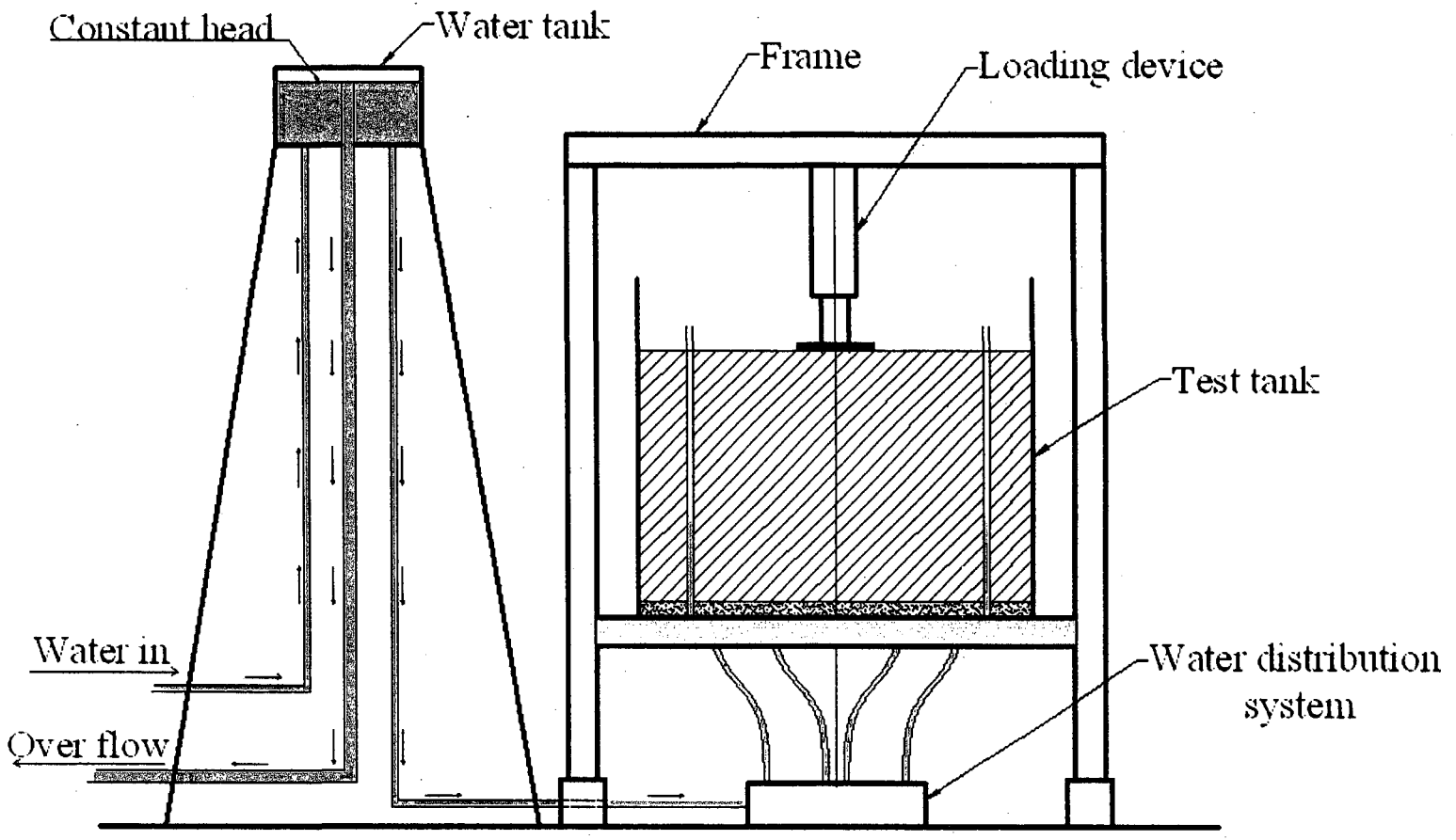

Figure (3-1): sketch shows test setup

3.2.1. Model test tank

The tank is made of Plexiglas walls 12.5mm thick with two sides made of Aluminum alloy channels. The tank is 1000mm wide, 400mm long and 650mm high, braced with steel angles to ensure no deformation while placing and compacting the soil and during loading of the footing. Plexiglas allows observation of the failure mechanism and the deformation in the reinforcement materials during testing and further to minimize the friction between the soil and the walls of the testing tank. In addition, silicon grease was spread over the walls, which are in contact with the soil. The test tank is placed on a steel frame, which allows the fixation of the loading device as well as the inlet of the water to the soil in the tank. Two thin tubes are connected to the bottom of the tank and extended along the tank height to allow observation of water level in the collapsible soil during inundation. Figure (3-2) shows a picture for the testing tank.

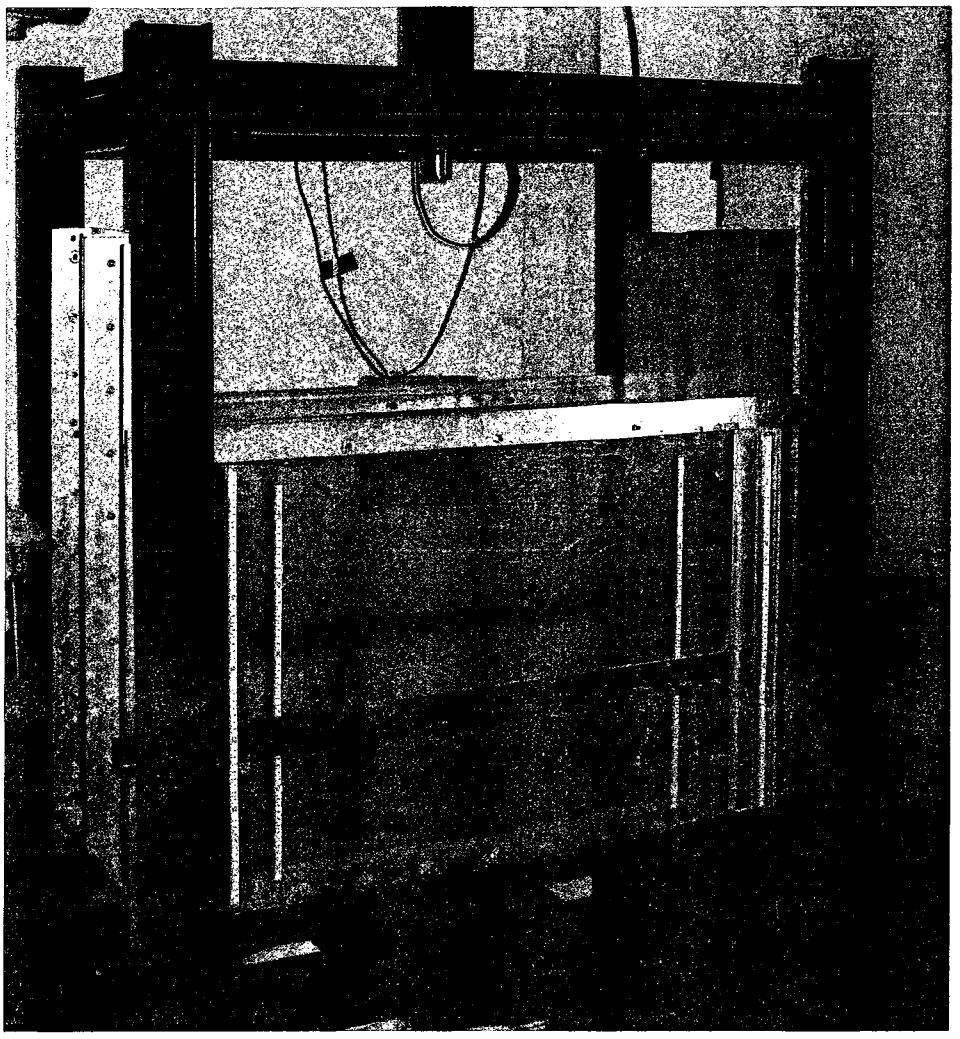

Figure (3-2): Testing tank

3.2.2. Model footing

The model footing is made of rigid Aluminum alloy plate 12.5mm thick, 75mm wide and 400mm long. With these dimensions, a plane strain condition is achieved that allows the horizontal strain of the elastic soil to occur only in the direction perpendicular to the long axis of the footing (Day, 2006). To simulate the rough condition between the footing base and the soil in the field, a sheet of sand paper was glued to the base of the model footing

by epoxy glue. A rigid Aluminum alloy plate 12.5 mm thick, 75 mm wide and 100 mm long was placed at the center of the footing and fixed by means of a steel pin. This plate had a groove made on it and a half sphere of steel rested in this groove through which the load is applied as shown in Figure (3-3). This setup keeps the applied centric load vertical throughout the test.

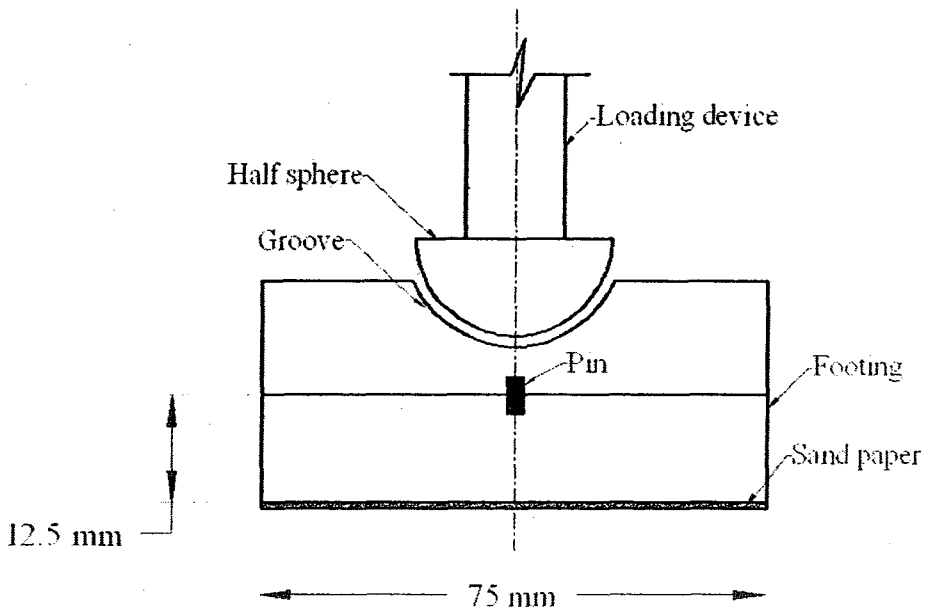

Figure (3-3): Schematic diagram of the model footing

Preliminary tests showed with these testing arrangements, no boundary effects were noted. Andrawes et al. (1983) carried out tests using strip footing on geotextile reinforced sand; they reported that for tests carried on homogeneous sand extended laterally to a maximum of six times the footing width from the centerline of the footing, the failure surface extends to maximum depth equivalent to two times the footing width. Lee et al. (1999) in their study of strip footing supported by a reinforced granular fill-soft soil recommended that the boundaries of the testing tank should extend beyond 4 times the

footing width from the footing centerline to ensure that the entire failure zone is contained

In this experimental investigation, the depth of the soil in the test tank is equal to $6B$, where B is the footing width, and when investigating the effect of collapsible soil depth on the collapse settlement of the footing, the minimum depth used was $4B$; consequently, the pressure contour at that depth will be about 0.11 B, which is accepted for the common engineering practice (French 1999).

3.2.3. Elevated water tank and water distribution system

An elevated tank, made of Plexiglas and rested on a steel frame, is connected to the testing tank by a thin plastic tube, which was branched into 4 tubes, through which the water is charged to the bottom of the test tank, simulating the rise of groundwater table. The water level in the water tank is kept constant during the inundation process, water is charged from a water source and an overflow pipe is fixed inside the water tank that keeps water at a constant head. A layer of slightly compacted coarse silica sand was placed at the bottom of the testing tank to ensure an even distribution of the water throughout the collapsible soil. Figure (3-4) and Figure (3-5) show pictures for the elevated water tank and the water distribution system respectively.

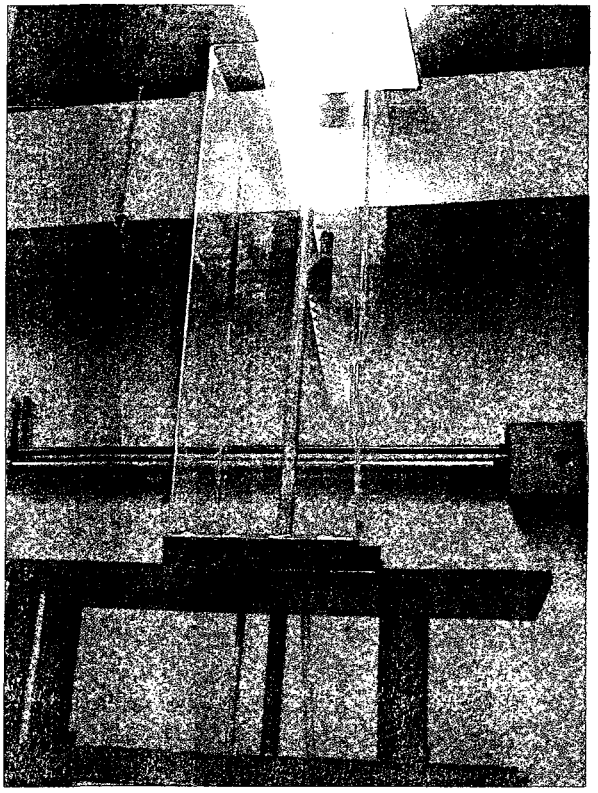

Figure (3-4): Elevated water tank

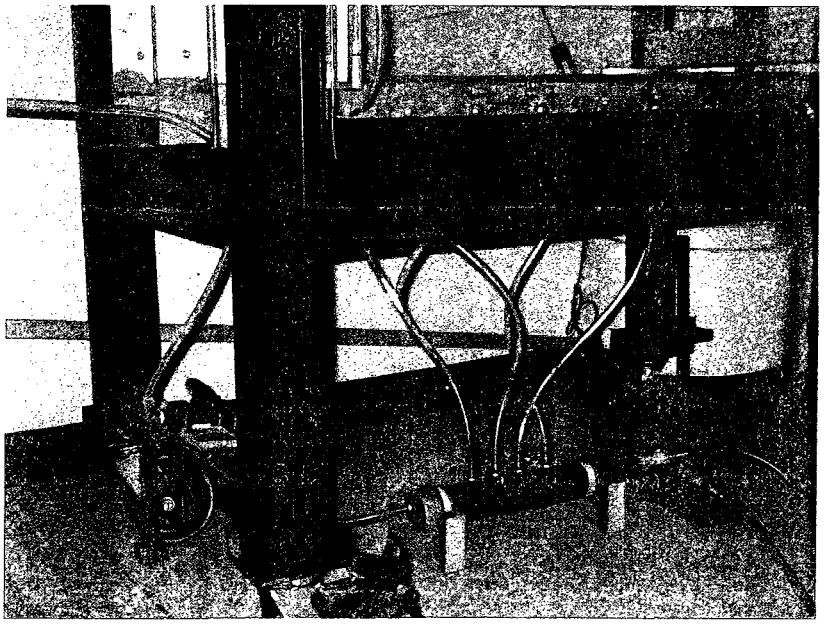

Figure (3-5): Water distribution system

3.2.4. Material placing techniques

Soil is placed in the testing tank manually by means of thin layers spread evenly then compacted. A device, which was supported on the testing tank's sides by means of bearings and moves along the testing tank length and guided by two guide rails, extend downwards and vertically with an aluminum plate fixed at its end, which is used to spread and level the soil. The height of the vertical plate can be adjusted to suit the height of each sub-layer needed to be placed before compaction. After ensuring that the soil layer was leveled at the required height, compaction started by means of dropping weight falling on two aluminum plates placed on the top of the soil layer. The reason for using two aluminum plates is to ensure the distribution of the energy produced from the dropping weight to the entire soil layer. The dimensions of the plate in contact with the soil are 510mm wide and 400mm long. The soil in the testing tank was compacted in two stages with an overlap of 10mm.

3.2.5. Loading system

Load was applied on the footing by means of stress control loading system, measured by means of load cell 5000 LB capacity, excitation 10 Vdc, output 3mV/V ± 0.25%, linearity 0.10% and repeatability 0.05%. An actuator was used to apply the load, which was controlled by Proportional-Integral-Derivative controller (PID controller) programmed by (labVIEW) software. Figure (3-6) shows a picture of the block diagram for programming a single loop PID. Figure (3-7) shows a picture of the front panel of this program where parameters controlling the loading system were varied and tested such as: proportional gain, integral time, derivative time and sampling time. The three main parameters controlling the design of this program are proportional gain, integral and

derivative times, which were tuned to provide the required control action for the loading device. Trials were carried out leading to program a PI system (Proportional-Integral controller) and the value for the derivative was set to zero. Sampling time was adjusted at 0.01 second to ensure the load applied is satisfying the required value.

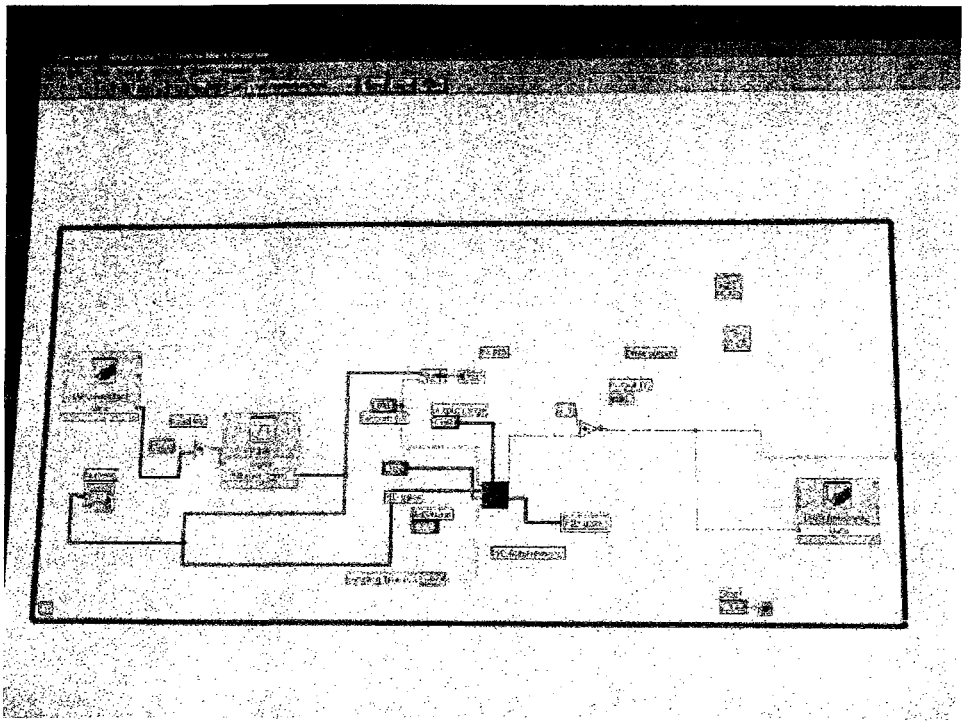

Figure (3-6): Block diagram for a single loop PI controller

Settlement of the footing was measured by two long stroke displacement transducers (DCR 150) placed at the third of the footing length from both ends with a linear stroke equal ± 150mm and the input voltage range is 9-15 volts (typical 10 V dc). The sensitivity of the LVDT is 13.3 mV/mm at 10 V dc with nonlinearity of 0.3%. Settlement of the footing was calculated as the average of the two LVDT readings. Figure (3-8) shows a picture of the final arrangement for the loading device, load cell, footing and LVDTs.

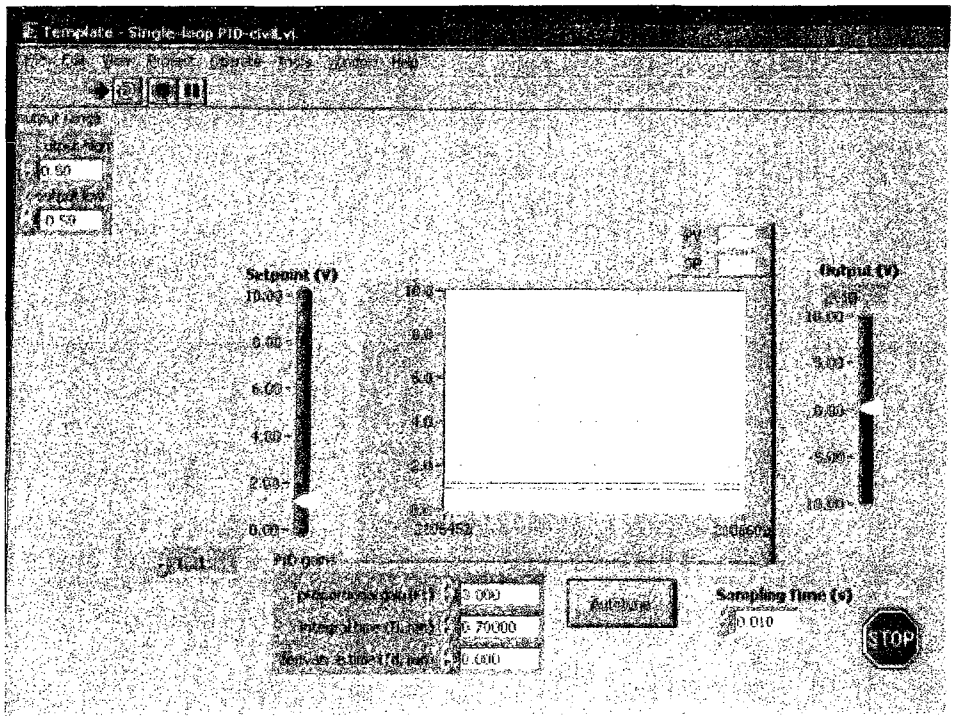

Figure (3-7): Front panel of the PI controller

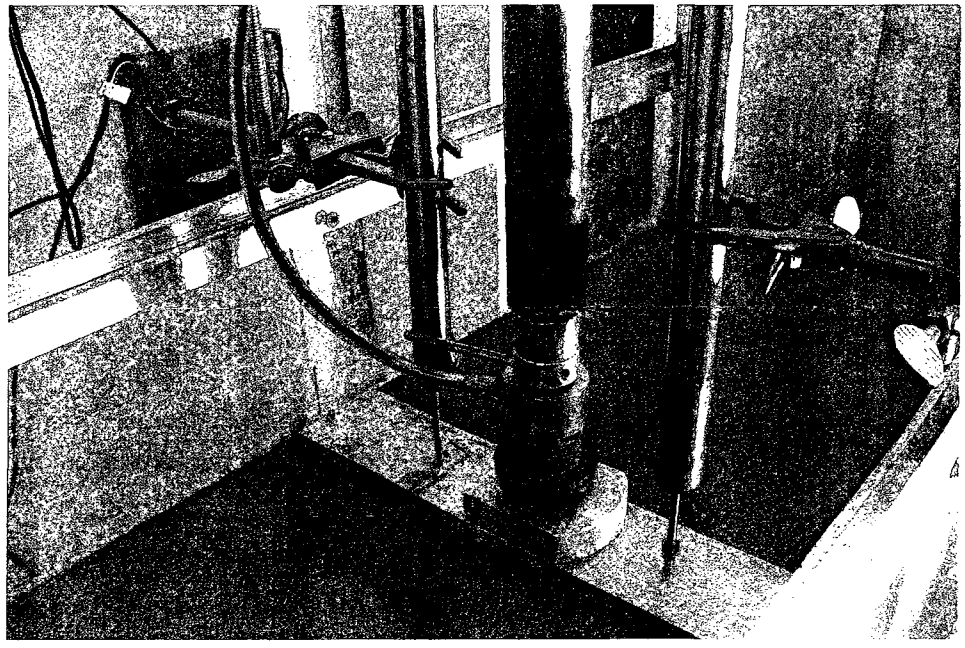

Figure (3-8): Loading device, load cell, footing and LVDTs

Readings from LVDT and load cell were recorded on a computer through Data Acquisition System (DAS) and software (vee.pro). The Data Acquisition System allowed the measurement of millivolts from the devices till 10^{-6} mV. The output of the LVDTs and the load cell were transformed from millivolts to millimeters and kilopascals, respectively, by using the software (vee.pro), (Figure 3-9), through formulas recorded on the software (vee. pro) and obtained from the calibration of these devices. The software allowed data recording till each 5 seconds.

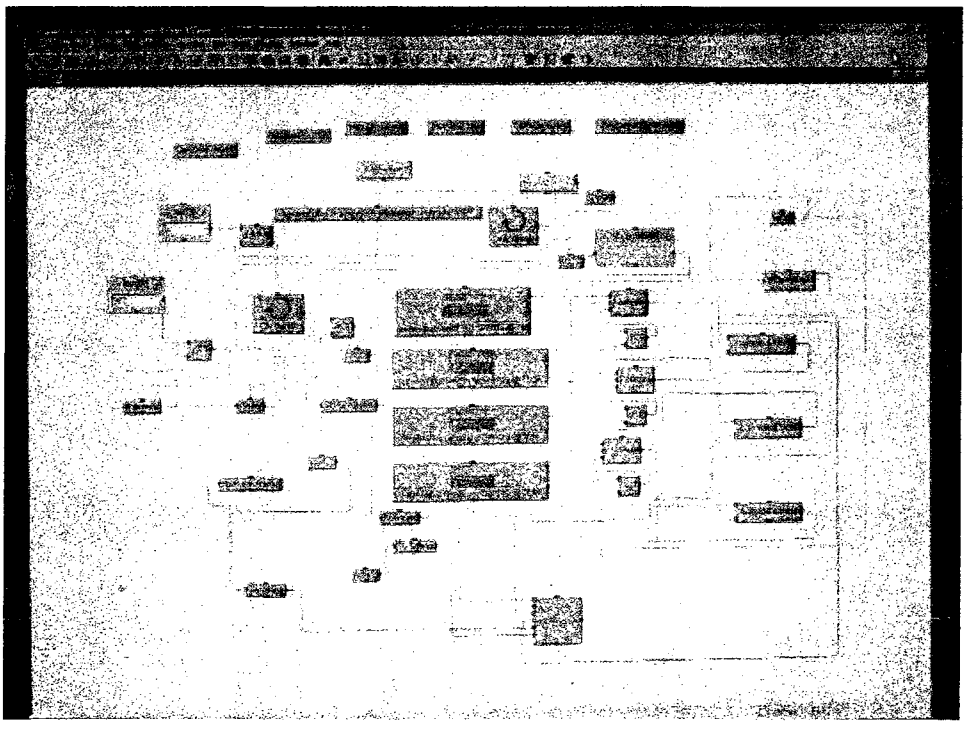

Figure (3-9): Programming of vee.pro

Figure (3-10) presents a picture of the testing setup with all accessories.

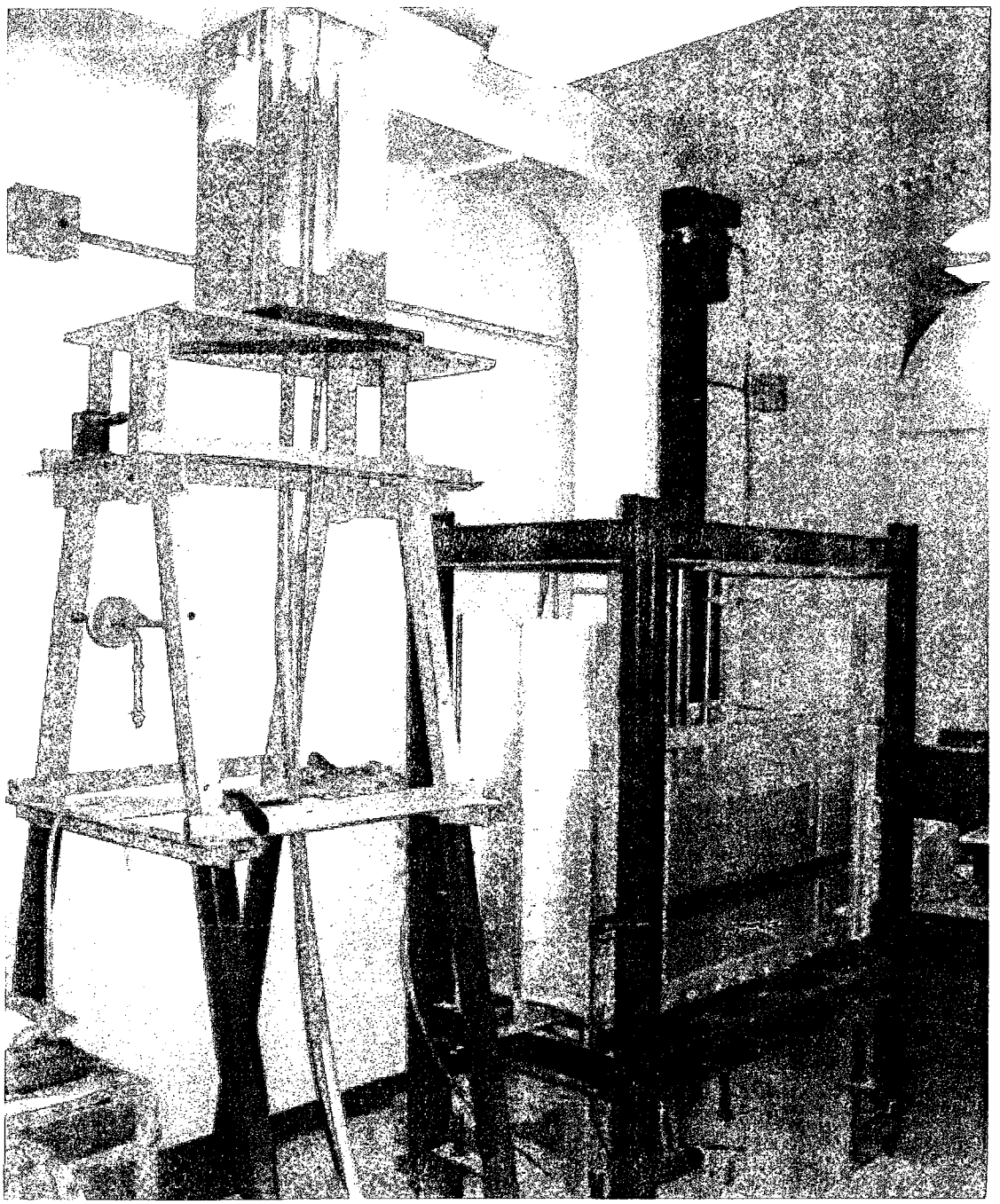

Figure (3-10): Test setup

3.3. MATERIALS

3.3.1. Soils

The experimental study was conducted on laboratory prepared collapsible soils by mixing a clay mineral (Kaoline) with sand at different percentages. In general, the higher the clay content the higher the collapse potential. However, it has to be noticed that there is a limit of clay content after which soils are expected to swell rather than to collapse (Adnan and Edril, 1992). Miller et al., (1998), have concluded that the maximum collapse occurs at approximately 18% clay (Kaoline) content. Single oedometer tests were carried out on the prepared samples to determine the collapse potential for each mix tested. This procedure allows obtaining soil samples with different collapse potentials ranging from about 4% to 13%, which presents a wide range of the problem severity and the majority of the field cases.

Properties for sand and clay mineral that have been used in these tests are given in the following sub-sections.

3.3.1.1. Sand

All-purpose sand, commercially known as Tech-mix sand and packed in 30 kg packages, was used to form collapsible soils. This sand was also used as a replacement material for some tests. Basic laboratory tests were conducted on the sand to determine its geotechnical properties including the grain size distribution, coefficient of uniformity, C_u, coefficient of curvature C_c, optimum water content and maximum dry unit weight. Table (3-1) presents the value of sand properties and Figure (3-11) presents the grain size distribution.

Table (3- 1): Sand properties

C_u	C_c	w_c	$\gamma_{d\,max}$
2.78	1.07	16.5%	16.93 kN/m^3

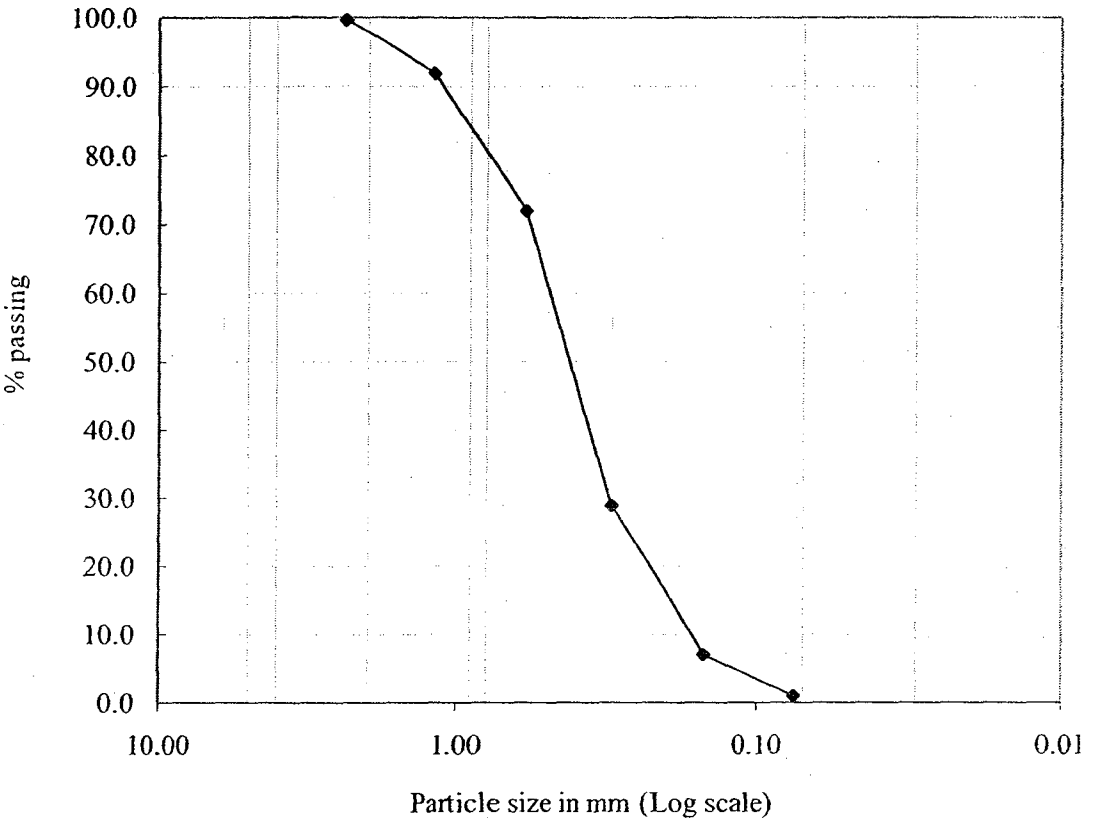

Figure (3-11): Particle size distribution for Sand

3.3.1.2. Kaoline

Different types of Kaoline were tested in the laboratory to produce the predetermined Collapse Potential (C_p) for the mix. The types used are known commercially as: KT-Cast, Sapphire and Rogers. Sieve analysis, chemical analysis and physical properties for

these three types provided by the manufacture are as shown in Figure (3-12) and Table (3-2).

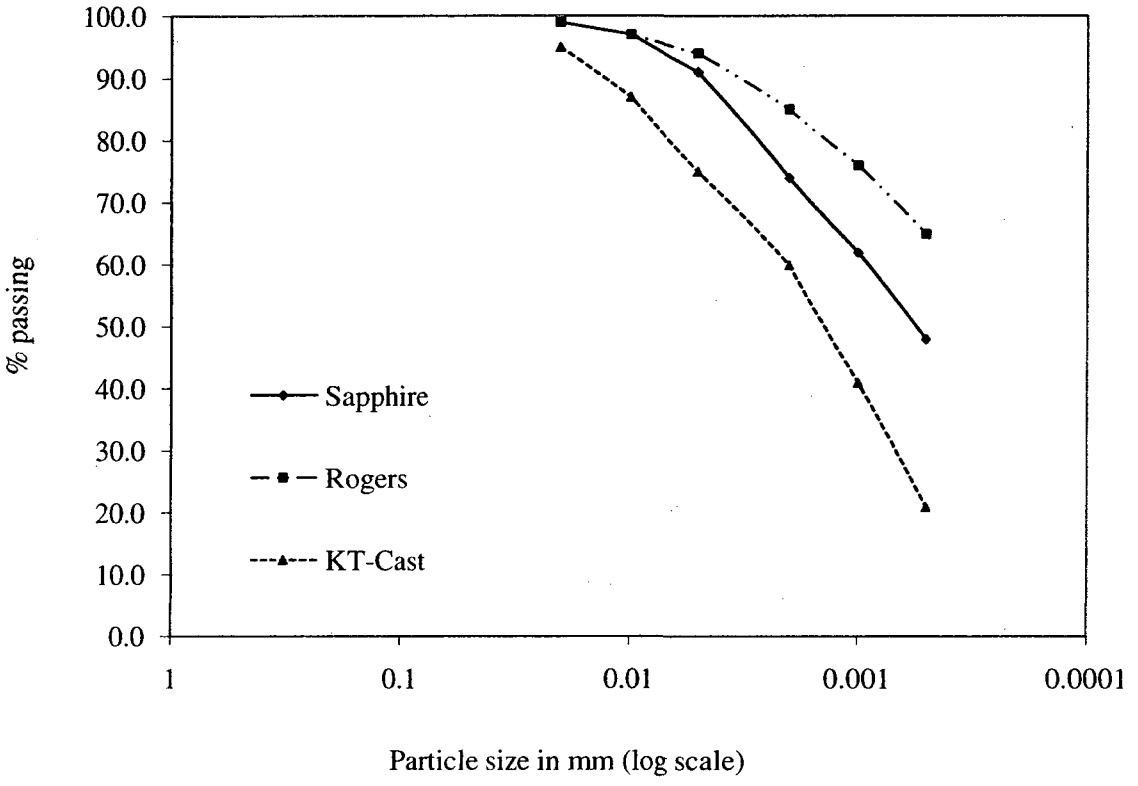

Figure (3-12): Particle size distribution for different Kaoline types

Table (3-2): Chemical analysis and Physical properties for different types of Kaoline

Chemical analysis	**KT-Cast**	**Sapphire**	**Rogers**
% SiO_2	45.1	46.3	46.5
Al_2O_3	38.8	38.2	37.5
Fe_2O_3	0.4	0.7	1
TiO_2	1.6	1.4	1.3
CaO	0.1	0.2	0.3

MgO	0.1	0.2	0.3
K_2O	0.1	0.2	0.2
Na_2O	0.1	0.1	0.1
Carbon	0.03	0.08	0.1
Sulfur	0.03	0.1	0.13
Physical properties	**KT-Cast**	**Sapphire**	**Rogers**
Dry Modulus of rupture psi	225	650	950
Surface area, m^2/g	12	22	24
pH	5.5	5	4.5

3.3.1.3. Collapsible soil

Following ASTM-D 5333-03 (2003), comprehensive parametric study was carried out to establish a procedure for producing collapsible soils at the laboratory with different collapse potentials. To achieve the most effective mixing percentages that give the required collapse potentials, parameters such as; Kaoline type, Kaoline percentage, water content and compaction energy were examined.

The effect of Kaoline type on the collapse potential of the soil was investigated by mixing a constant percentage (15%) of each type of Kaoline (KT-Cast, Sapphire and Rogers) with Tech-mix sand at constant water content of 5%. The mix was then placed and compacted in the oedometer ring in three layers by means of a 100 gm weight falling from 200mm height and for 10 blows. Figure (3-13) presents the results of the oedometer tests. The trend of the Kaoline type effect on the collapse potential is given in Figure (3-

14), which shows that collapsible soil formed by mixing the Kaoline type commercially known as Rogers with sand produces the highest collapse potential on the three mixes.

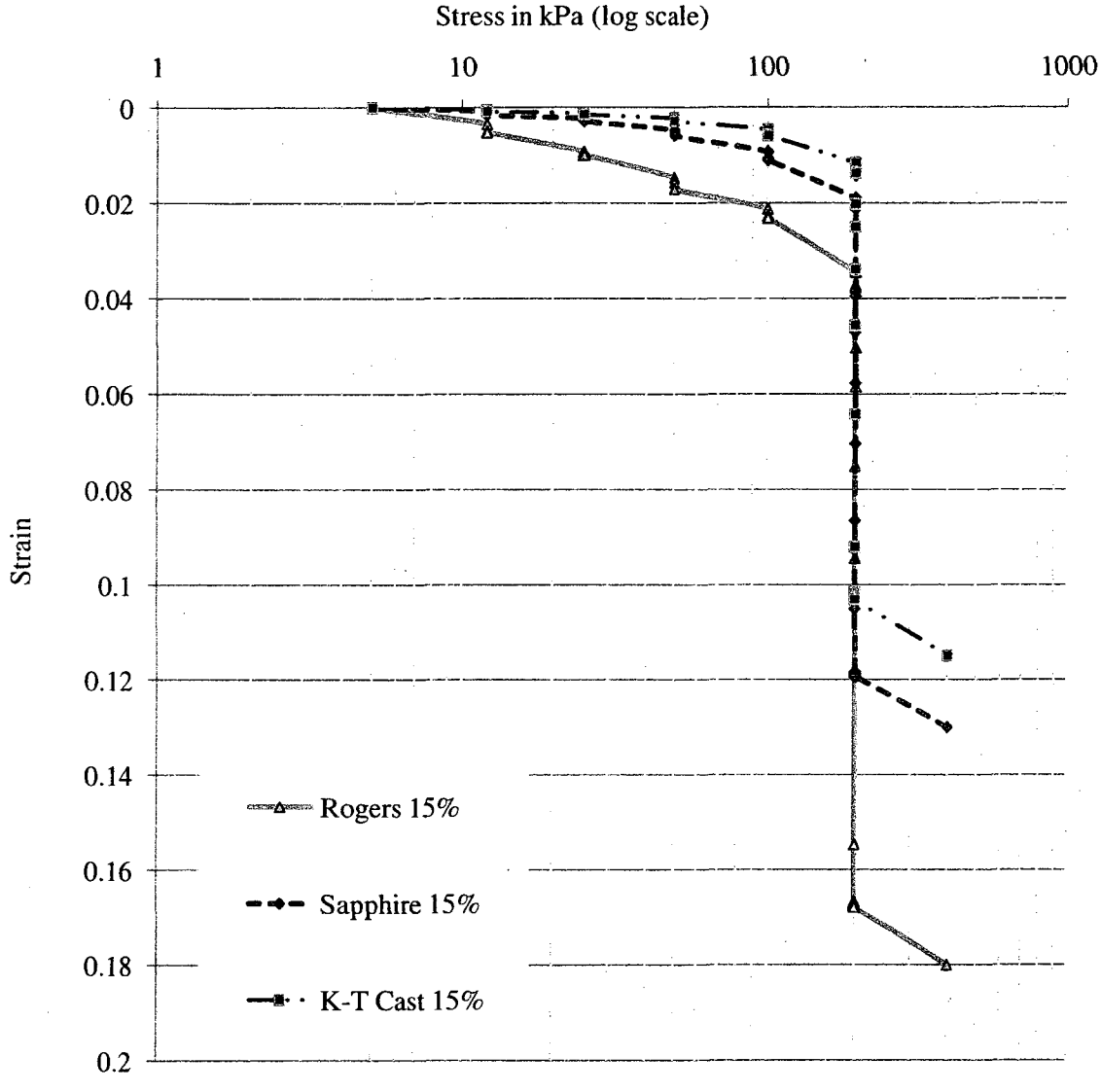

Figure (3-13) Oedometer test results for 15% Kaoline percentage for different Kaoline types under constant compaction energy and constant water content

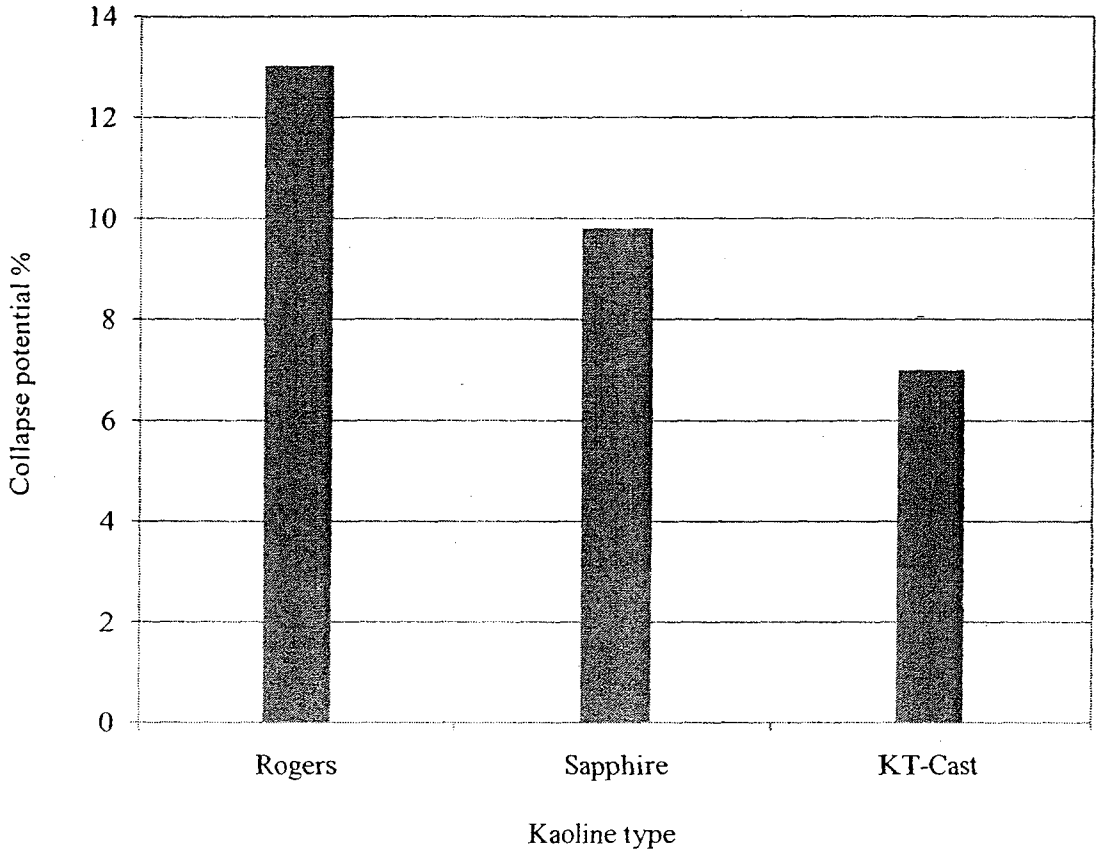

Figure (3-14): Kaoline type versus collapse potential for 15% Kaoline content, 5% water content and constant compaction energy

Another series of tests were carried out to investigate the effect of varying the Kaoline percentage on the collapse potential of the mix. All the three types of tested Kaoline were used, water was added to the mixes at 5% by weight and soils were compacted in the consolidation ring in three layers by 100 gm weight falling from 200mm for 10 blows. Results of this series of oedometer tests are shown in Figure (3-15). It can be noted from this Figure that for any Kaoline percentage at the mix, Rogers type produced the highest collapse potentials for the tested soils.

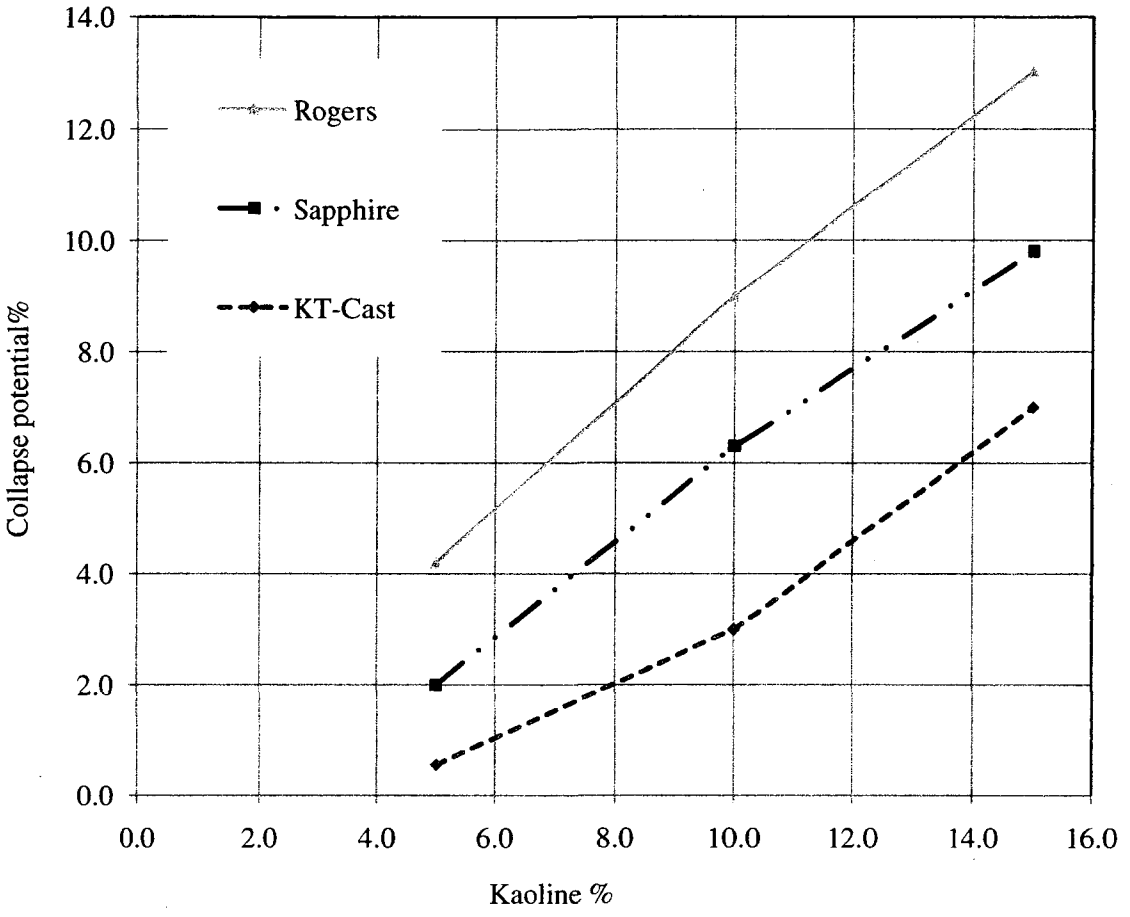

Figure (3-15): Kaoline percentage versus collapse potential for different Kaoline types

From these series of tests with various Kaoline types, and as there is limitation for the maximum percentage of Kaoline for the soil not to swell (Adnan and Edril, 1992), it can be noted that using Kaoline type commercially known as Rogers, within reasonable percentages, allowed the achievement of a wide range of collapse potential that represents variety of field cases. For this reason, the effect of compaction energy was studied on samples resulted from mixing sand with different percentages of Rogers. This parameter was investigated by changing the number of the drops on each of the three soil layers in the consolidation ring while the height of the drops was kept constant at 200mm.

Water content was constant at 5% by weight. The results are shown in Figure (3-16) from which it can be noted that for all soils tested having different Rogers percentages collapse potential decreases due to an increase of the compaction energy.

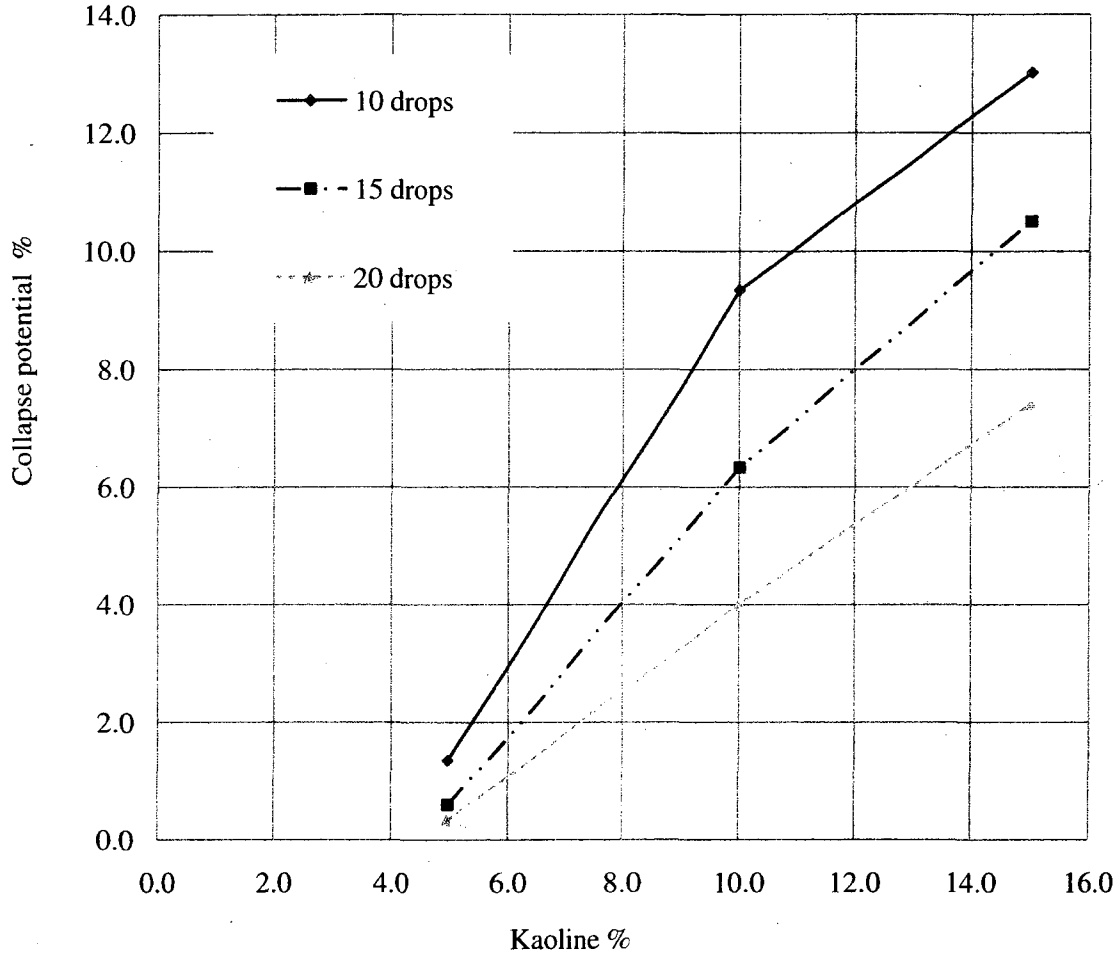

Figure (3-16): Compaction energy versus collapse potential for different percentages of kaoline (type Rogers)

To examine the effect of water content on collapse potential; Rogers Kaoline was used at a constant percentage (10%) and the compaction energy was kept constant for the three soil layers in the consolidation ring (8 drops by 100gm falling from 150mm). Figure (3-17) presents these results. It can be seen from this Figure that the collapse potential was decreased sharply due to increasing the water content, especially in the range between 5% to 7% water content, after that the rate of decreasing the collapse potential decreases.

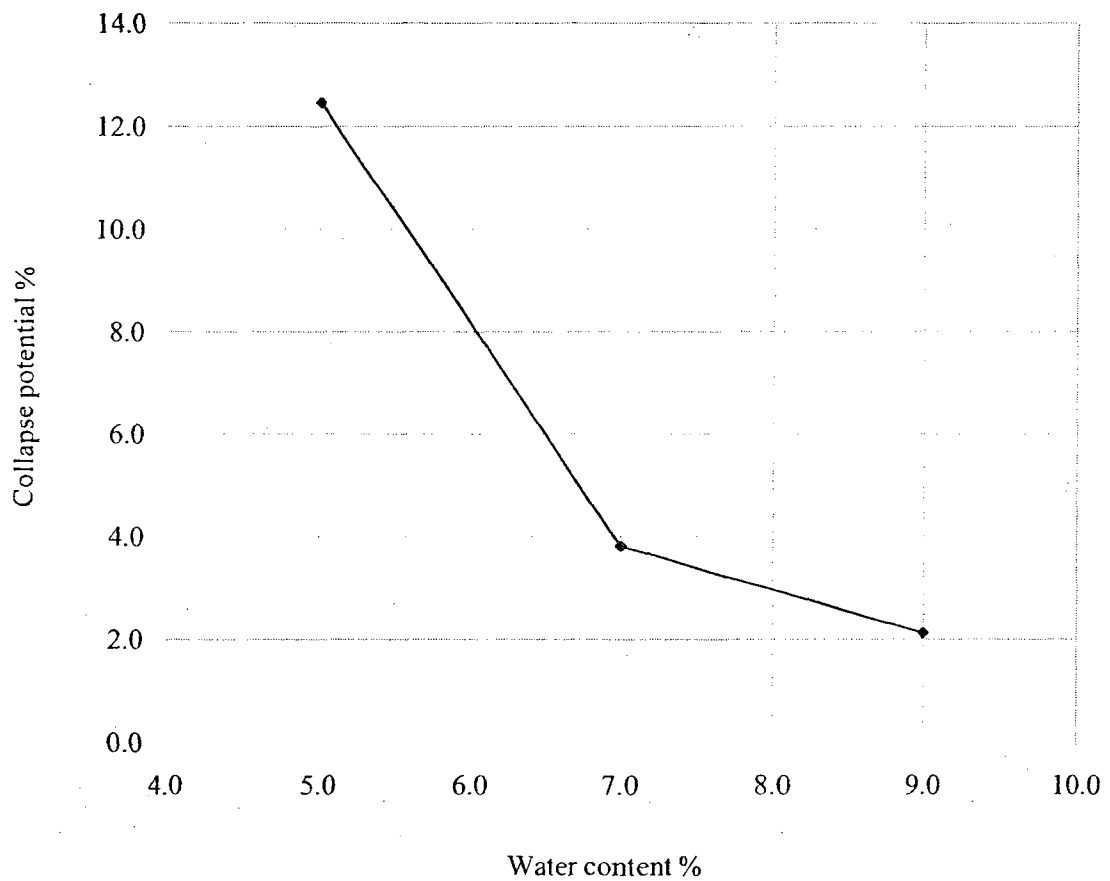

Figure (3-17): Water content versus collapse potential for constant clay content and constant compaction energy

From tests carried out on different mixes of sand and Kaoline with varying different parameters that affect the collapse potential and the performance of the collapsible soil, it was chosen then to mix the Tech-mix sand with Rogers in different percentages (6, 8, and 10%), constant water content (5%) and constant compaction energy (8 drops by 100 gm falling from height 150mm) in the oedometer test to gain average collapse potentials of 4.2% (soil A), 9% (soil B), and 12.5% (soil C) respectively as shown in Figure (3-18).

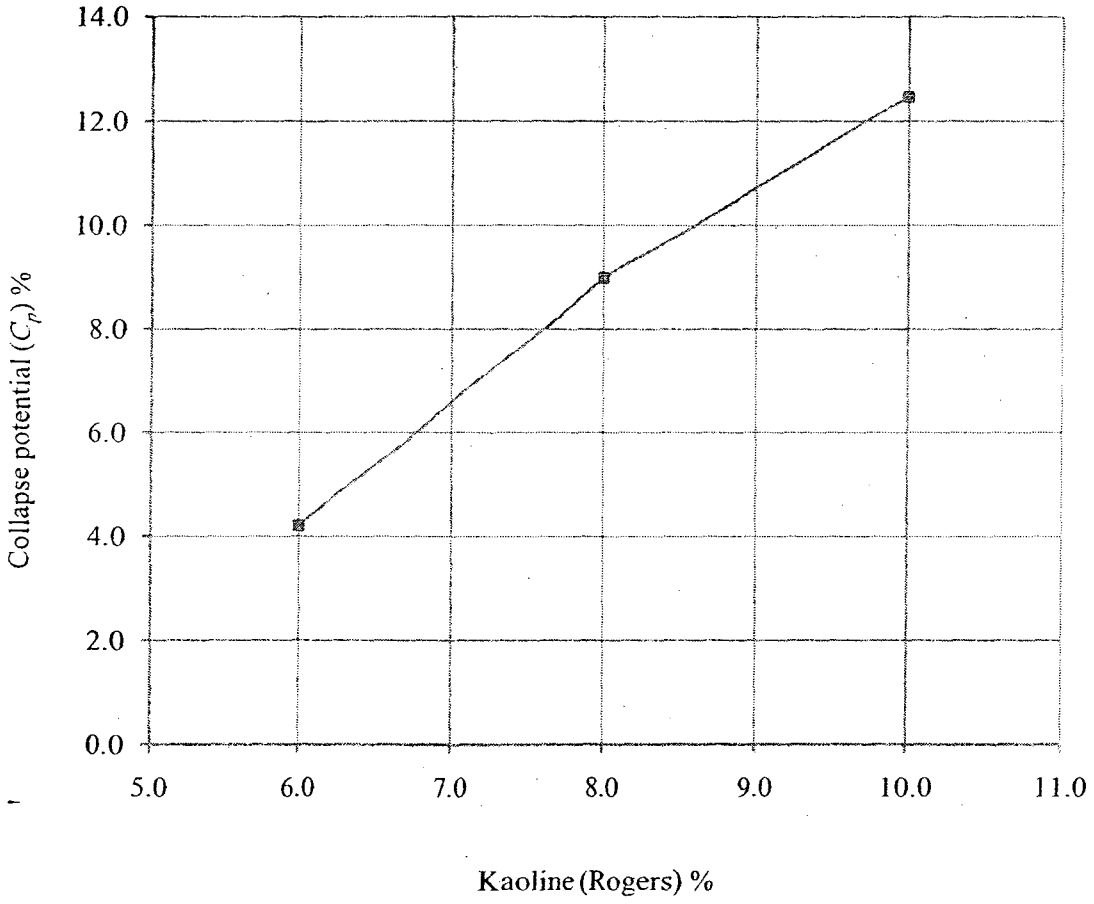

Figure (3-18): Kaoline (Rogers) percentages and the corresponding collapse potentials for the collapsible soils used in this research

For the aforementioned mixes with 6, 8 and 10% Rogers, three repeated oedometer tests were carried out for each Kaoline percentage to confirm the obtained values of the collapse potential. The sample mean, standard deviation and Coefficient of variance for each soil were computed by the following formulas:

$$\bar{X} = \frac{\sum V}{N} \quad \text{(3-1)}$$

Where,

$\bar{X}$ = sample mean, V = test value, N = Number of tests

$$\bar{\sigma}^2 = \frac{1}{N}(\sum_1^N V^2 - N\bar{X}^2) \quad \text{(3-2)}$$

Where,

$\bar{\sigma}^2$ = sample variance, $\bar{\sigma}$ = standard deviation, $\bar{C}$ = Coefficient of variance is computed as

$$\bar{C} = \frac{\bar{\sigma}}{\bar{X}} \quad \text{(3-3)}$$

Table (3-3) presents the results of the various oedometer tests, the sample mean, standard deviation and Coefficient of variance for each soil.

Table (3-3) indicates that standard deviation of 0.327 to 0.356 was obtained from the oedometer tests, which were carried out on collapsible soils used in these investigation, which is considered to be an acceptable range (Bowles 1984).

Laboratory tests were carried out on these soils to determine basic properties. Results obtained from these tests are summarized in Table (3-4).

Table (3-3): Oedometer test results and statistics

Soil	Rogers %	C_p %	Sample mean $\bar{X}$	Sample variance $\bar{\sigma}^2$	Standard deviation $\bar{\sigma}$	Coefficient of variance $\bar{C}$
A	6	4.6 3.8 4.2	4.2	0.107	0.327	0.078
B	8	8.8 9.5 8.7	9	0.127	0.356	0.04
C	10	12.3 13.0 12.2	12.5	0.127	0.356	0.085

Table (3-4): Collapsible soil properties

Soil property	Soil A (C_p= 4.2%)	Soil B (C_p= 9.0%)	Soil C (C_p= 12.5%)
Unit weight in kN/m^3	16.28	16.25	16.2
Maximum unit weight kN/m^3	18.05	18.3	19.25
Optimum water content (w_{opt}%)	12.6	12.25	12
Cohesion (C) in kPa	9	12.5	15.5
Angle of internal friction (φ)	40	38.5	35

Liquid limit (w_L)	-	9.2	15.9
Plastic limit (w_P)	N.P.	N.P.	13.35
Plasticity index (PI)	-	-	2.55
Coefficient of uniformity (C_u)	4	5.4	21.9
Coefficient of curvature (C_c)	1.27	1.65	6.47
Soil classification (unified) AASHTO	SP-SM A – 3	SP-SM A – 3	SP-SM A – 2 – 4
Specific gravity (G_s)	2.66	2.67	2.67
Clay %	6	8	10

3.3.2. Geosynthetic materials

3.3.2.1. Geotextile

Geotextiel, commercially known as (Texel Geo-9), was used in this study. It is a reinforcement geocomposite made of polypropylene fibers. In this research, the Geo-9 was placed at the interface between the collapsible soil and the granular material (sand). The role of this reinforcing material is to distribute the tension received from the soil over greater surface area.

Stress-strain relationships in addition to the geotextile technical data sheet, provided by the manufacture, are presented in Figure (A-1) and Table (A-1) in the Appendix respectively.

3.3.2.2. Geogrid

Geogrids, commercially known as (BX1100) and manufactured by Tensar Corporation, was used as reinforcing material to reinforce the upper replaced soil layer. Technical data sheet and specifications and Stress-strain relationship in machine direction and transverse direction provided by the manufacture are presented in Table (A-2) and Figure (A-2) in the Appendix respectively.

3.4. TEST PROCEDURES

1. A layer of coarse silica sand was placed and slightly compacted at the bottom of the testing tank to allow even and uniform distribution of water throughout the collapsible soil during inundation.
2. The laboratory prepared collapsible soil was prepared by mixing Tech-mix dry sand with three different percentages of Rogers Kaoline Clay. Sand and Kaoline are mixed dry first in a mortar mixer. The mixing dry procedure ensures that Kaoline and sand are thoroughly mixed. 5% water by weight is added to the mix and all are mixed together for additional period of time.
3. The previously prepared collapsible soil was placed, spread and leveled in the test tank in layers, each of 50mm by means of the spread device described in section (3.2.4). Each two layers (total height of 100mm) are compacted by means of the dropping weight. The resulting energy was the same as the one used in the oedometer test to ensure having the same collapse potential for the soil tested. The height of each compacted layer reaches 75mm with a resulting unit weight of 16.28, 16.25, and 16.2 kN/m^3 for soils A (4.2% C_p), B (9.0% C_p) and C (12.5%

C_p) respectively. These steps are repeated until reaching the desired collapsible layer depth (d_c).

4. In case of tests on homogenous collapsible soil, the collapsible soil was placed in 6 layers till reaching a height of 450mm.
5. In case of tests where the compacted sand layer was to partially replace the collapsible soil, the collapsible soil placement was stopped at the predetermined depth and a geotextile sheet (Geo-9) is / is not placed at the interface between the collapsible soil and the compacted sand depending on the test series that is carried out. When the geotextile sheet is placed, it has the length and width of the test tank and is placed to cover the whole contact area between the two layers.
6. Sand was mixed with the optimum water content in the mortar mixer then placed, spread, leveled and compacted with the same compaction method mentioned in step 3 reaching relative density of 80% and a unit weight of 17.5 kN/m^3.
7. For tests using geogrid within the upper sand layer, it is placed at the predetermined depth (d_g).
8. When reaching the desired depth of the soil in the test tank, the footing is placed and centered; LVDTs and load cell are installed in place and connected to Data Acquisition System, which is connected to a computer to record the load applied on the footing and the settlement of the footing.
9. Load is applied on the footing in increments of 20 kPa and the corresponding settlement was constantly recorded. Load increments were applied when the settlement readings are less than 0.01mm.

10. For tests on dry homogeneous collapsible soils, load-settlement curves are obtained and the ultimate load (q_u), for each soil used, is determined.
11. For tests on saturated soils, load increments continue till reaching the predetermined inundation stress. Settlement for this load is recorded till the settlement readings are less than 0.01 mm and then water is introduced to the soil from the bottom of the test tank, in a slow rate controlled by a valve, simulating the case of ground water rise while the applied load is kept constant. This procedure is continued till the whole soil is fully saturated and that is confirmed by observing the water appearing on the surface of the soil in the tank. Load and settlements are recorded for the following 24 hours.

3.5. PRELIMINARY TESTS

Two Series of preliminary tests were carried out prior to the investigation of the main parameters on the test program as follows:

3.5.1. Effect of compaction energy on the collapsible soil performance:

The main objective of these tests is to ensure that the collapsible soil mixes obtained from section (3.3.1.3) with specific properties will perform in the same manner when mixing, placing and compacting with the same energy in the testing tank. Also, these tests were carried out to investigate the effect of changing the compaction energy on the performance of the collapsible soil tested in the testing tank. Three tests were carried out on a mix of 90% sand, 10% Rogers and 5% water content. Soil was spread and compacted in layers with the similar thickness for the three tests. Compaction energy was changed in each test by changing the number of drops and keeping the weight constant or by changing the weight and keeping the number of drops constant or changing the height

of dropping the compaction weight. The resultant load – settlement relationships are in Figure (3-19).

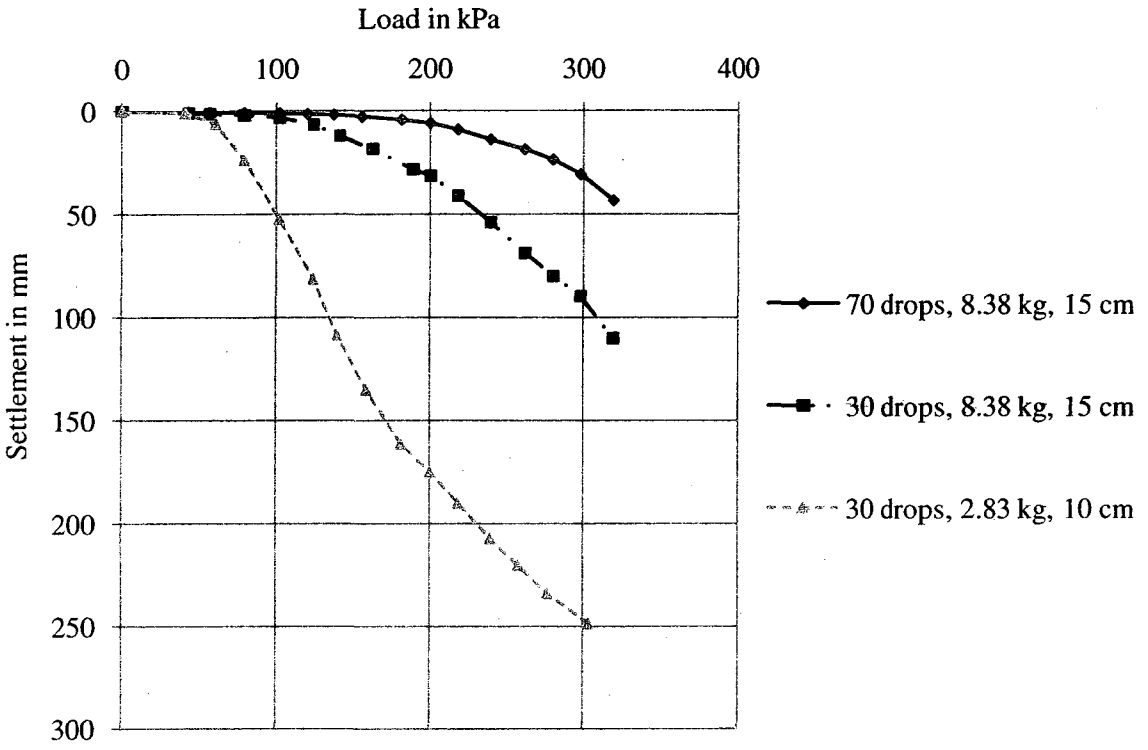

Figure (3-19): load-displacement curves for collapsible soils having 10% Kaoline (Rogers) and compacted at different compaction energies

Results in Figure (3-19) show that the compaction energy (unit weight and relative density) has great effect on the settlement that the collapsible soils experience in their initial moisture content i.e. the ultimate load that they can carry. Samples from collapsible soil compacted by 8.38 kg falling weight from 15cm for 70 drops (same compaction energy / cm^3 as soil C in table 3-4) were tested to obtain the collapse potential and the unit weight and compare them to the properties obtained from oedometer test and they were in good agreement.

3.5.2. Repeatability of test setup:

Prior to starting the test program, it was essential to ensure the repeatability of the test setup by conducting some tests under the same conditions and checking the variation in the results between these tests. One of these comparisons was between two tests that were carried out on a mix of 90% sand, 10% Rogers and 5% water content. Soil was placed in the test tank and compacted in layers (10 cm each) with constant weight (2.83 kg) falling from specific height (10 cm) for constant number of blows (70 drops). The resulting dry unit weight of the collapsible soil was 12.28 kN/m^3. Figure (3-20) shows the load – settlement relationship for these two tests. The two curves are almost identical, which means that the results obtained from the experimental setup are repeatable.

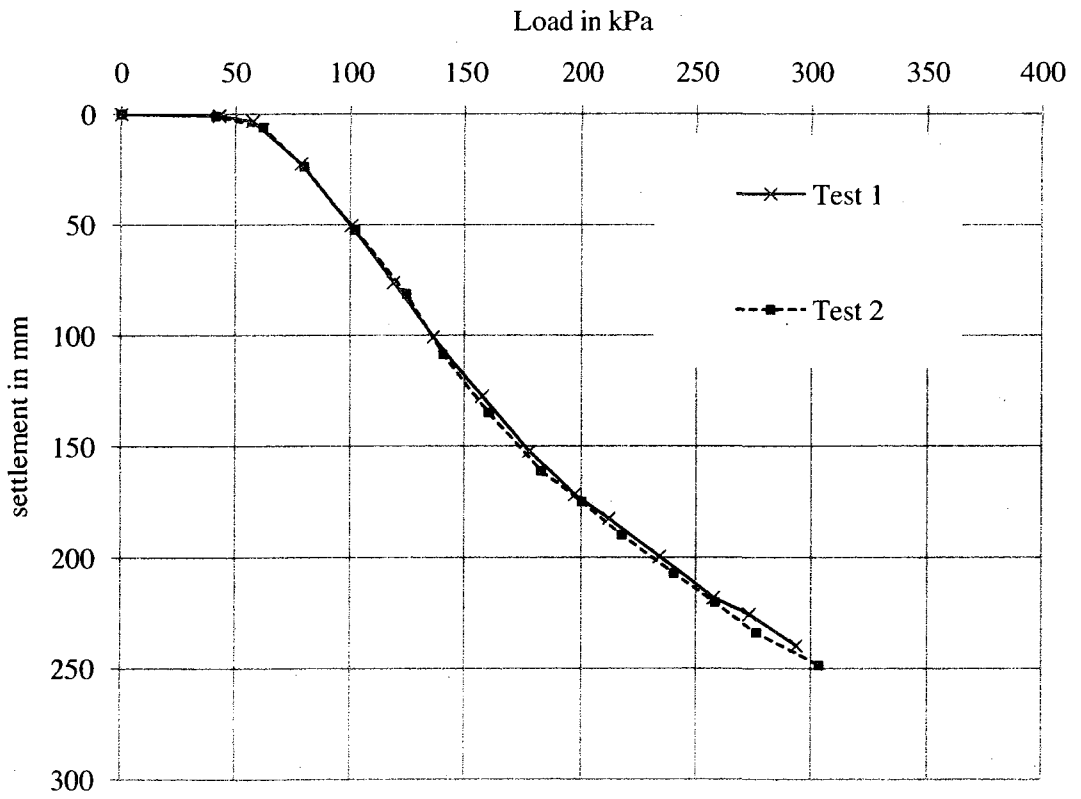

Figure (3-20): load versus footing settlement for repeatability tests

3.6. TEST PROGRAM

Parameters considered in this investigation are:

1. Collapse potential (C_p), varied between 4.2%, 9.0 % and 12.5% to have the variation of the severity of the problem from moderate to severe and to cover wide practical range of collapsibility.
2. Collapsible soil depth ratio (d_c/B), varied between 4, 5 and 6.
3. Inundation stress (σ), varied from ($q_u/4$) to ($q_u/2$).
4. Compacted sand layer thickness ratio (d_s/B), varied between 0 (homogeneous collapsible soil), 1, 2 and 3.
5. Geogrid layer depth ratio (d_g/d_s), varied between 0.3 and 0.7.
6. Geogrid layers number as one or two layers of geogrid are used.

Figure (3-21) presents a sketch for the testing tank showing the parameters considered in this investigation. The test program is presented in Tables (3-5, 6, 7 and 8)

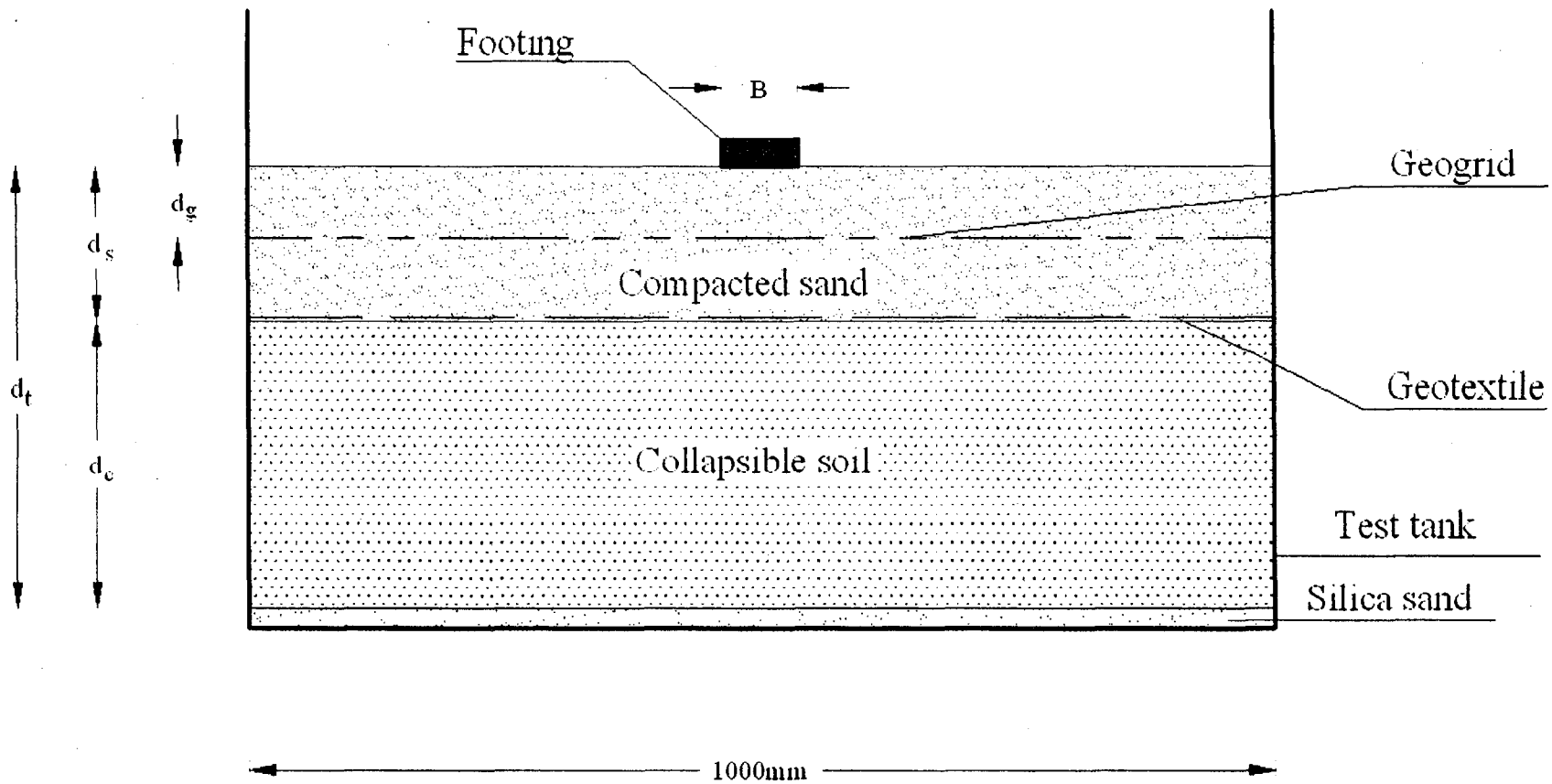

Figure (3-21): Sketch for the test tank showing the studied parameters

Table (3-5): Test program for homogeneous collapsible soils (series I)

Series	Tests No.	Soil type	Degree of saturation	Collapsible soil depth (d_c)	Inundation stress (σ) kPa	Total soil depth (d_t)	Collapse settlement (mm)
I	1	A	Initial W_c	*6B*	-	*6B*	-
	2	B	Initial W_c	*6B*	-	*6B*	-
	3	C	Initial W_c	*6B*	-	*6B*	-
	4	A	Initial W_c then inundated	*4B*	125	*4B*	187.05
	5	A	Initial W_c then inundated	*5B*	125	*5B*	234.88
	6	A	Initial W_c then inundated	*6B*	125	*6B*	280.78
	7	B	Initial W_c then inundated	*6B*	125	*6B*	282.84
	8	C	Initial W_c then inundated	*6B*	125	*6B*	284.81
	9	C	Initial W_c then inundated	*6B*	140	*6B*	290.53
	10	C	Initial W_c then inundated	*6B*	180	*6B*	307.51

Table (3-6): Test program for partially replaced collapsible soils (series II)

Series	Tests No.	Soil type	Collapsible soil depth (d_c)	Sand thickness (d_s)	Collapse settlement (mm)
II	1	A	*5B*	*1B*	240.02
	2	A	*4B*	*2B*	250.58
	3	A	*3B*	*3B*	261.47
	4	C	*5B*	*1B*	246.67
	5	C	*4B*	*2B*	261.90
	6	C	*3B*	*3B*	278.75

- Total soil depth (d_t) was constant and equal to *6B*
- Tests were carried out on soils in their initial moisture content then subjected to inundation at 125 kPa

Table (3-7): Test program for partially replaced collapsible soils reinforced with geotextile (series III)

Series	Tests No.	Soil type	Collapsible soil depth (d_c)	Inundation stress (σ) kPa	Sand thickness (d_s)	Collapse settlement (mm)
III	1	A	*5B*	125	*1B*	66.44
	2	A	*3B*	125	*3B*	163.067
	3	C	*5B*	125	*1B*	109.76
	4	C	*4B*	125	*2B*	192.85
	5	C	*3B*	125	*3B*	228.00
	6	A	*5B*	60	*1B*	47.96
	7	A	*5B*	100	*1B*	51.71
	8	C	*5B*	60	*1B*	70.07
	9	C	*5B*	100	*1B*	79.98
	10	C	*5B*	140	*1B*	slip

- Total soil depth (d_t) was constant and equal to *6B*
- Tests were carried out on soils in their initial moisture content then subjected to inundation at different inundation stresses (σ).

Table (3-8): Test program for partially replaced collapsible soils reinforced with geotextile and geogrid (series IV)

Series	Tests No.	Collapsible soil depth (d_c)	Sand thickness (d_s)	Geosynthetics configuration			Collapse settlement (mm)
				Geogrid depth ratio (d_g/d_s)	Geogrid number	Geogrid spacing	
IV	1	*5B*	*1B*	0.33	2	0.33*B*	98.59
	2	*4B*	*2B*	0.67	2	0.67*B*	72.92
	3	*3B*	*3B*	1	2	1*B*	77.80
	4	*5B*	*1B*	0.3	1	-	105.21
	5	*5B*	*1B*	0.7	1	-	105.63

- Tests were carried out on soil C.
- Total soil depth (replacement layer and collapsible soil) was constant and equal to *6B*.
- Tests were carried out on soils in their initial moisture content then subjected to inundation at 125 kPa.

CHAPTER 4

RESULTS AND ANALYSIS

4.1. GENERAL

A total of 44 model tests were conducted in this investigation. Tests carried out in this research are divided into the following series (Tables 3-5, 6, 7, and 8):

1. Tests on homogeneous collapsible soils (series I).
2. Tests on partially replaced collapsible soil (series II).
3. Tests on partially replaced collapsible soil reinforced with geotextile (series III).
4. Tests on partially replaced collapsible soil reinforced with geotextile and geogrid (series IV).

4.2. HOMOGENEOUS COLLAPSIBLE SOILS (SERIES I)

In this series, tests were carried out on homogeneous collapsible soils and results were used as a reference to establish the benefit of using soil replacement and soil reinforcements. Based on the results obtained from this series an empirical formula is developed to determine the collapse settlement of homogeneous collapsible soil under various site conditions. Parameters studied in this series are: degree of saturation, collapse potential (C_p), collapsible soil depth (d_c), and inundation stress (σ). The details of each of the test groups in this series and the effect of each studied parameter on the collapse settlement of collapsible soils are explained as follows:

4.2.1. Effect of degree of saturation:

The purpose of this group of tests is to determine the ultimate bearing capacity of the collapsible soils used in this research, soils A, B and C (Table 3-4). Tests (I-1, I-2 and I-3) were carried out on collapsible soils in their initial water content (5%); each collapsible soil was prepared and test procedures were followed as in section (3.4) without applying any inundation to the soil. Load – settlement curves obtained from these tests are presented in Figure (4-1). The ultimate bearing capacity was determined at the intersection of the tangents slopes of the load – settlement curve, which ranged from 262 to 268 kPa with a variation of around 2%. This implies that the initial moisture content has no effect on the variation of the kaoline content; consequently on the collapse potential (within the range used) and on the ultimate bearing capacity of the soils tested in this investigation. The deduced settlement can be divided into two parts: the first part where the variation of the footing settlements for the three samples was relatively small and it continued up to a load of 200 kPa. The second part where settlement of the footing on soil A and B was the same but it varies considerably for soil C, and that was up to the load of about 260 kPa (almost the value of the ultimate load). After this stage, footing settlements on soil B and C start getting closer with the increase of the load applied on the footing, while footing on soil A settles dramatically reaching a settlement of more than double the settlement of soil B and C under applied load of 300 kPa.

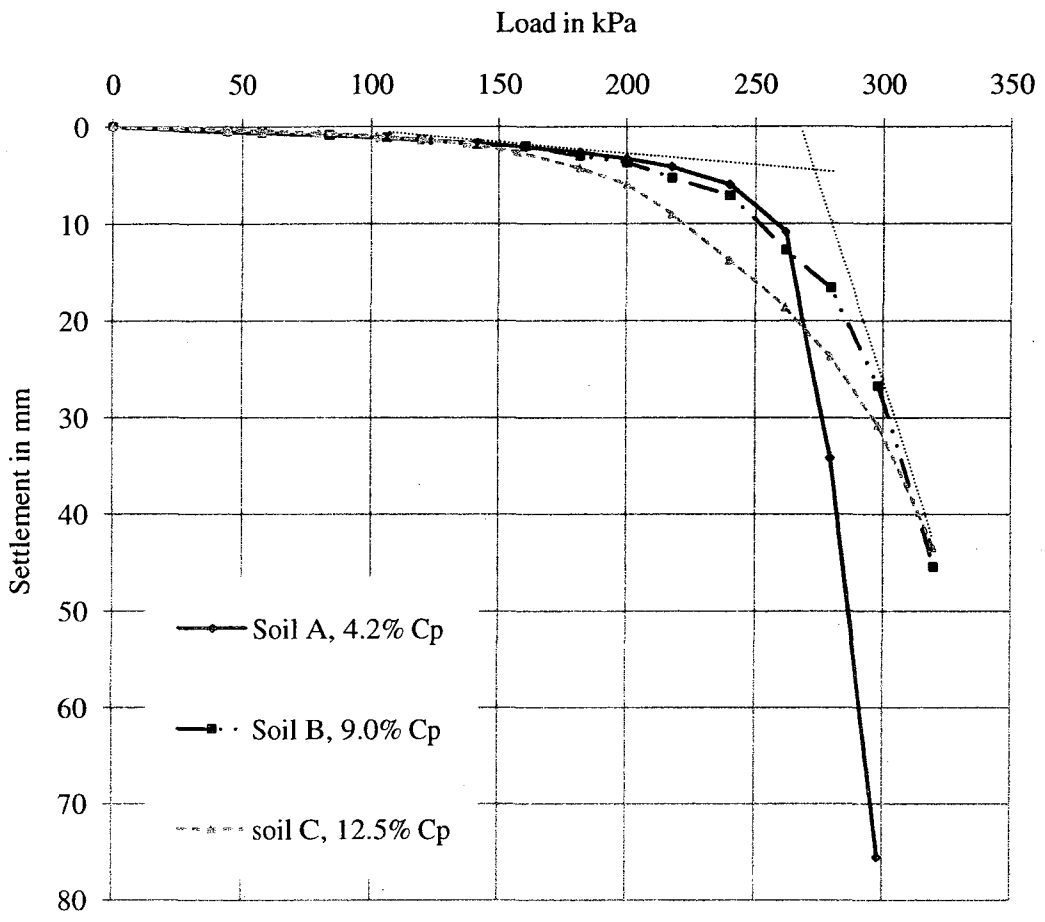

Figure (4-1): Load – settlement curves for different collapsible soils

Another group of tests was carried out when collapsible soils are subjected to inundation (tests I-6, I-7 and I-8). The purpose for this group of tests is to determine the collapse settlement the footing experiences when it is subjected to the design load and experiences inundation resulting from the groundwater rise. These tests were carried out for the different soils used in this research that have different collapse potentials (C_p).

In these tests and for the different collapsible soils, a factor of safety of about 2 is used to determine the design load for these soils (as an average, it was chosen to be 125

kPa). The footing is loaded till reaching the value of the design load and the water is introduced to the soil in a slow rate while the footing is subjected to this load, simulating the case of the groundwater table rise. Test procedures for saturated tests (section 3-4) were followed and relationships between applied load (σ) and the settlement ratio (footing settlement / footing width = Δ_h / B) for the different collapsible soils are drawn and presented in Figure (4-2), which shows that increasing the collapse potential (4.2% for soil A, 9.0% for soil B and 12.5% for soil C) increases the collapse settlement ratio. The variation of collapse settlement versus collapse potential is presented in Figure (4-3).

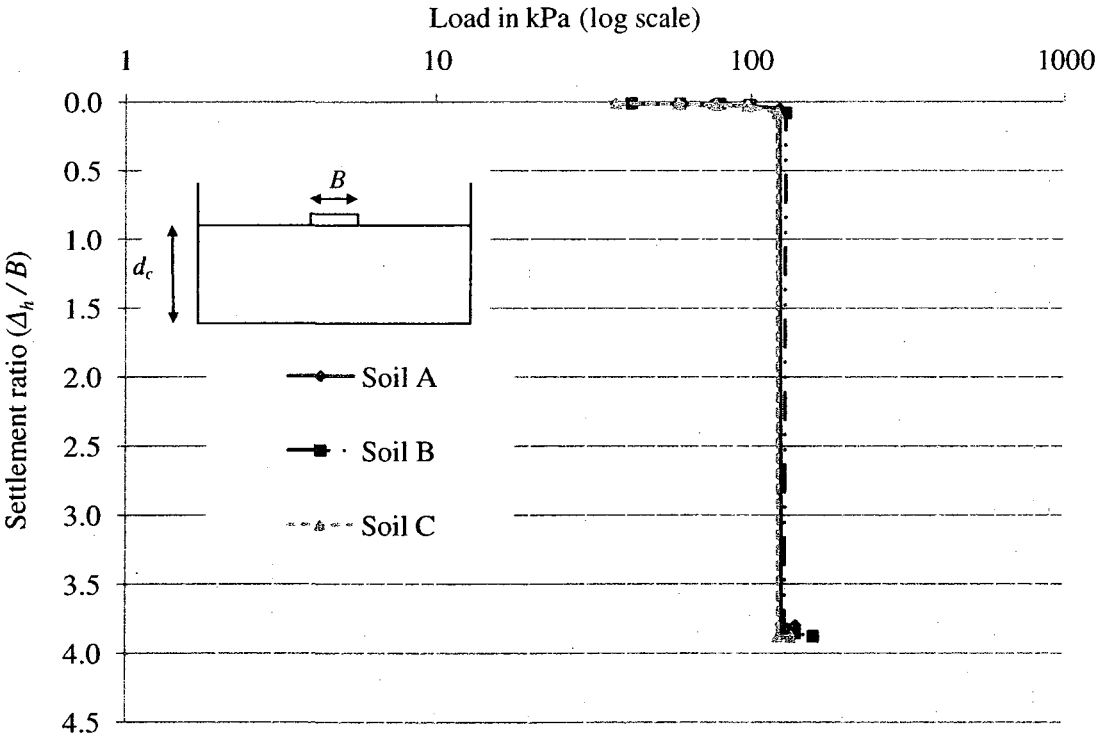

Figure (4-2): Settlement ratio versus applied stress for different collapsible soils (tests I-6, I-7 and I-8)

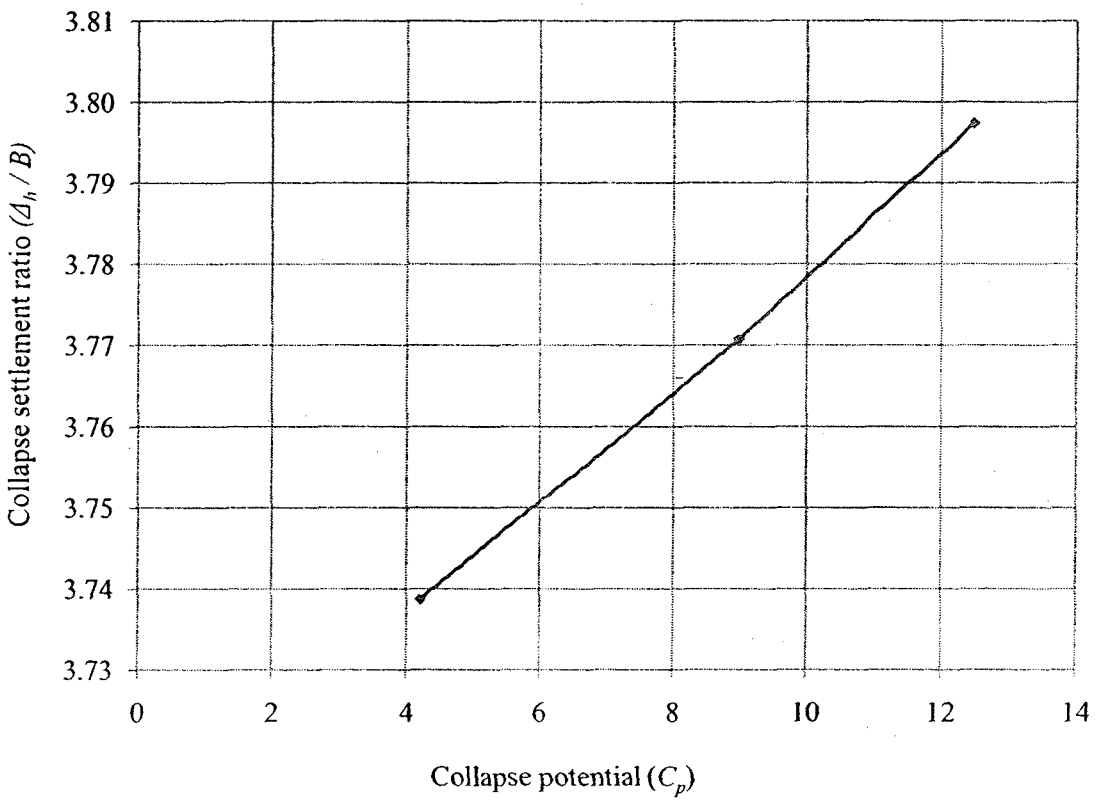

Figure (4-3): Collapse settlement versus collapse potential at 125 kPa inundation stress

The settlements obtained from these tests were expected to be directly proportional to the height of the collapsible soils by the collapse potential values obtained from laboratory oedometer tests. The results obtained showed the same trend but in a smaller scale, which can be related to the differences between the oedometer tests and the experimental setup. Firstly, the variation between the height of the soils in the oedometer tests (20 mm) and the height of the soils in the test tank (450 mm) allows soil particles to rearrange and occupy less space when inundated. Secondly, the soils in the oedometer tests are confined between the ring walls and the porous stone, while in the test tank there is ability for the movement between the footing and the walls of the test tank, which

could give the possibility for more settlement for the footing in the experimental model investigation.

The response of each soil to the wetting process from its natural water content till saturation is different. Two main parameters can be analyzed: the first is the time the soil takes to start the settlement due to the access of water to the soil and the second is the time in which the collapse settlement occurs. As shown in Figure (4-4), soil A with 4.2% collapse potential starts responding to the presence of water in the soil after relatively long period of time but the collapse settlement happens in a short period of time (suddenly). For soil C with 12.5% collapse potential, the response for wetting starts almost immediately and progresses rapidly till certain stage and then continues in a moderate rate till reaching the final collapse settlement. In other words, settlement of collapsible soils with low collapse potential (soil A) starts when the water level reaches certain extent within the soil while for collapsible soils with high collapse potential the settlement starts shortly after the water reaches the soil. This analysis of different collapsible soils response to wetting can be very helpful in avoiding some disasters related to the collapse settlement due to water level increase within collapsible soils.

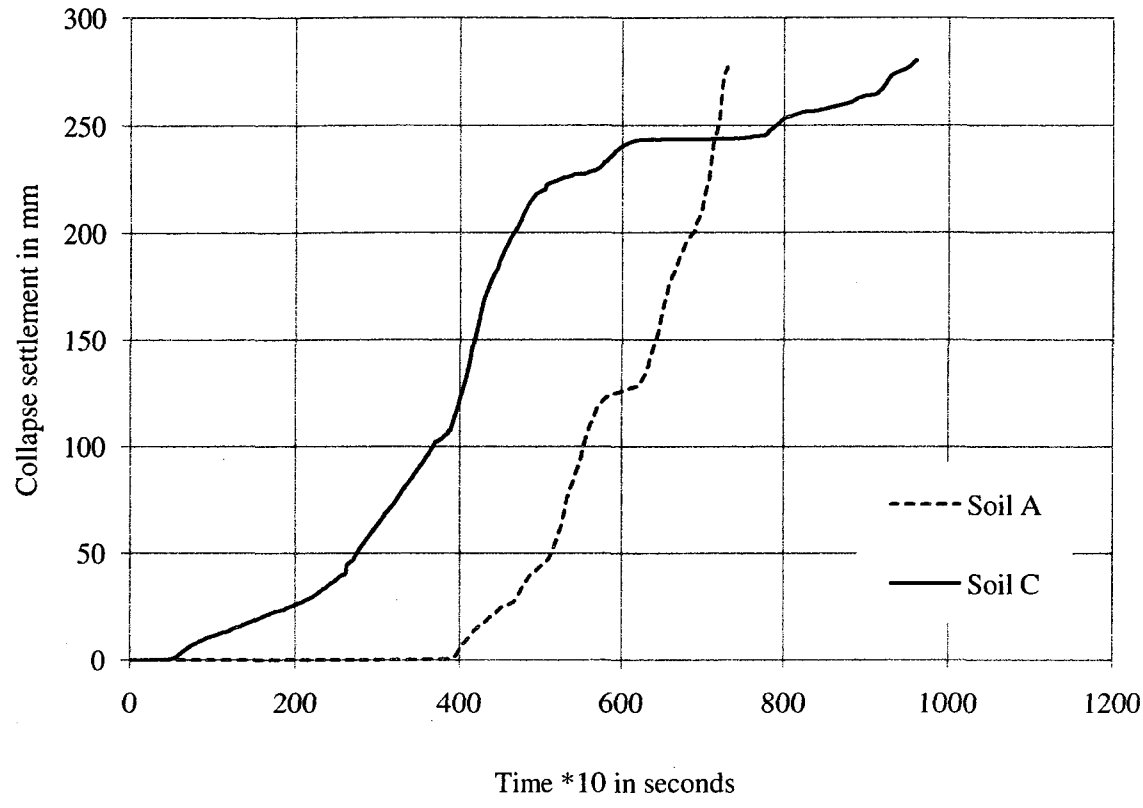

Figure (4-4): Collapse settlement versus time for different collapsible soils

4.2.2. Effect of collapsible soils depth:

In these tests, (I-4, I-5 and I-6), the effect of varying the collapsible soil depth (d_c) was studied. Tests were carried out on soil A (4.2% C_p), 125 kPa inundation stress (σ), and collapsible soil depths of $4B$, $5B$ and $6B$. The results of these tests are given in Figure (4-5).

The effect of the collapsible soil depth on the collapse settlement ratio (Δ_h / B) of the footing concluded from Figure (4-5) is that collapse settlement ratio increases by increasing the collapsible soil depth.

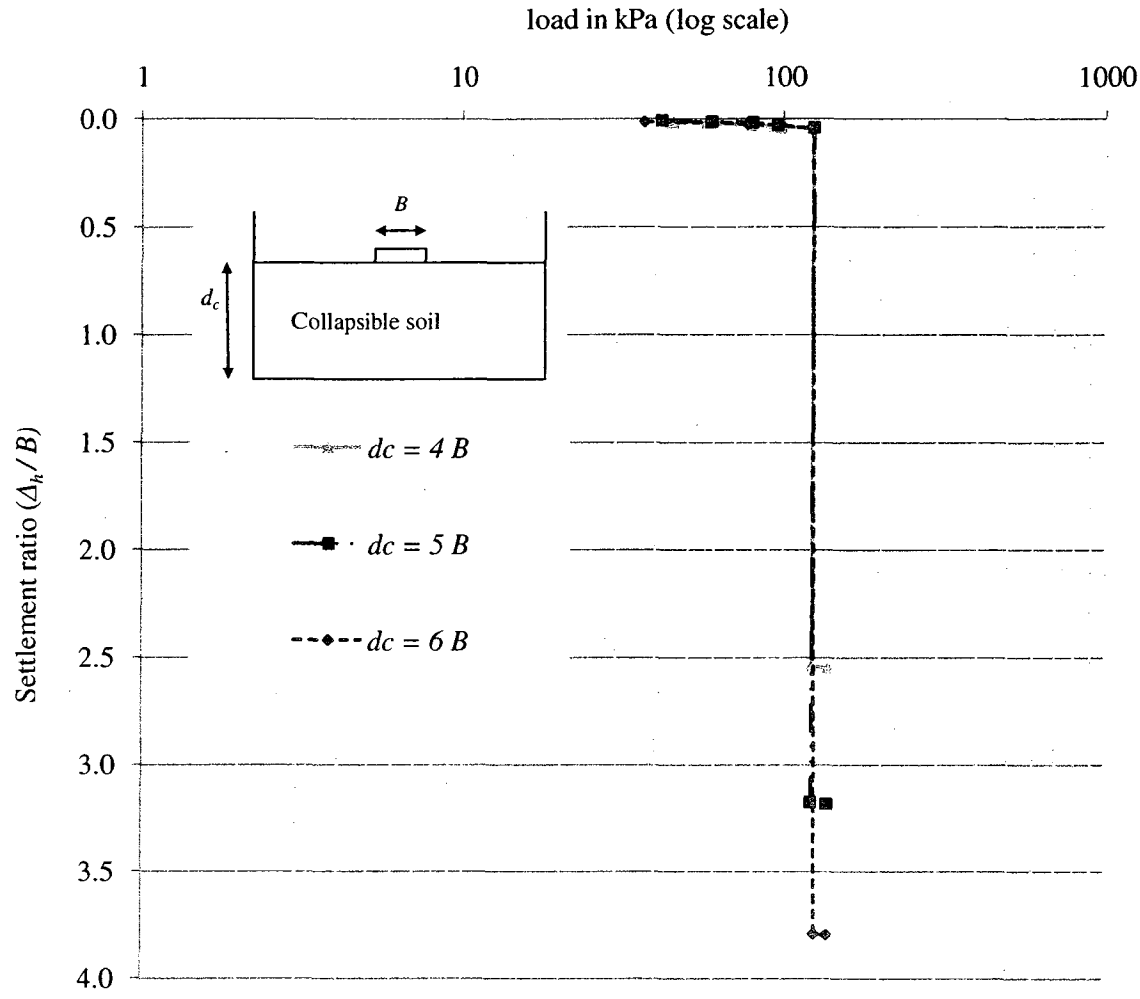

Figure (4-5): Settlement ratio versus applied stress for different depths of collapsible soil A (tests I-4, I-5 and I-6)

This relationship between the collapsible soil depth and the collapse settlement ratio is presented in Figure (4-6) that shows an almost linear relationship between collapse settlement ratio and collapsible soil depth. This means that the collapsible soil depth is a major contributor to the amount that the collapsible soil settles when inundated.

The obtained results were expected as the depth of the collapsible soil is one of the main reasons of the large settlement that this type of soil experiences. For this reason,

when a site has a deep deposit of collapsible soil that will not be economical to remove or the settlement experienced after different mitigation methods is still higher than the allowable limits, the solution of deep foundations might be considered

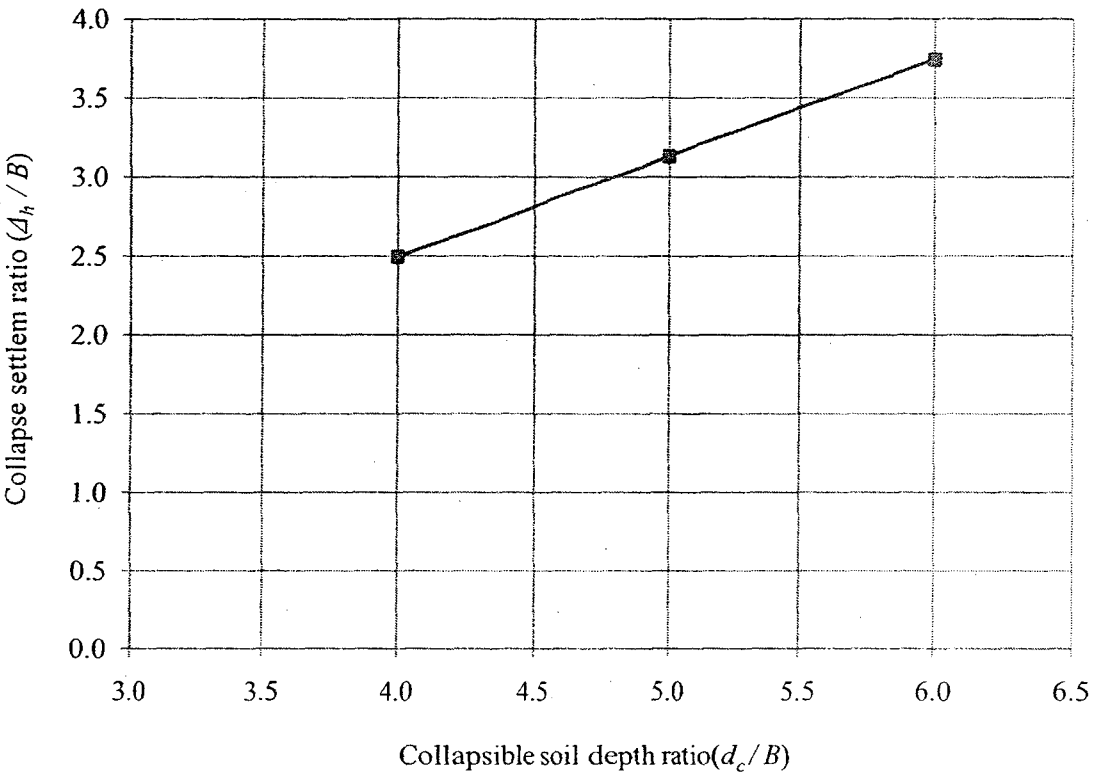

Figure (4-6): Collapse settlement versus collapsible soil depth ratio (soil A)

4.2.3. Effect of inundation stress variation:

These tests concern about the stress acting on the strip footing when the inundation occurs. Tests (I-8, I-9 and I-10) were carried out on collapsible soil C (collapse potential of 12.5%), collapsible soil depth (d_c) is constant and equal to $6B$. The inundation stress was varied between 125, 140 and 180 kPa. Results of these tests are given in Figure (4-7) from which it can be noted that increasing the inundation stress, (σ), increased the collapse settlement ratio (Δ_h / B).

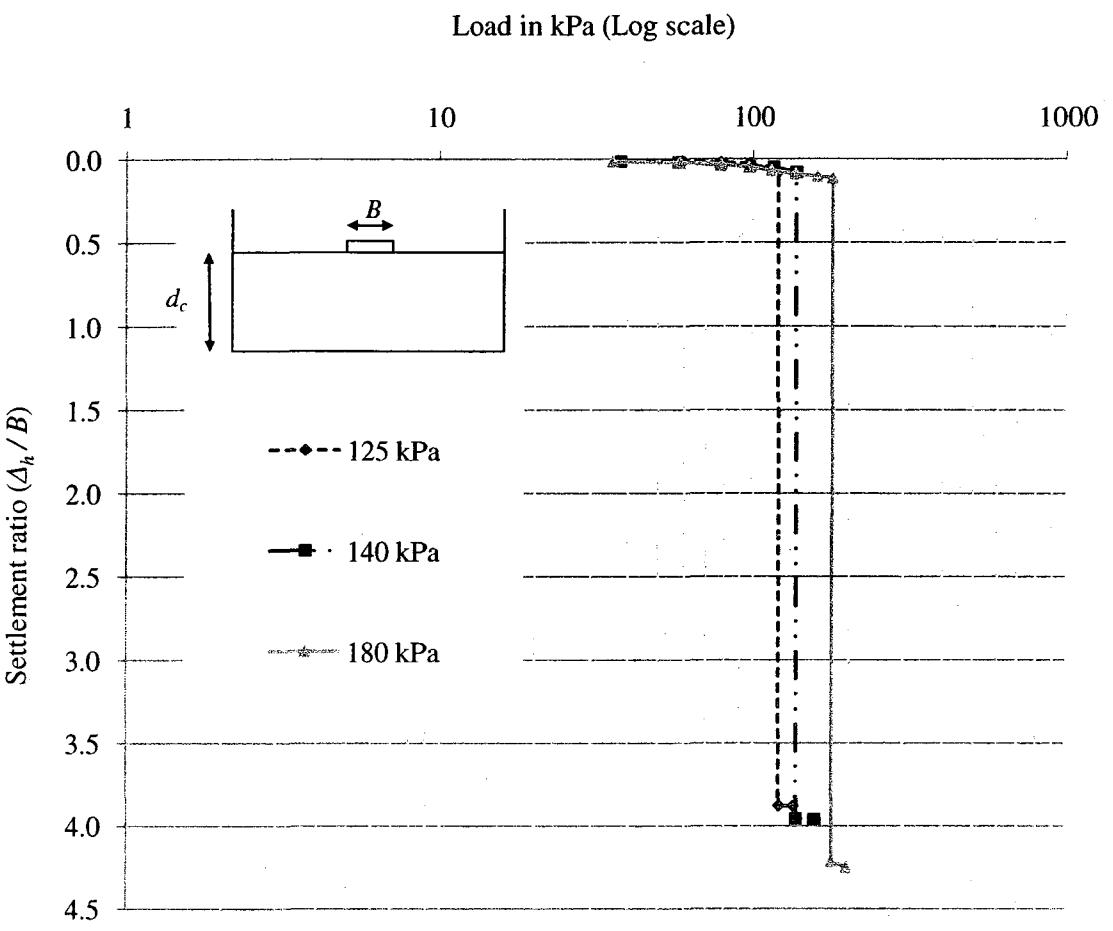

Figure (4-7): Settlement ratio versus applied stress for collapsible soil C at different inundation stresses (tests I-8, I-9 and I-10)

The variation of collapse settlement ratio versus inundation stress is presented in Figure (4-8), which shows that changing the inundation stress has a great effect on the collapse settlement ratio of the strip footing used in this research.

These results were expected as the settlement of footings constructed on different types of soils is highly affected by the load induced on these footings. For the rest of the investigation in this research, the inundation stress will be within the range between q_u / 2 and q_u / 4, where q_u are the ultimate bearing capacities for the different collapsible soils obtained from tests (I-1, I-2 and I-3) described in section 4.2.1 in this dissertation.

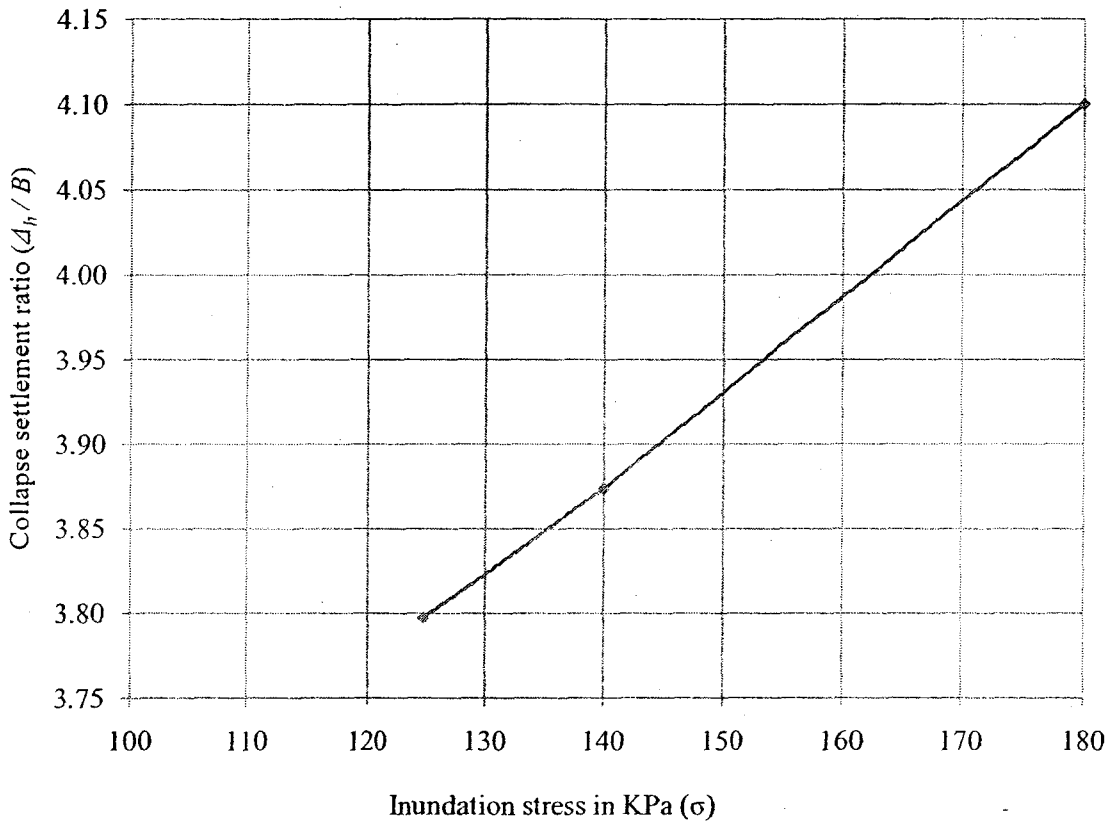

Figure (4-8): Collapse settlement ratio versus inundation stress (soil C)

From the parametric study carried out in these series (series I), an attempt was carried out to develop an empirical formula that allows the geotechnical engineer to determine the expected collapse settlement of strip footing constructed on homogeneous collapsible

soil. The collapse strain for a collapsible soil (ε_c) subjected to stress (σ) while inundation reaching full saturation is related to the soil's collapse potential (C_p) obtained from conventional laboratory oedometer tests under stress ($\bar{\sigma}$) equal to 200 kPa. This relation takes the following form:

$$\frac{\varepsilon_c}{Log\sigma} = a_1 \frac{C_p}{Log\,\bar{\sigma}} + a_2 \quad \text{..... (4-1)}$$

Where:

a_1 and a_2 are constants

(ε_c) collapse strain = Δ_h / d_c,

(Δ_h) collapse settlement for homogeneous collapsible soil

(d_c) collapsible soil depth

(σ) stress acting on the footing in kPa, and

(C_p) soil collapse potential measured at $\bar{\sigma}$ equals to 200 kPa.

From the experimental data collected from tests carried out on various homogeneous collapsible soils having different depths and subjected to various values of inundation stresses, constants a_1 and a_2 can be determined and Formula (4-1) will be:

$$\frac{\varepsilon_c}{Log\sigma} = 0.0011 \frac{C_p}{Log\,\bar{\sigma}} + 0.296 \quad \text{..... (4-2)}$$

As ($\bar{\sigma}$) is equal to 200 kPa, Formula (4-2) can be rearranged as follows

$$\frac{\varepsilon_c}{Log\sigma} = 0.0005C_p + 0.296 \quad \text{..... (4-3)}$$

Formula (4-3) and the experimental results are shown in Figure (4-9).

Knowing the collapse potential form the results of a traditional oedometer test and the stress applied on the footing in the field, the collapse strain can be obtained by using formula (4-3), from which the collapse settlement for homogeneous collapsible soil (Δ_h) can be calculated when knowing the depth of collapsible soil in the site (d_c).

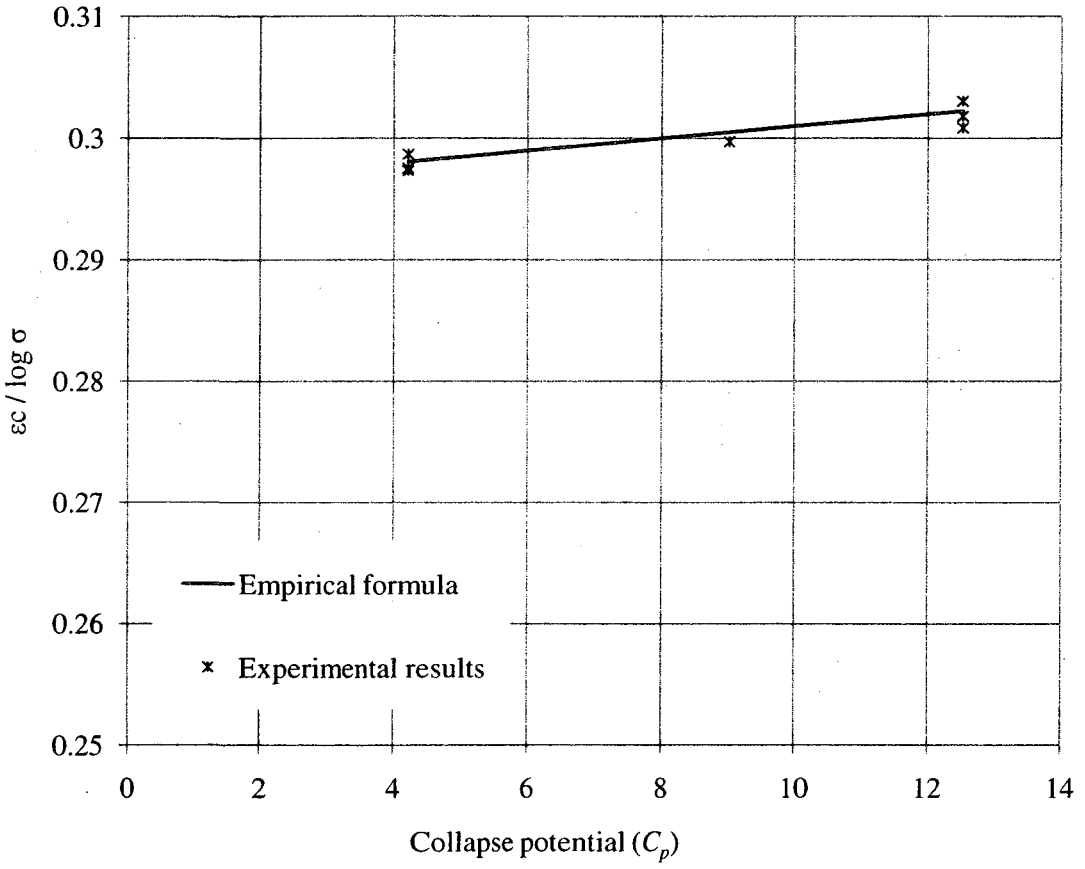

Figure (4-9): Empirical formula versus experimental results

4.3. PARTIALLY REPLACED COLLAPSIBLE SOILS (SERIES II)

In this series of tests, an investigation is carried out to examine the effect of partially replacing collapsible soils by various thicknesses of compacted sand layers on the

reduction of the collapse settlement caused by inundation. The sand used as replacement layer is Tech-Mix sand mixed at 16.5% water content and compacted in the test tank reaching unit weight of 17.5 kN/m^3 and a corresponding relative density of 80%. Compacted sand layer thickness (d_s) is varied between 1B, 2B and 3B. The total soil depth (d_t) was constant and equal to 6B. Tests were carried out on soil A (tests II-1, II-2 and II-3) and on soil C (tests II-4, II-5 and II-6). The results are presented in (Figure 4-10) and (Figure 4-11) respectively.

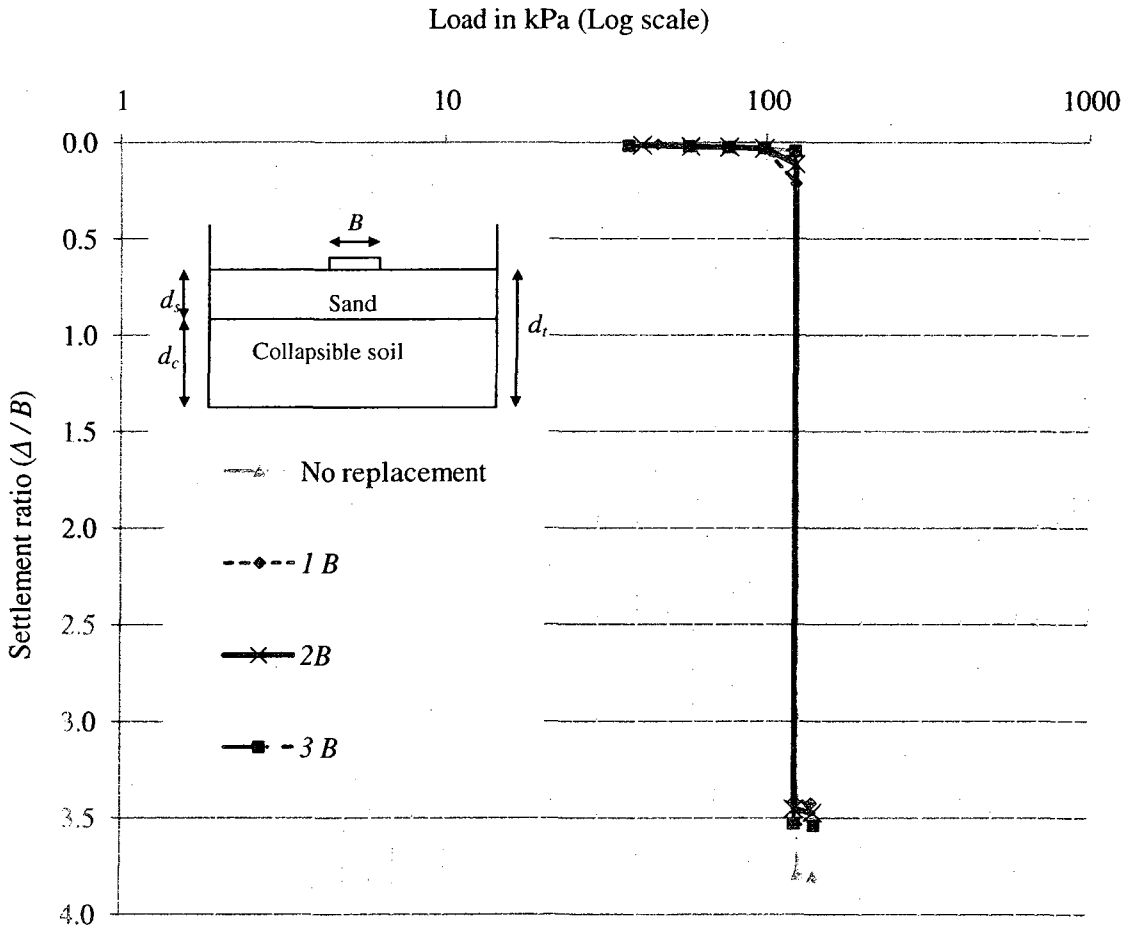

Figure (4-10): Settlement ratio versus applied stress for different replacement thicknesses for collapsible soil A (tests I-6, II-1, II-2 and II-3)

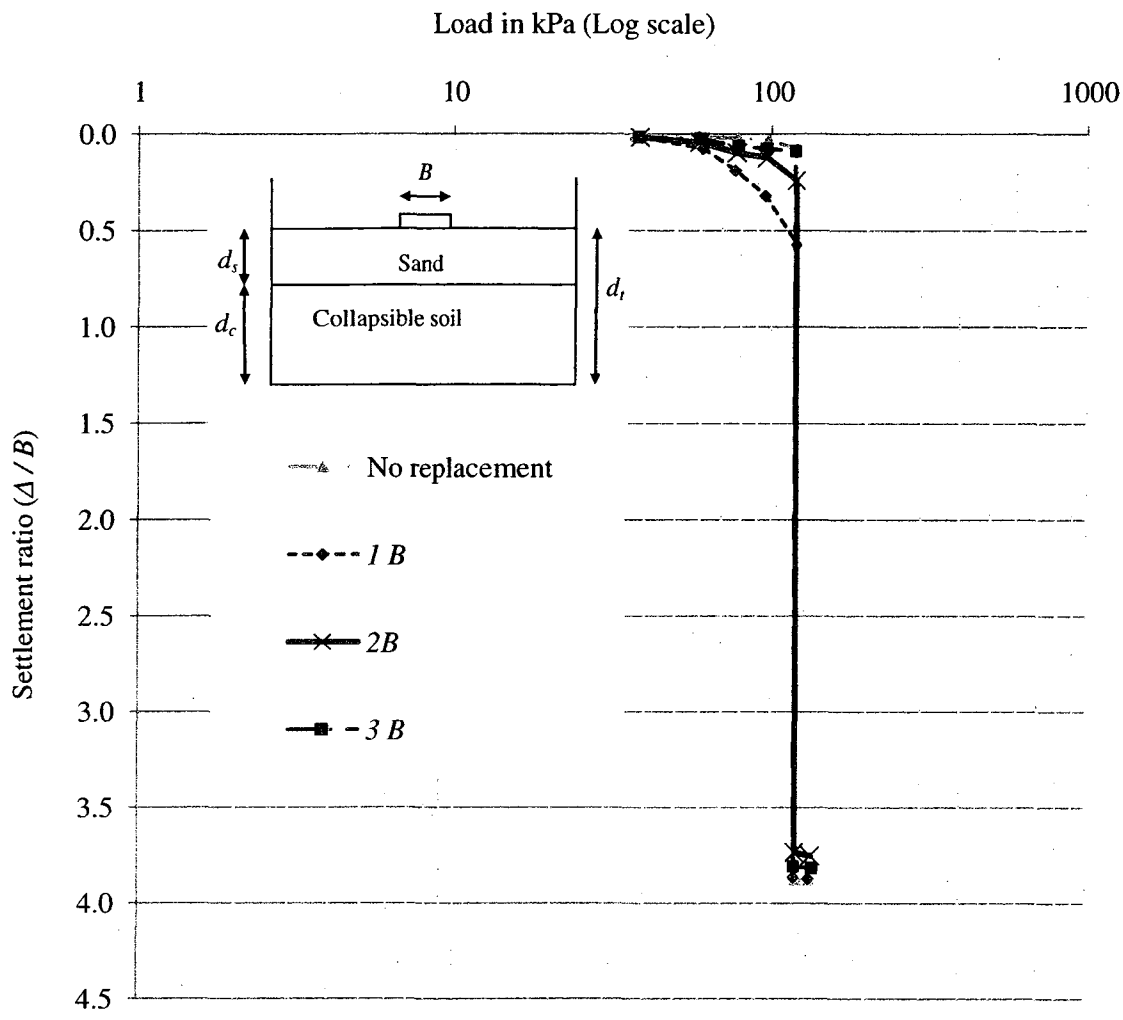

Figure (4-11): Settlement ratio versus applied stress for different replacement thicknesses for collapsible soil C (tests I-8, II-4, II-5 and II-6)

Figures (4-10) and (4-11) illustrate that partially replacing the collapsible soils by compacted sand slightly decreases the collapse settlement. The most effective sand layer thickness that reduced the collapse settlement was equal to $1B$ for both types of collapsible soils tested in this series. On the other hand, results obtained from tests (II-2

and II-5) show that the response for replacing the collapsible soil varies according to the collapse potential. Figure (4-12) shows the case of the replacement thickness equal to *2B*.

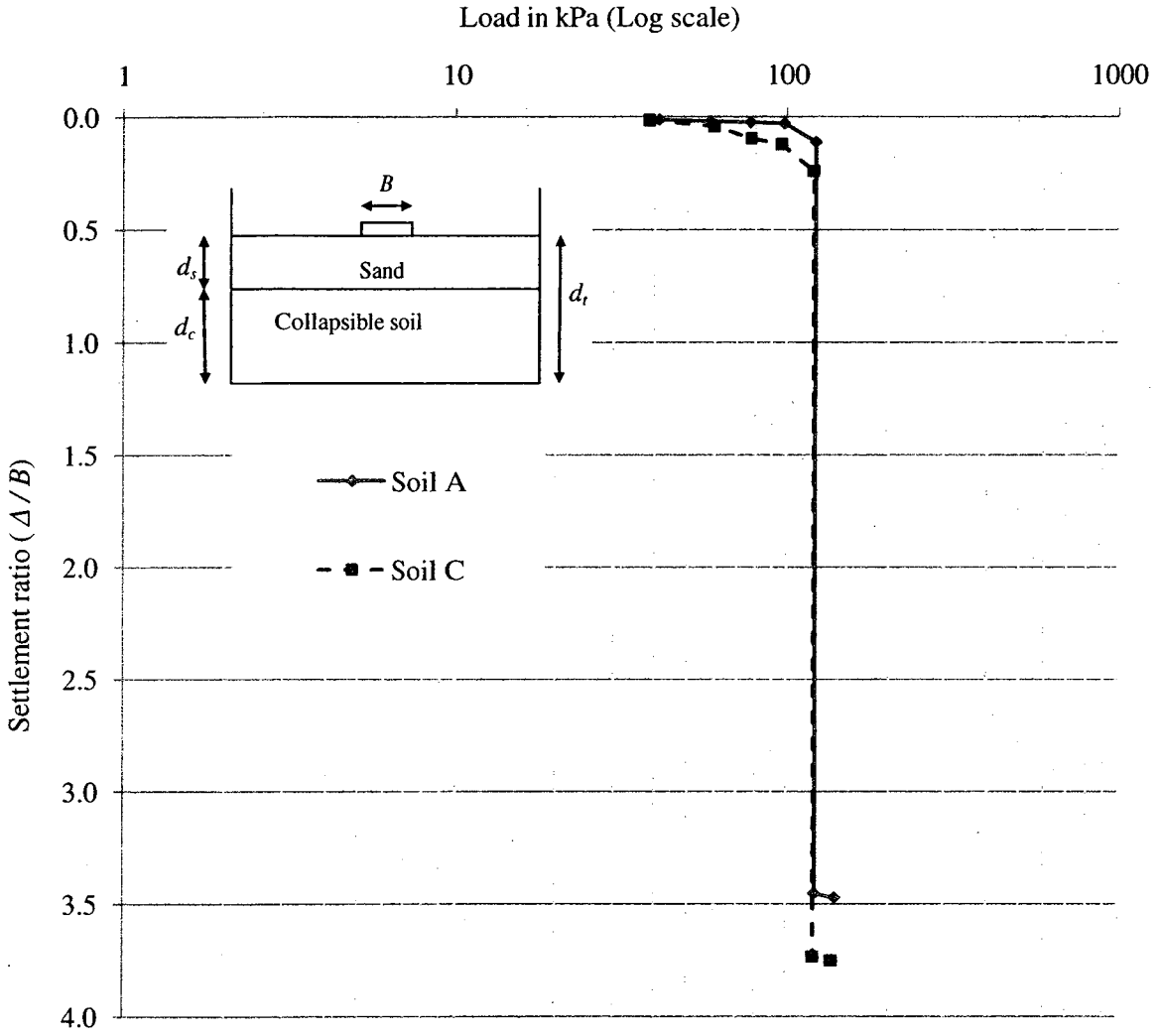

Figure (4-12): Settlement ratio versus applied stress for replacement thickness of *2B* (tests II-2 and II-5)

Collapse settlement ratios (Δ / B) for different replacement thickness ratio resulting from these tests are shown in Figure (4-13). This Figure shows that, starting from sand thickness equal to 1B, the collapse settlement ratio increased with the increase of the compacted sand layer thickness and, for the tested range where 1B being the smallest replacement thickness, the most effective replacement thickness to reduce the collapse settlement ratio is equal to 1B. The effect of the partial replacement of the collapsible soil technique on reducing the collapse settlement ratio is more evident in soil A with less collapse potential (4.2%) than soil C with higher collapse potential (12.5%).

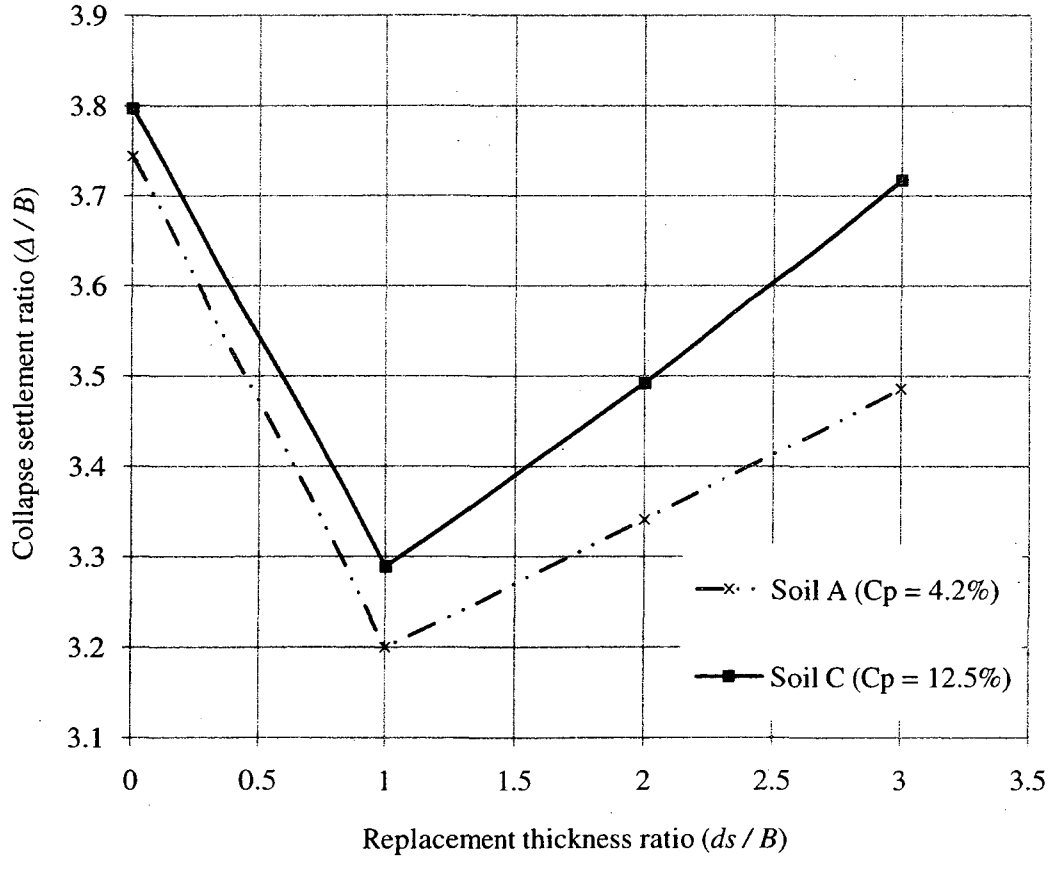

Figure (4-13): Collapse settlement ratio versus replacement thickness ratio

The smallest replacement thickness used in these tests was equal to $1B$, which is considered to be a reasonable assumption in practice and in laboratory testing. Based on the results obtained from this group, it can be reported that the sand layer acted as a surcharge on the collapsible soil, i.e. increasing the stress acting on the collapsible soil and the corresponding collapse settlement, while the collapsible layer depth was simultaneously decreasing, i.e. decreasing the collapse settlement.

To simplify the results obtained and the effect of the different studied parameters on reducing the collapse settlement of the strip footing, the collapse settlement reduction factor (*CSRF*) is introduced to represent the effect of sand replacement, with / without reinforcements, on the collapse settlement of the surface strip footing as follows:

$$CSRF = \frac{\Delta_h - \Delta}{\Delta_h} \quad \text{..... (4-4)}$$

Where,

CSRF = collapse settlement reduction factor

Δ_h= Collapse settlement of homogeneous collapsible soil.

Δ = Collapse settlement of partially replaced collapsible soil with / without reinforcements.

By using the (*CSRF*) on the results obtained from tests in series (II) the effect of the compacted sand layer thickness on the collapse settlement reduction factor is given in Figure (4-14).

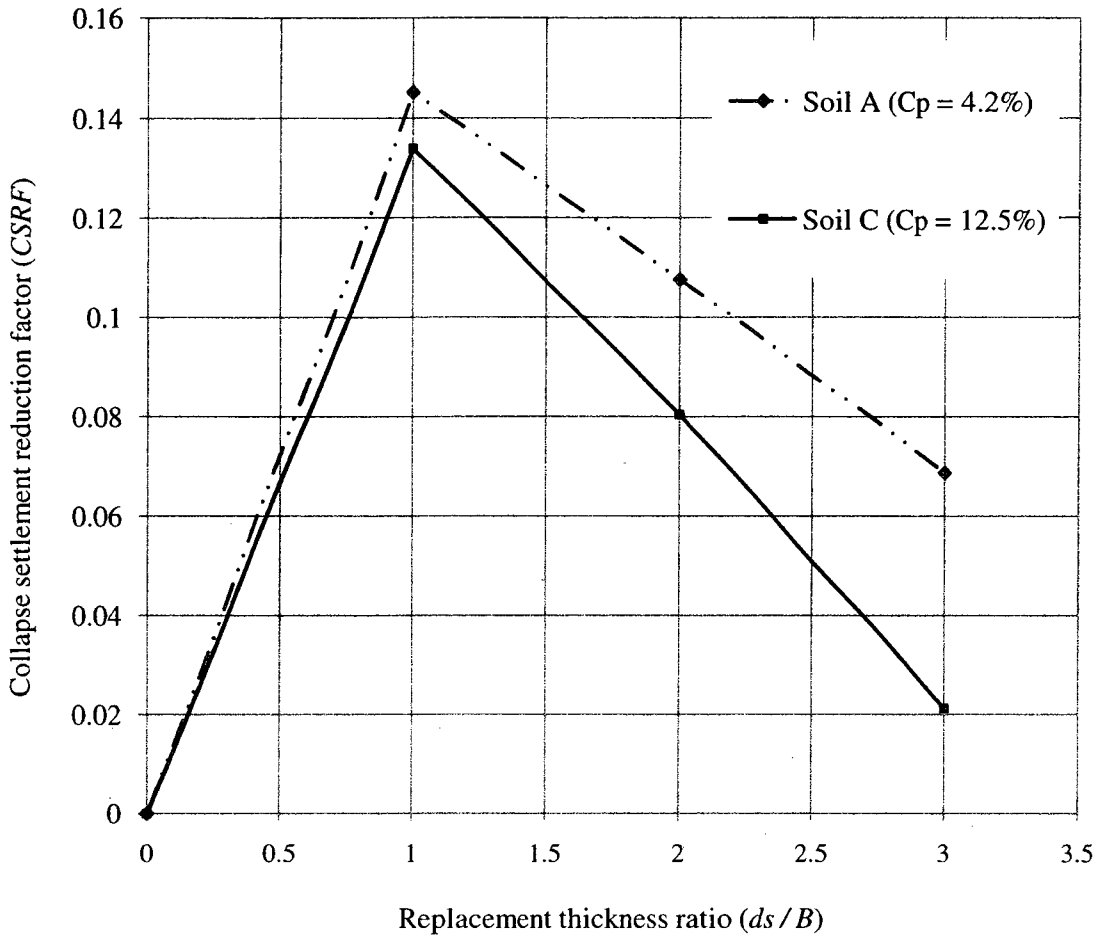

Figure (4-14): Collapse settlement reduction factor versus replacement thickness ratio

Figure (4-14) indicates that the optimum value for the compacted sand layer thickness (within the tested limit) equals to 1*B*, where a reduction on the collapse settlement of about 14% can be obtained regardless of the value of the collapse potential of the collapsible soil. When increasing the sand layer thickness beyond 1*B*, the *CSRF* decreases and the decrease is sharper in soils having higher collapse potential. For example, when increasing the compacted sand layer thickness ratio (d_s/B) to three a reduction in settlement of almost 7% is achieved for soil A, while this reduction is only 2% for soil C.

4.4. PARTIALLY REPLACED COLLAPSIBLE SOILS REINFORCED WITH GEOTEXTILE (SERIES III)

Tests in this series are carried out by partially replacing the collapsible soils with compacted sand with the inclusion of geotextile layer at the interface between collapsible soil and sand. The function of the geotextile used in the investigation is reinforcement in addition to separation between collapsible soil and sand. In these tests, thickness of compacted sand layer is varied in addition to varying the inundation stress and the effect on the collapse settlement is studied under these variations.

The compacted sand layer thickness was varied between $1B$, $2B$ and $3B$ and tests were carried out on soil A (tests III-1 and III-2) and soil C (tests III-3, III-4 and III-5). In these tests, the total soil depth (d_t) is $6B$ and the inundation stress acting on the strip footing is 125 kPa. The results obtained from these tests in addition to the case of homogeneous collapsible soils (tests I-6 and I-8) are shown in Figure (4-15) for soil A and in Figure (4-16) for soil C.

The Figures show that, regardless of the collapsible soil collapse potential value, the most effective sand replacement thickness with the inclusion of geotextile at the interface is equal to $1B$.

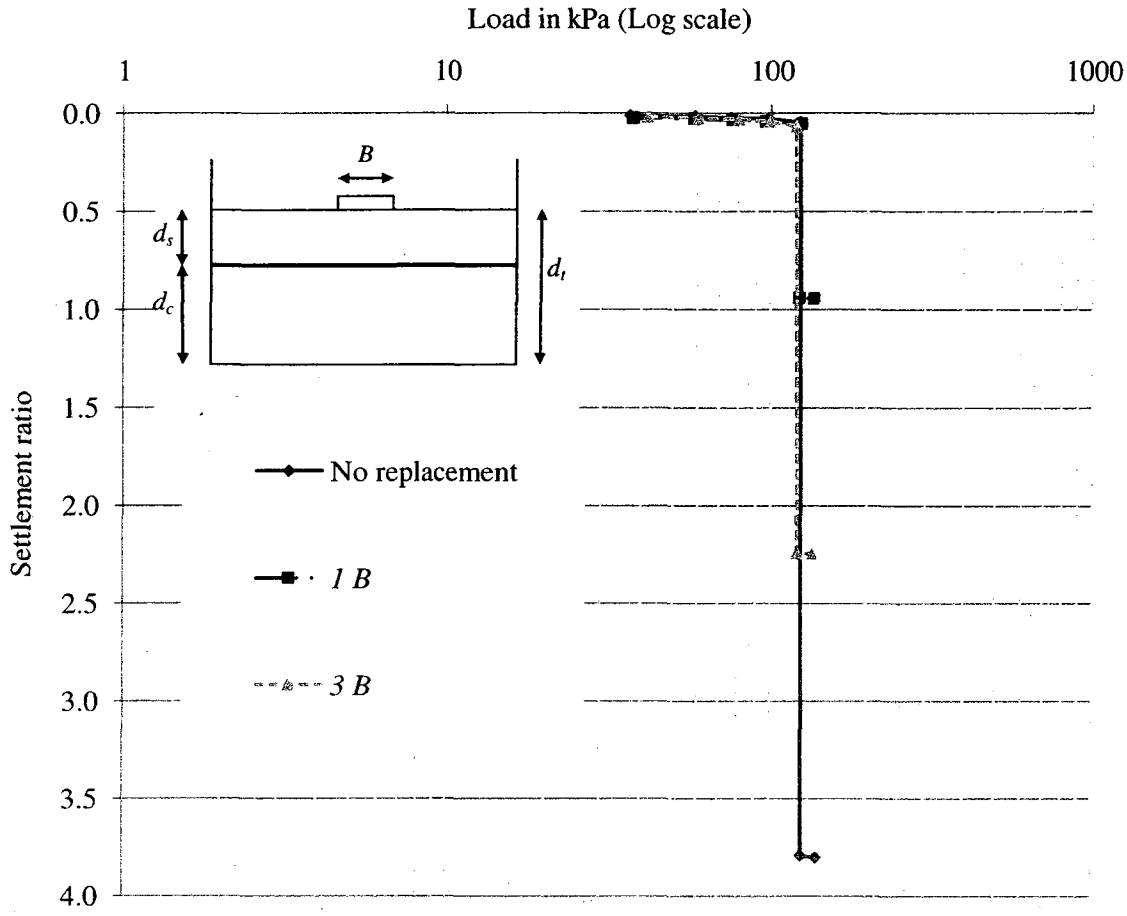

Figure (4-15): Settlement ratio versus applied stress for different replacement thicknesses for collapsible soil A (tests I-6, III-1 and III-2)

Variation of collapse settlement ratio versus compacted sand layer thickness with the inclusion of geotextile layer placed at the interface between the two soil layers is shown in Figure (4-17). Also, the Collapse settlement reduction factor versus replacement thickness ratio is shown in Figure (4-18).

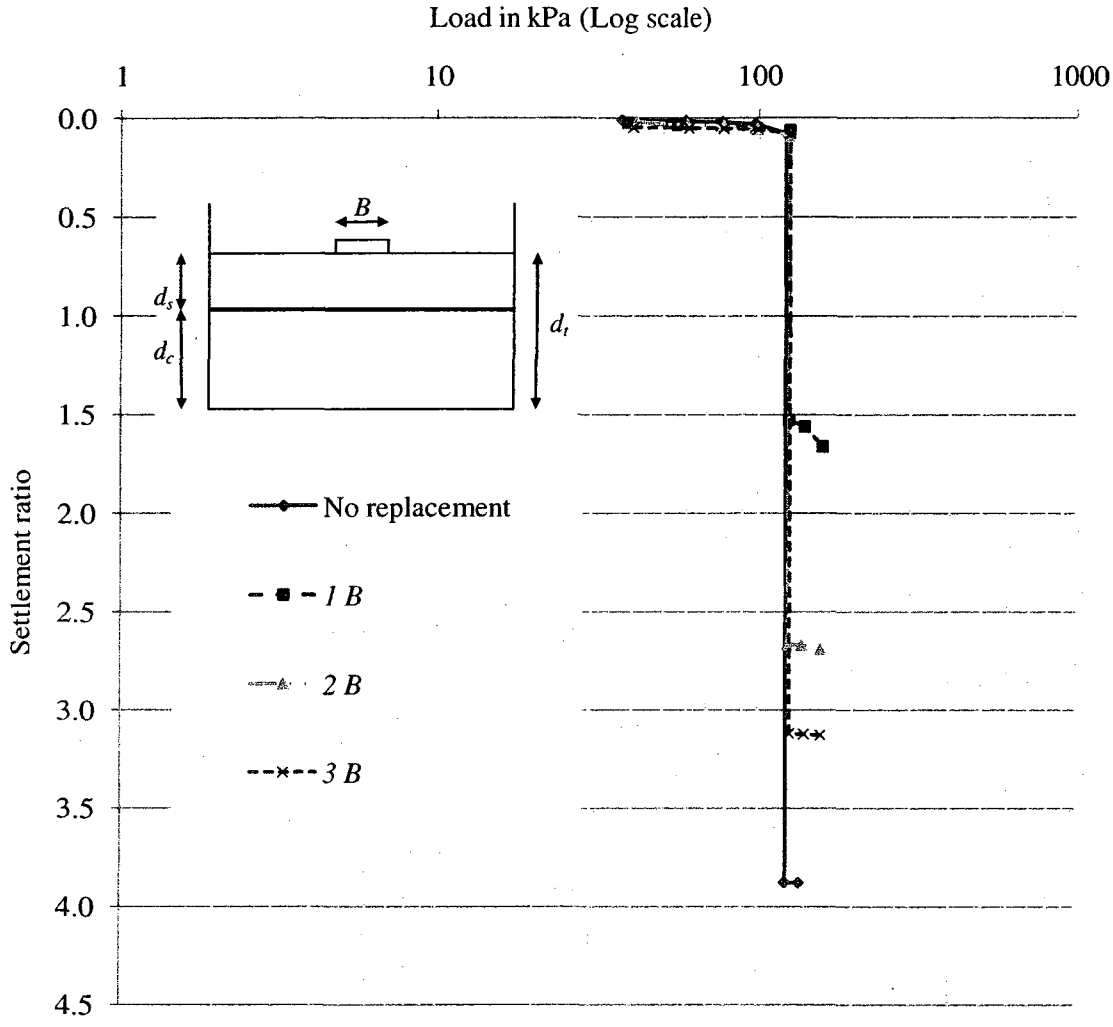

Figure (4-16): Settlement ratio versus applied stress for different replacement thicknesses for collapsible soil C (tests I-8, III-3, III-4 and III-5)

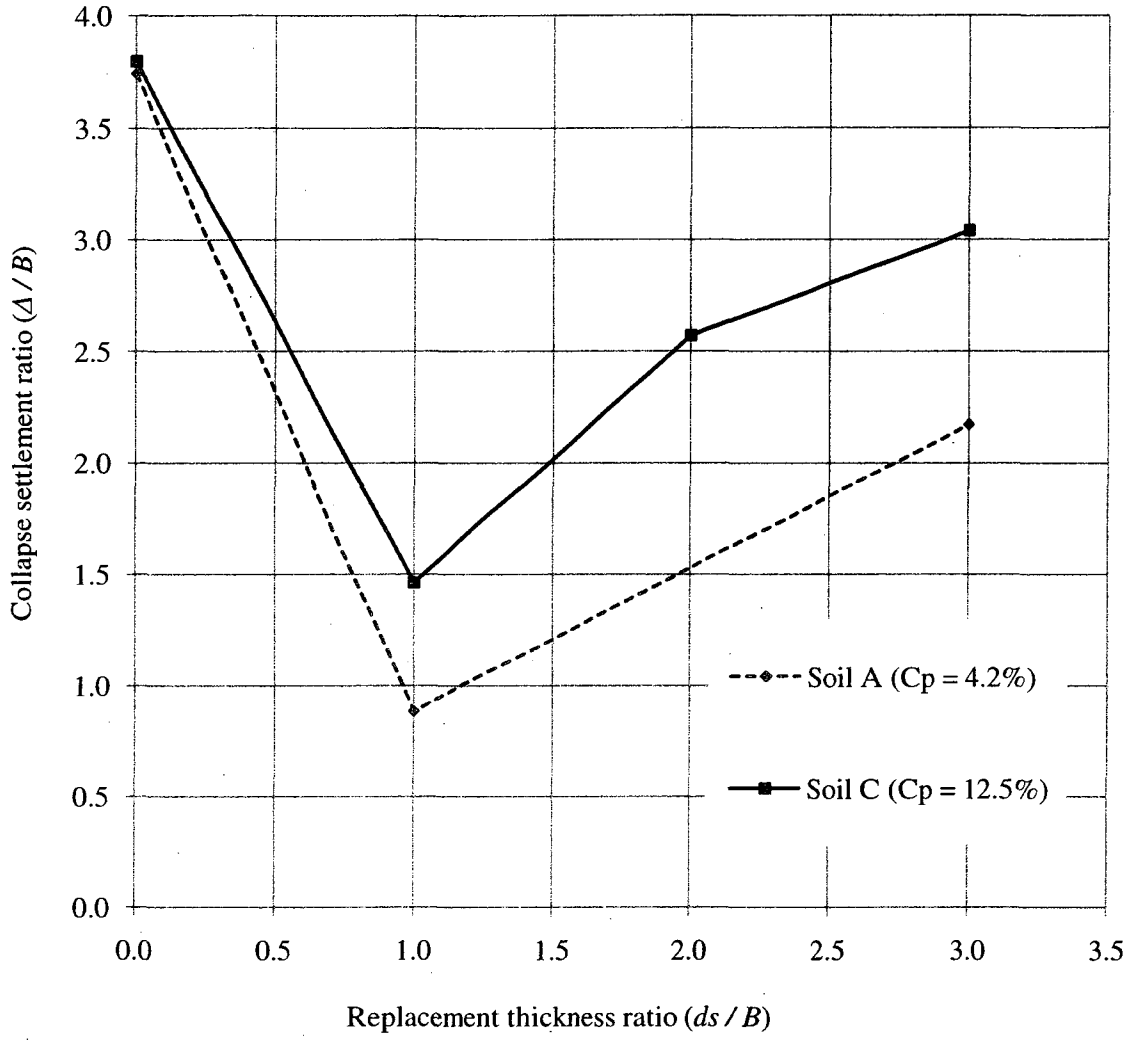

Figure (4-17): Collapse settlement ratio versus replacement thickness ratio for partially replaced reinforced collapsible soils

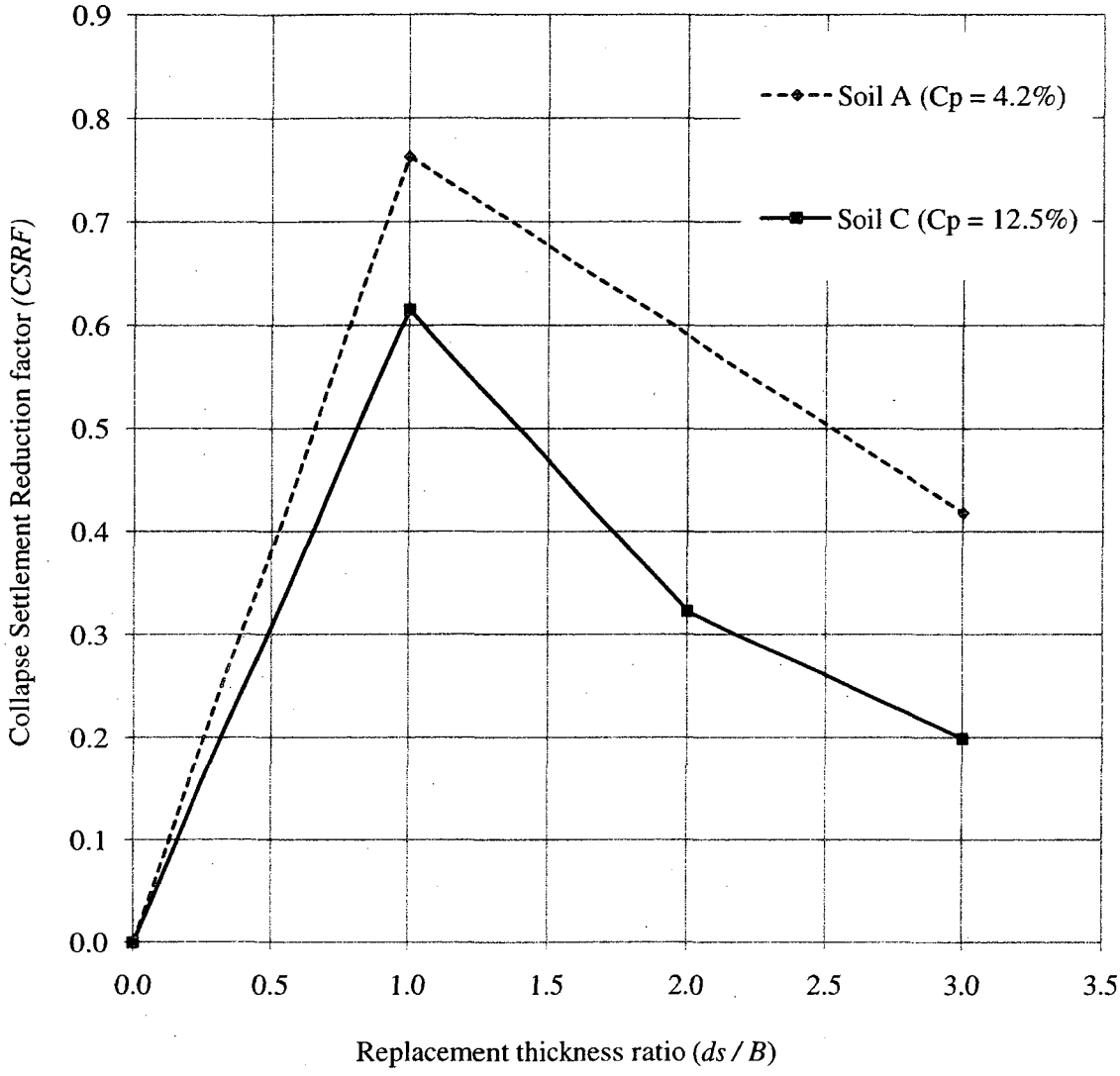

Figure (4-18): Collapse settlement reduction factor versus replacement thickness ratio for partially replaced reinforced collapsible soils

Figures (4-17) and (4-18) show that *1B* is the most effective replacement thickness (the least settlement and the highest collapse settlement reduction factor) when using geotextile as reinforcement. This finding is close to the results obtained from investigation carried out by Lee et al. (1999) where they studied the case of dense sand

overlying soft clay with geotextile at the interface and found that no benefits can be achieved by using granular material for depths more than 1.5 the footing width. Das et al. (1998), in case of granular soil overlying soft clay, found this ratio to be 4/3. Basudhar et al. (2008) found that under certain properties for modulus of elasticity for soil and geotextile, the optimum placement depth for the geotextile layer at the interface equals to 0.6 the footing width.

Figure (4-17) indicates that when using the same replacement thickness of compacted sand with the inclusion of geotextile layer at the interface between the two soil layers, the effect in reducing the collapse settlement is higher in soil A, which has smaller value of collapse potential than soil C with higher collapse potential value.

From Figure (4-18), when replacing the collapsible soils by sand thickness ratio of 1 in addition to the inclusion of geotextile at the interface, reduction in collapse settlement up to 76% can be achieved in soil A while in soil C this reduction is 61.5%.

To analyze the trend of the footing settlement while varying the compacted sand layer thickness, a sketch representing the relationship in Figure (4-17) is given in Figure (4-19), which can be divided into four sections: Section I: where $d_s / B = 0$, meaning the soil is homogeneous collapsible soil and the values of the settlement for different collapsible soils can be determined using the empirical formula (4.3). Section II: where $0 < d_s / B < 1$. For this section no experimental tests were carried out for practical and laboratory tests considerations. Section III is where $1 \leq d_s / B \leq 3$, experimental investigation was

carried out within this range and was not extended to section IV for practical and economical considerations.

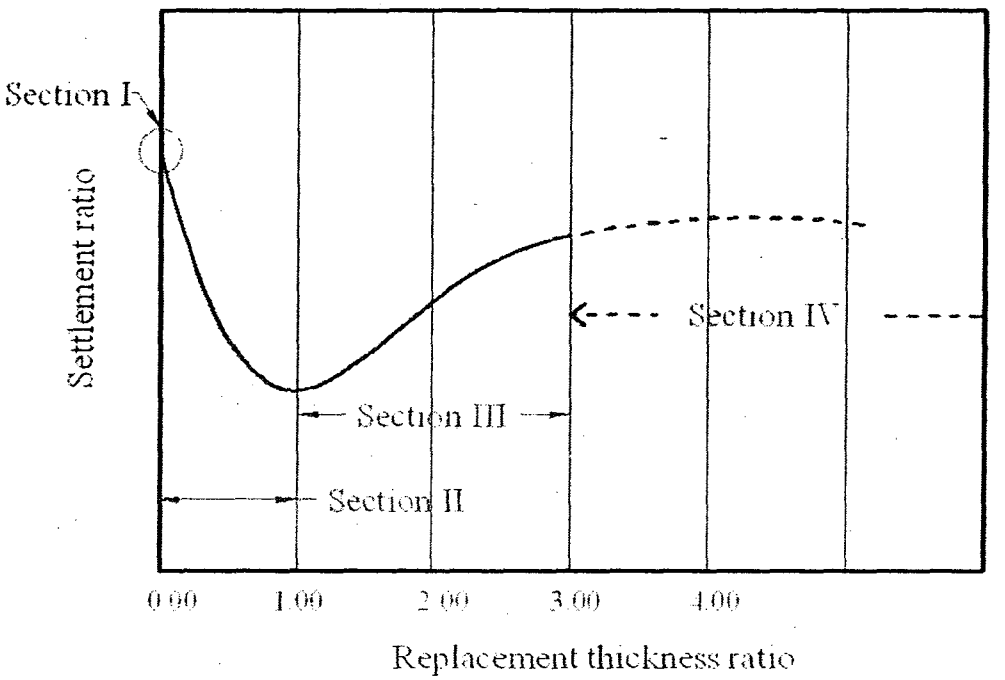

Figure (4-19): Sketch for the relationship between replacement thickness ratio and settlement ratio

From results obtained in this group of tests it can be noted that the foundation goes through two types of collapse settlement simultaneously when it is subjected to inundation. The first is due to the surcharge caused by the weight of replacement layer, which increases with the increase of the replacement thickness, while the second is due to the collapse of the collapsible soil that decreases with the decrease of the collapsible soil height. The summation of the two is the total collapse settlement that the footing experiences.

Additional tests were carried out to examine the effect of varying the applied inundation stress on the settlement of the strip footing on the replaced reinforced collapsible soils. Soils A, (tests III-6, III-7 and III-1), and C (tests III-8, III-9 and III-3) are used in these tests, collapsible soils were partially replaced by sand thickness of $1B$, total depth of the soil is $6B$ and geotextile layer is placed between collapsible soil and compacted sand. Inundation stress is varied between 60, 100 and 125 kPa, which represent range between $q_u / 4$ to $q_u / 2$. Results of this group of tests are presented in Figures (4-20) and (4-21). These results indicate that for any type of collapsible soil, increasing the applied inundation stress increased the settlement ratio for the footing. The variation of collapse settlement ratio versus inundation stress for soils A and C is given in Figure (4-22). This Figure indicates that regardless of the collapse potential value, the trend of the increase in the collapse settlement ratio is similar. The increase in the collapse settlement ratio is gradual between the values of the inundation stresses that are equal to q_u / 4 to almost q_u / 2.6 after that the trend of the increase is sharper. For example, for soil C increasing the inundation stress from 60 kPa to 100 kPa (65% increase) increased the collapse settlement by about 14%, while increasing it from 100 kPa to 125 kPa (25%) increased the collapse settlement by almost 37%. That leads to the conclusion that a factor of safety of 2.5 or more is preferred when constructing in this type of soils to maximize the benefits of the methods used to reduce the footing settlement.

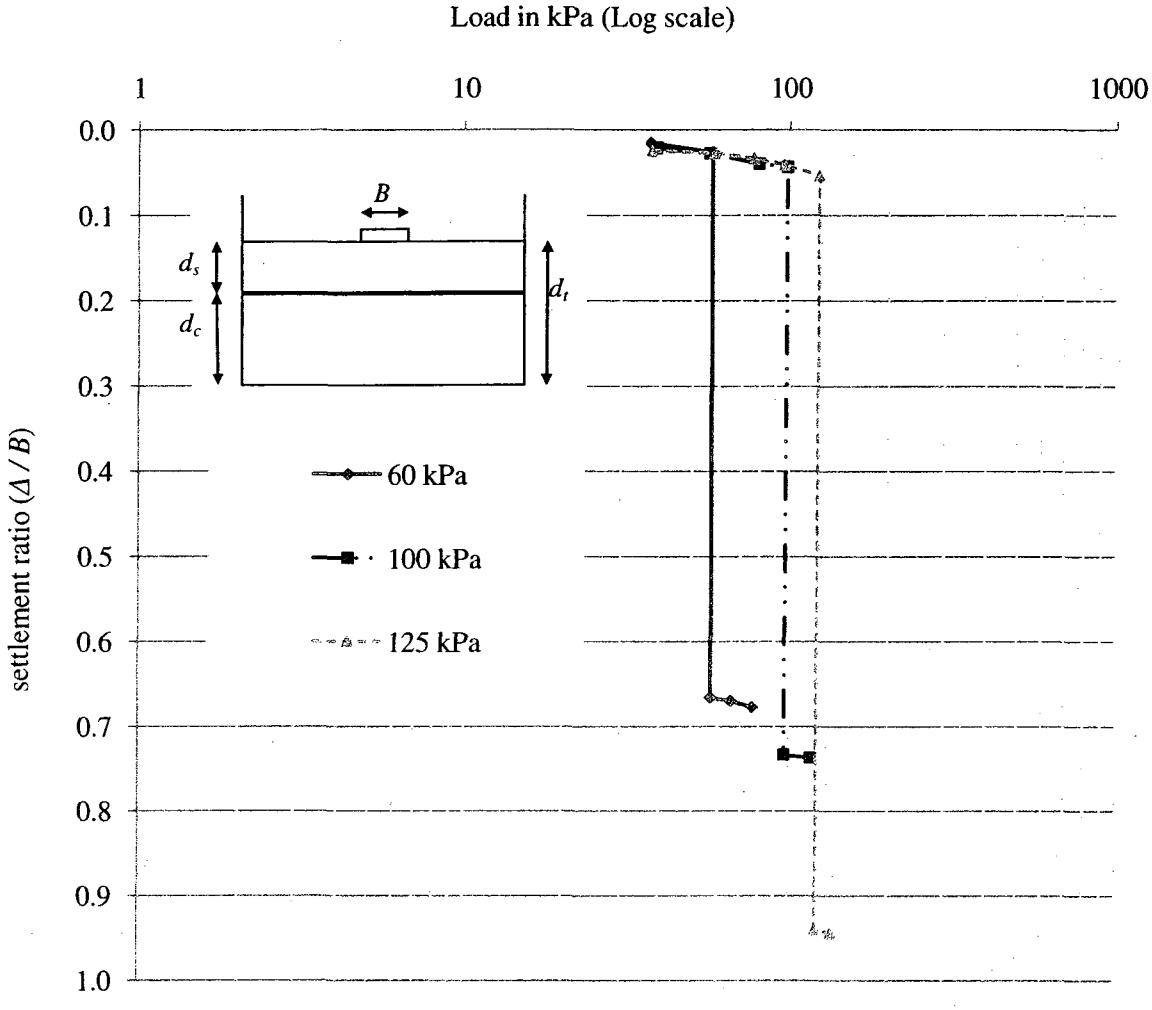

Figure (4-20): Settlement ratio versus applied stress for different inundation stresses for collapsible soil A, $d_s / B = 1$, (tests III-6, III-7 and III-1)

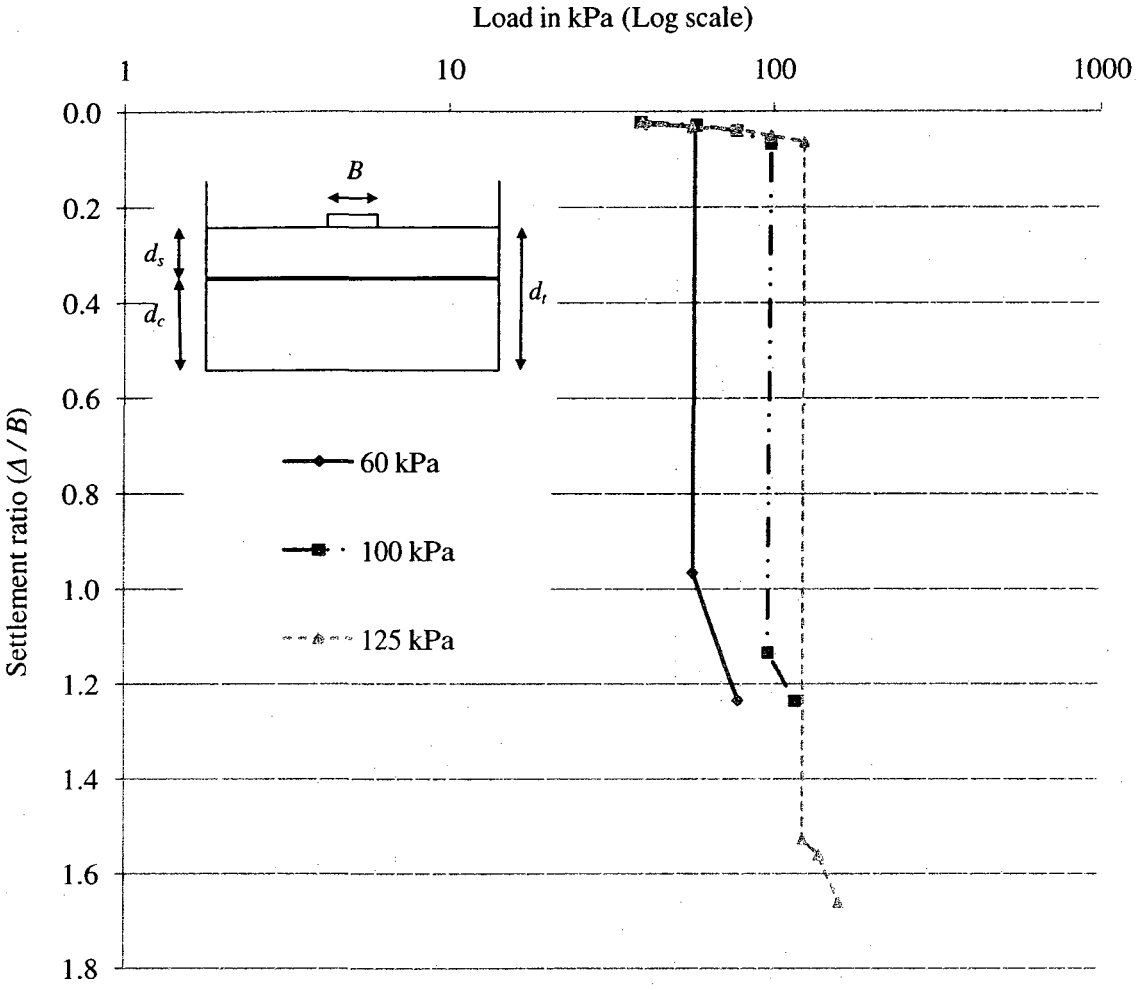

Figure (4-21): Settlement ratio versus applied stress for different inundation stresses for collapsible soil C, $d_s / B = 1$, (tests III-8, III-9 and III-3)

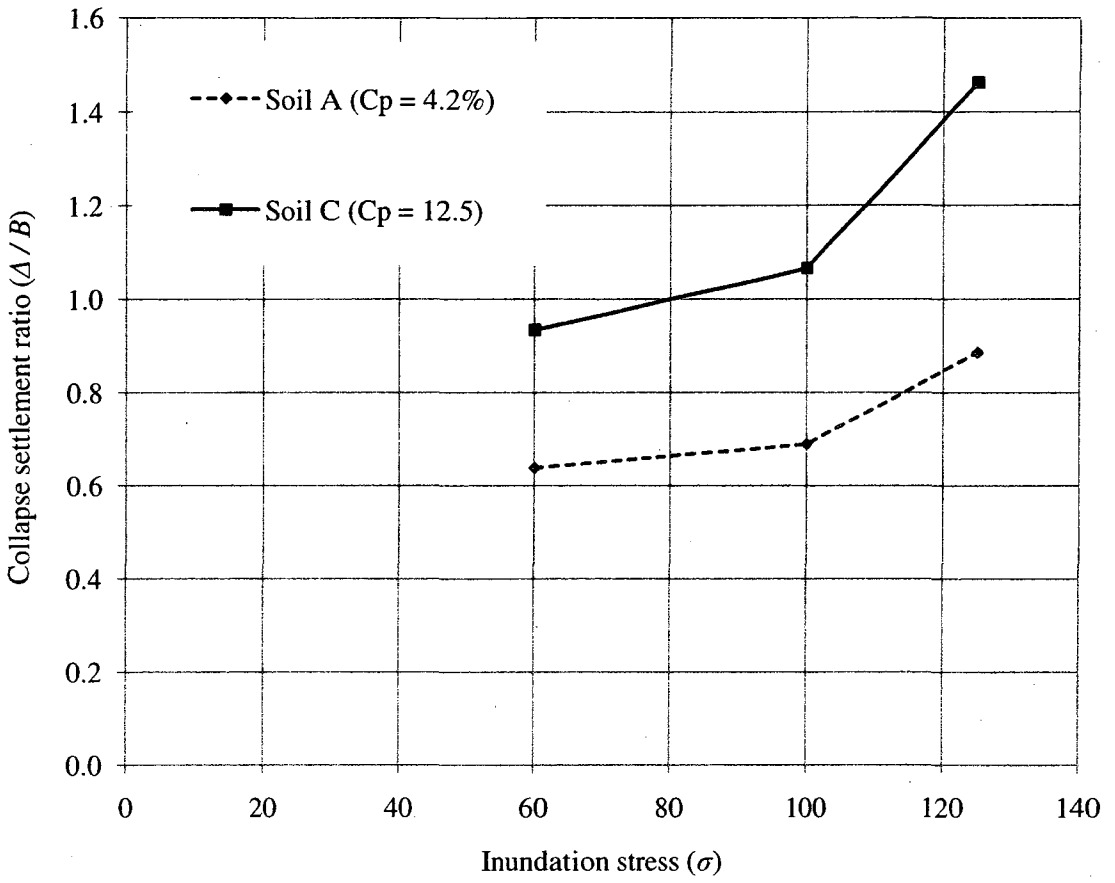

Figure (4-22): Collapse settlement ratio versus inundation stress for partially replaced reinforced collapsible soils

It was also noted from test (III-10), where the inundation stress was 140 kPa (factor of safety less than 2), that slip between the soil layers and the geotextile layer occurs, which supports the conclusion of using higher factor of safety to determine the working load to be applied on the strip footing as this case was not part of this investigation.

4.5. PARTIALLY REPLACED COLLAPSIBLE SOILS REINFORCED WITH GEOTEXTILE AND GEOGRID (SERIES IV)

Tests in this series are carried out by partially replacing the collapsible soils with compacted sand with the inclusion of geotextile at the interface between collapsible soil and sand in addition to placing geogrid layer(s) within the compacted sand. Various compacted sand thicknesses are used to partially replace the collapsible soil. Geogrid layer is placed at different depths. Additional tests were carried out using 2 layers of geogrid. Only soil C was used in this series with total soil depth of $6B$ and subjected to inundation stress of 125 kPa. The details of this series are:

Tests (IV-1, IV-2 and IV-3) were carried out to investigate the effect of partially replacing collapsible soil with different thicknesses of compacted sand with the geotextile layer at the interface between the two soil layers in addition to the inclusion of two geogrid layers within the compacted sand. While varying the sand thickness, the geogrid layers are placed in equal spacing of $d_s / 3$. Results for these tests in addition to the case of homogeneous collapsible soil (test I-8) are given in Figure (4-23).

From these results, it is concluded that, in case of using two geogrid layers within the compacted sand layer in addition to the geotextile layer at the interface, the most effective sand layer thickness that gives the least settlement ratio is equal to $2B$. Increasing the replacement thickness more than that value didn't have any effect on reducing the settlement ratio. Figure (4-24) presents the relation between the collapse settlement ratio and the replacement thickness ratio.

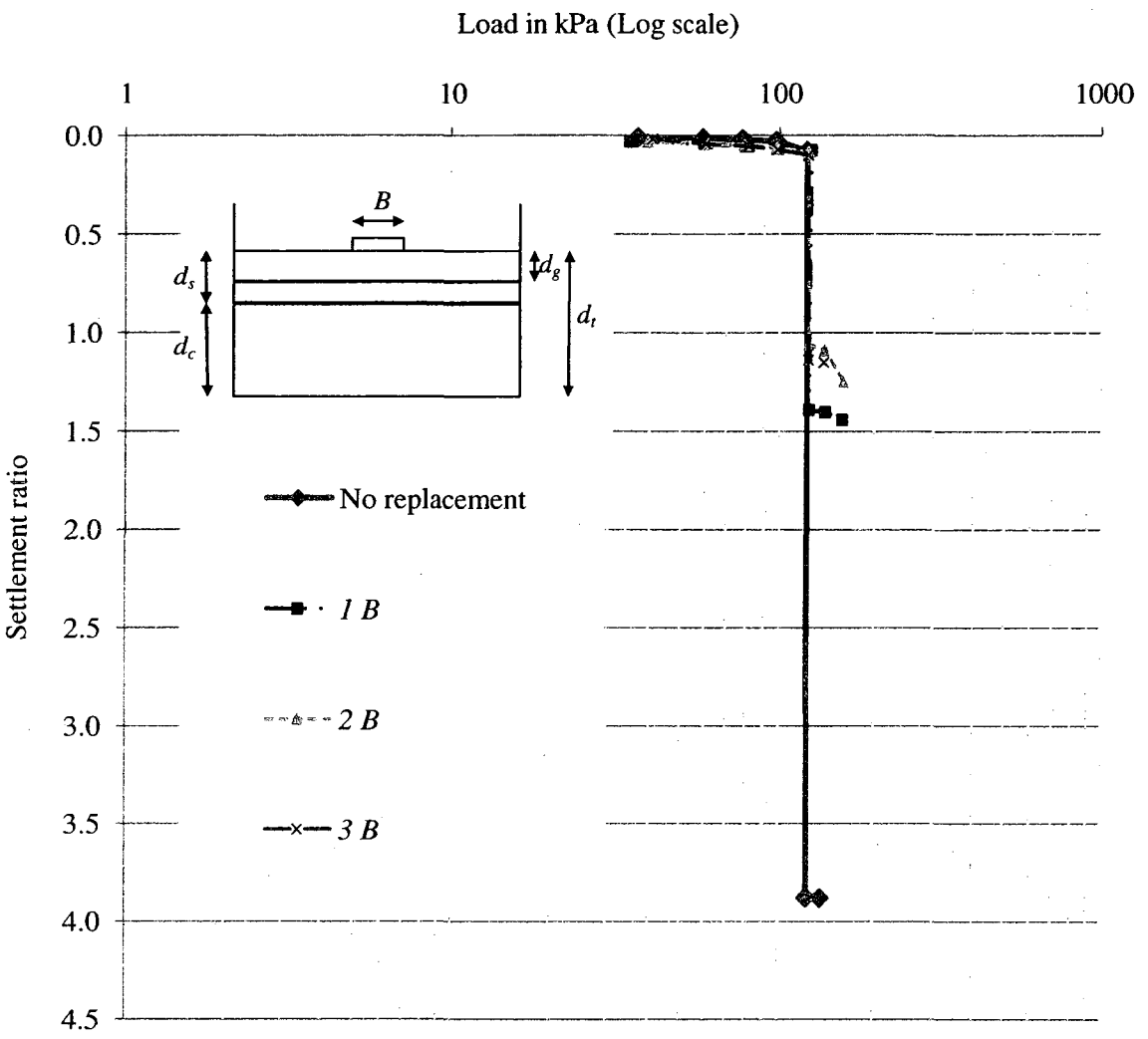

Figure (4-23): Settlement ratio versus applied stress for different replacement ratios for reinforced collapsible soil C (tests I-8, IV-1, IV-2 and IV-3)

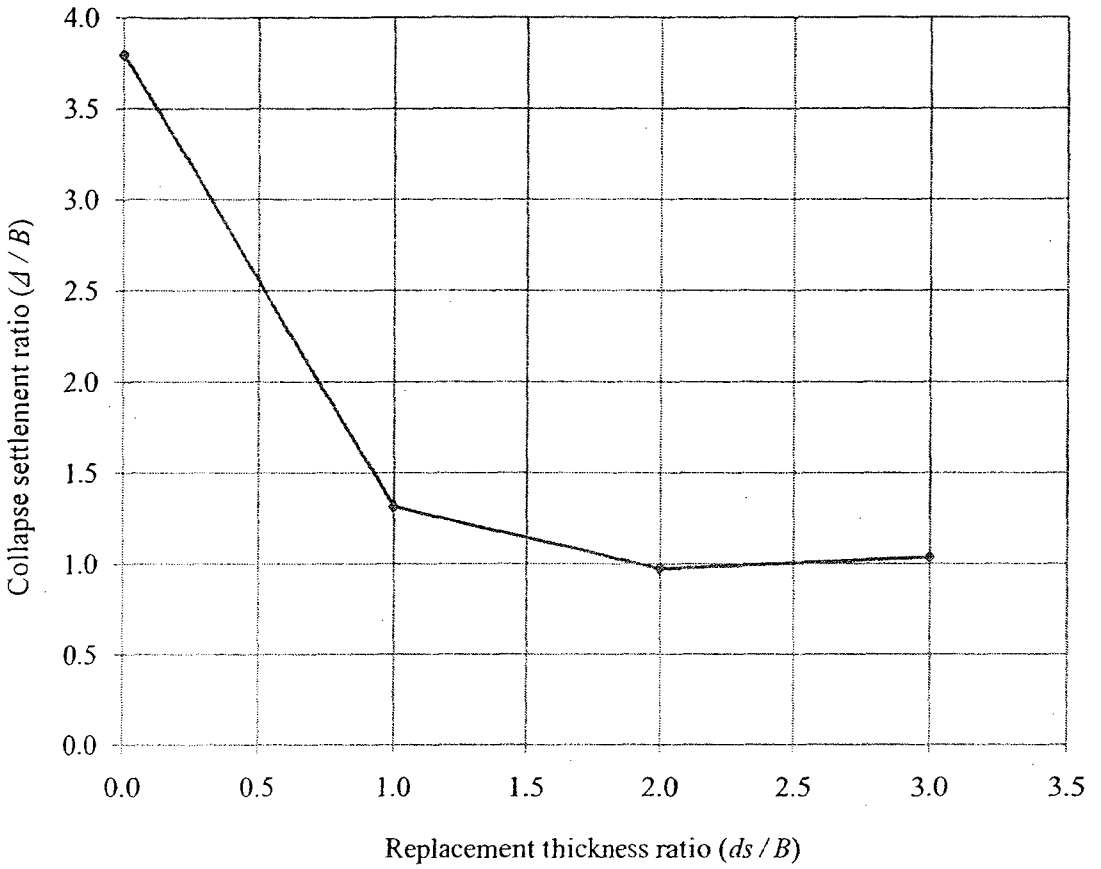

Figure (4-24): Collapse settlement ratio versus replacement thickness ratio for soil C reinforced with geotextile and 2 geogrid layers

Figure (2-24) shows that the collapse settlement ratio decreases with the increase of the compacted sand layer thickness ratio up to 2, after that it is almost constant. This means that in case of using two geogrid layers within the compacted sand layer in addition to geotextile layer at the interface the most effective replacement thickness is equal to $2B$ after which there is almost no effect on the collapse settlement ratio of the footing.

The effect of the compacted sand layer thickness on the collapse settlement reduction factor is presented in Figure (4-25), which illustrates that, with the inclusion of two layers of geogrid spaced at $(d_s / 3)$, increasing the replacement thickness ratio (d_s / B) increased the collapse settlement reduction factors till the replacement thickness ratio reached 2. In this case, the corresponding collapse settlement reduction factor has the value of 74.4% after that a slight decline in the collapse settlement reduction factor occurs reaching a value of 72.7%, which can be considered as constant value for the *CSRF*. This can be due to the fact that the geogrid needs to be subjected to higher stress to mobilize its effect. When the replacement thickness was equal to $1B$ the surcharge caused by the replacement layer was less than the case when the replacement thickness was $2B$. Increase in replacement thickness increases stresses in the geogrid layers leading to the effectiveness of the geogrid in the reduction of the settlement ratio, on the contrary of the results with the sand replacement with or without the geotextile layer at the interface between the two soil layers where the settlement ratio increased with the increase of the replacement thickness from $1B$ to $2B$. Increasing the replacement thickness afterwards to $3B$ with 2 geogrid layers within the replacement thickness didn't have significant effect compared to replacement thickness of $2B$.

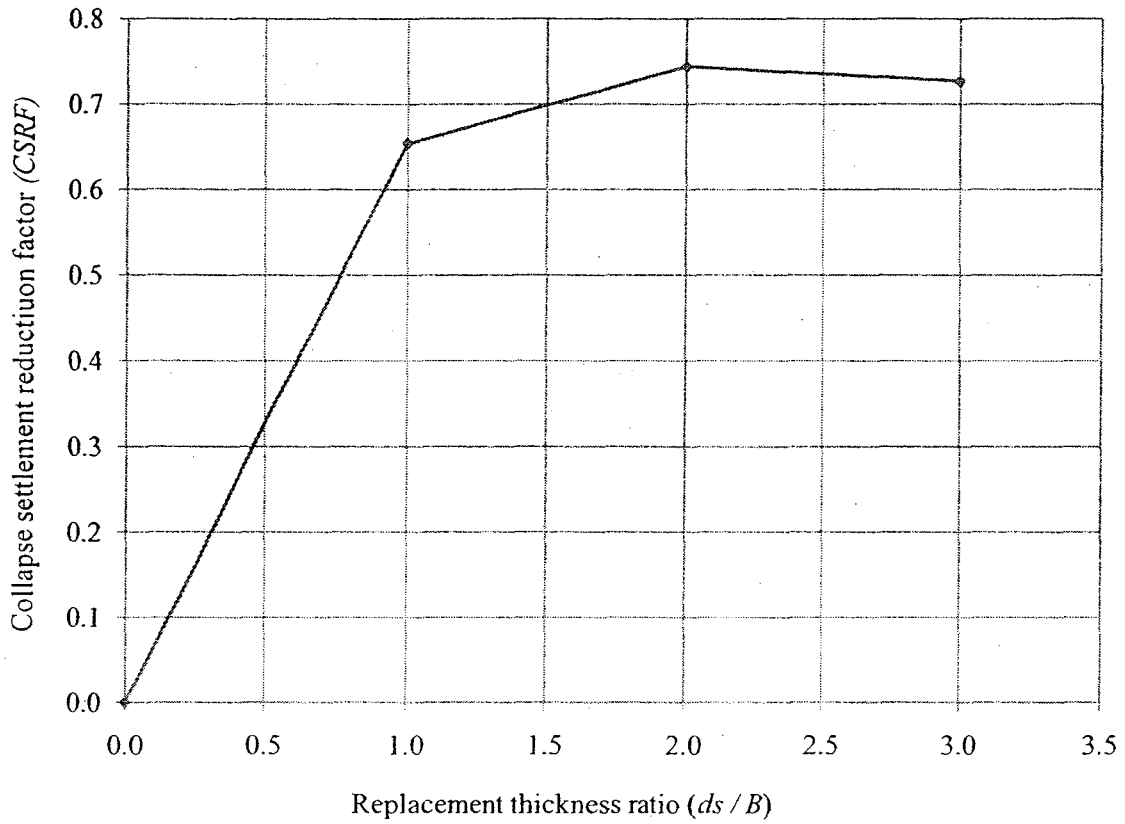

Figure (4-25): Collapse settlement reduction factor versus replacement thickness ratio for soil C reinforced with geotextile and 2 geogrid layers

This leads to the conclusion that, for soil C in this investigation, the use of a replacement thickness ratio (d_s / B) of 2 with the inclusion of two layers of geogrid spaced at ($d_s / 3$) and a layer of geotextile at the interface between the collapsible soil and the compacted sand, with length and width equal to the length and width of the test box, reduces the collapse settlement by 74.4% and any additional increase in the compacted sand layer thickness has almost no effect on the collapse settlement reduction factor.

Additional tests were carried out to investigate the effect of partially replacing collapsible soil with certain thicknesses of compacted sand equals to $1B$, geotextile layer at the interface between the two soil layers in addition to the inclusion of one geogrid layer within the compacted sand at different depths (0.3 d_s and 0.7 d_s). Tests were carried out on soil C, total depth of soil equal to $6B$ and subjected to inundation stress of 125 kPa. Results for these tests (IV-4 and IV-5) are presented in Figure (4-26), from which it is noted that changing the geogrid layer depth has almost no effect on the footing settlement ratio.

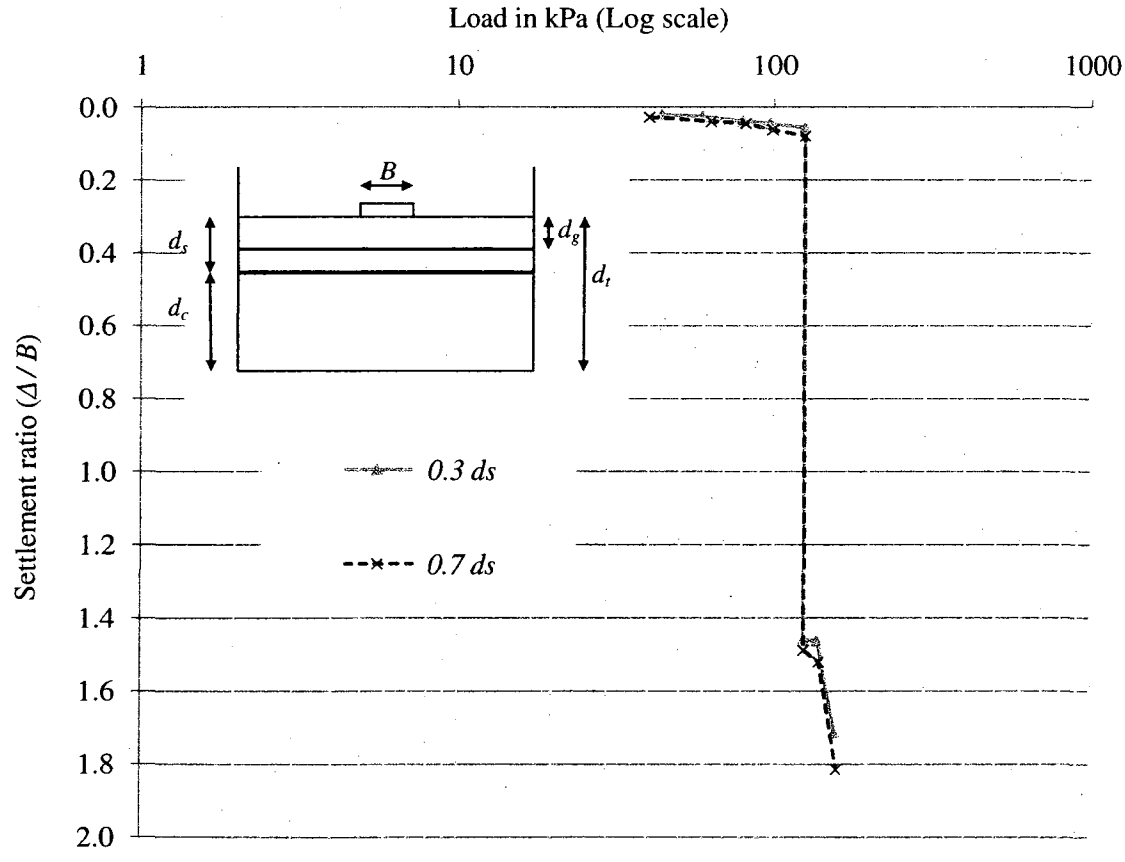

Figure (4-26): Settlement ratio versus applied stress for different geogrid depths for collapsible soil C, $d_s / B = 1$ (tests IV-4 and IV-5)

Combining these results from changing the geogrid layer depth (tests IV-4 and IV-5) with the results from test (III-3) where geotextile only was used at the interface between the two soil layers, it can be noted that adding one geogrid layer at any depth within the compacted sand layer has almost no effect on the footing settlement ratio as shown in Figure (4-27).

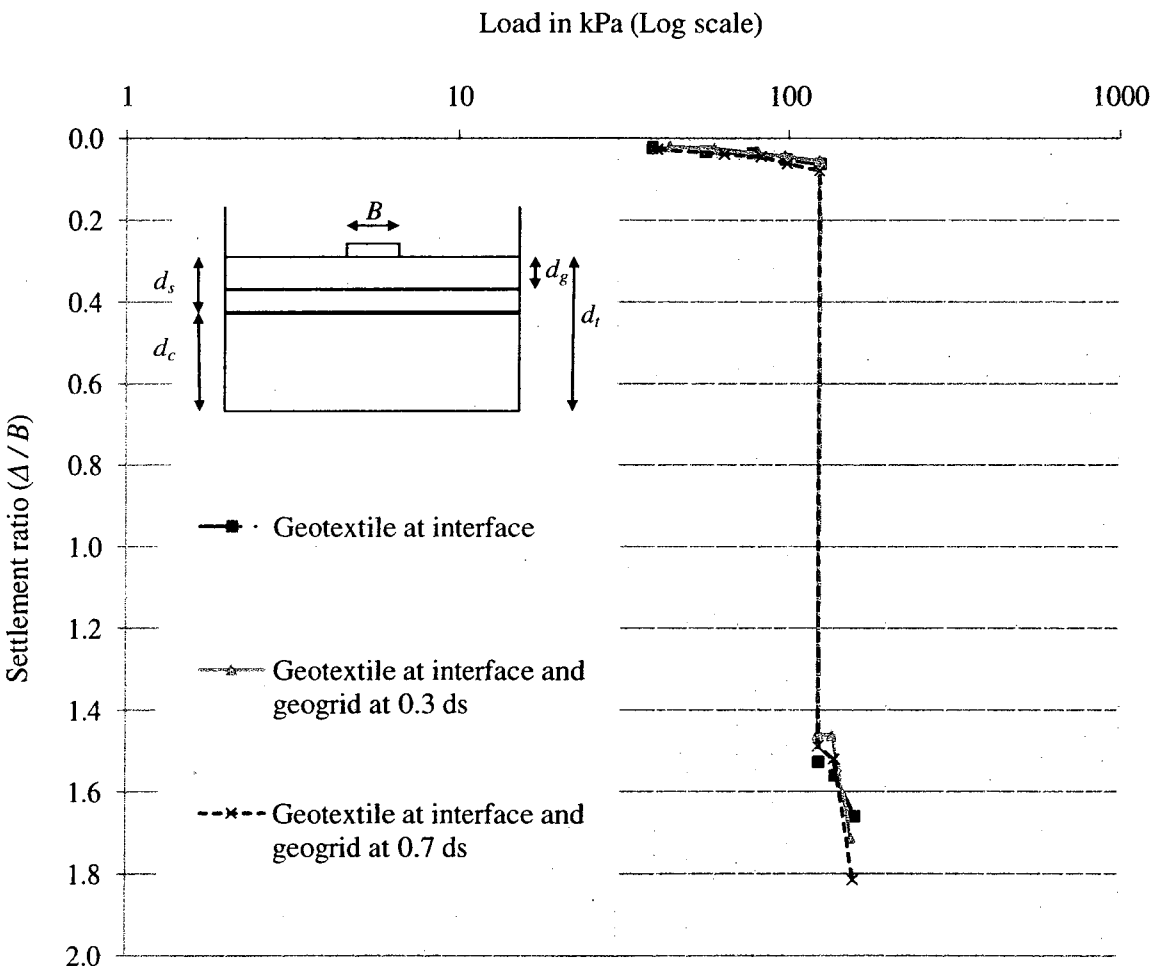

Figure (4-27): Settlement ratio versus applied stress for different reinforcement for collapsible soil C, $d_s / B = 1$ (tests III-3, IV-4 and IV-5)

The effect of changing the geogrid layer depth on the collapse settlement reduction factor is given in Figure (4-28) where it shows that changing the depth ratio of the geogrid layer doesn't have almost any effect on the collapse settlement reduction factor. At depth ratio of the geogrid layer equals to 0.3, the *CSRF* was equal to 63.1%, while at depth ratio of 0.7, the *CSRF* was equal to 62.9%. Furthermore, using geogrid layer at any depth within the compacted sand layer of thickness equal to $1B$ doesn't have significant effect on the collapse settlement reduction factor. The *CSRF* without using geogrid layer within $1B$ replacement thickness and using only geotextile at the interface was equal to 61.5% with almost 1.6% increase when placing the geogrid at depth ratio of 0.3.

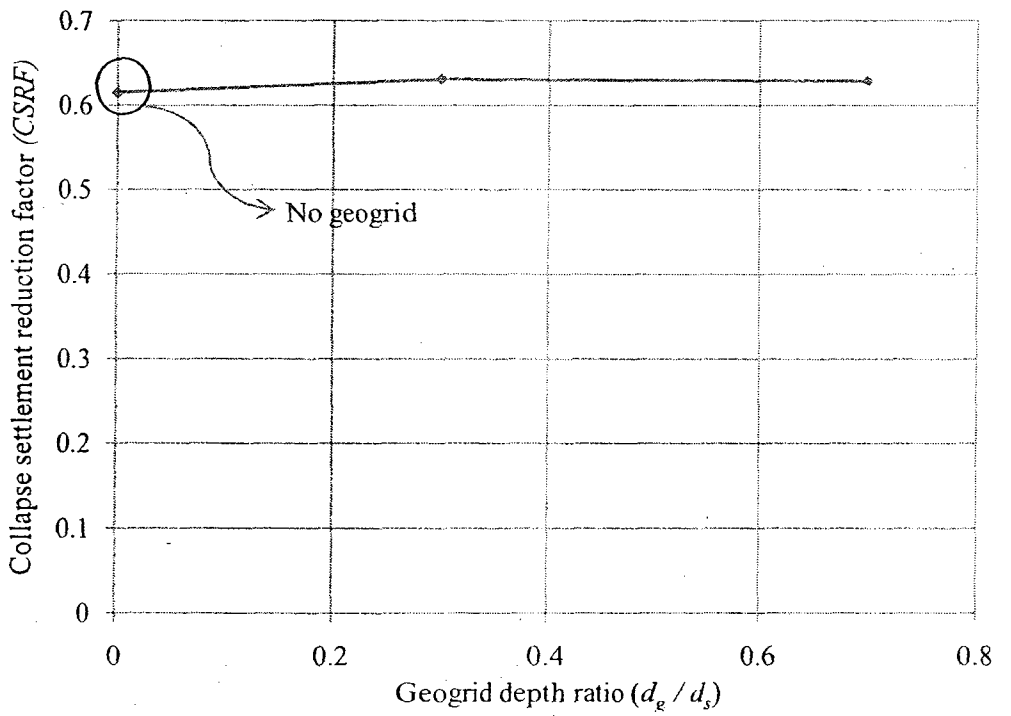

Figure (4-28): Collapse settlement reduction factor versus geogrid depth ratio for collapsible soil C, $d_s / B = 1$

The effect of geogrid placement is mobilized when it is subjected to higher stresses and this case was not reached yet in the case of replacement with $1B$ thickness and geotextile at the interface.

Figure (4-29) presents the collapse settlement reduction factors obtained in case of partially replacing collapsible soil C with compacted sand having thickness equal to $1B$ and different reinforcement possibilities. It can be seen from this Figure that using geotextile layer at the interface between the compacted sand, which has a thickness ratio of 1, and the collapsible soil (soil C) has a significant effect on reducing the collapse settlement of the footing (61.5%). On the other hand, adding geogrid layer at any depth doesn't considerably affect the settlement of the strip footing under consideration (63.1% for depth ratio of 0.3 and 62.9% for depth ratio of 0.7). Using two geogrid layers within the compacted sand has a slight effect on reducing the footing settlement as it increased the *CSRF* to 65.4%.

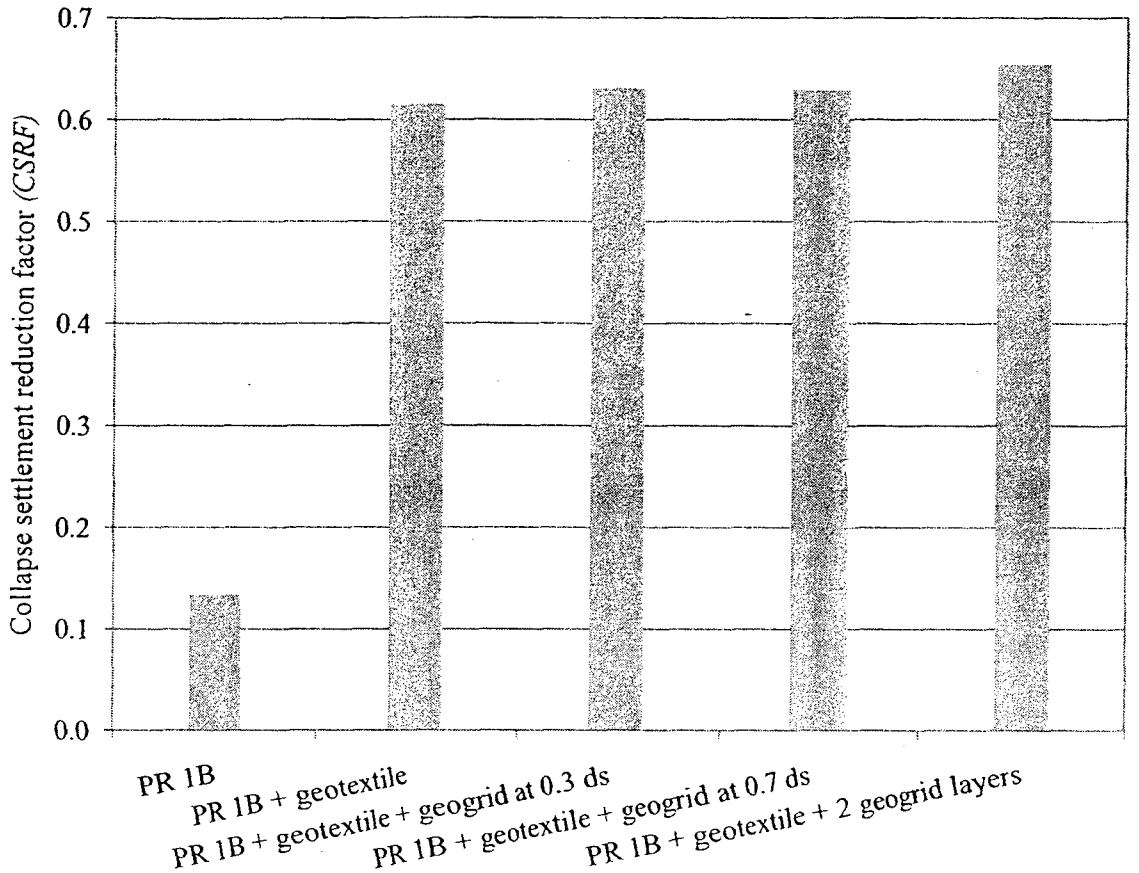

Figure (4-29): Collapse settlement reduction factor for different reinforcement configurations for soil C, $d_s / B = 1$

From all the suggested mitigation methods discussed in this chapter, it can be concluded that, for the collapsible soil C used in this study, and to achieve the highest reduction on the strip footing settlement, a replacement thickness of $2B$ is to be used with the inclusion of two geogrid layers, equally spaced, within the compacted sand and a geotextile layer at the interface between the two soil layers, as shown in comparison in Figure (4-30). However, the increase on the *CSRF* is only 9% from the case of using

replacement thickness of 1*B* with also two layers of geogrid equally spaced and about 13% from the case of using geotextile alone at the interface. Depending on the individual case in the field and the economical study that should be considered, the decision could be made to choose the most effective and appropriate method of reducing the collapse settlement of strip footing on collapsible soil, which is thought to be by partially replacing the collapsible soil with compacted sand with thickness equal to 1B with placing a geotextile layer at the interface between the collapsible soil and the compacted sand layer.

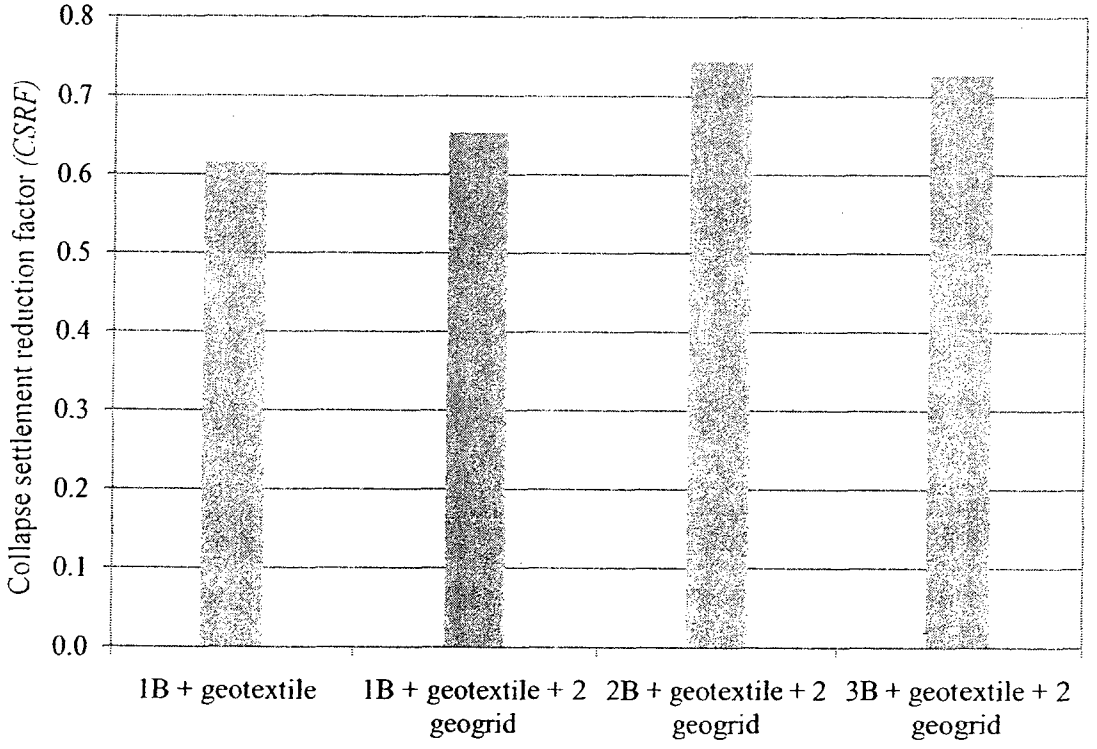

Figure (4-30): Collapse settlement reduction factor for different replacement thicknesses and reinforcement configurations

CHAPTER 5

ANALYTICL AND EMPIRICAL MODELS

5.1. GENERAL

The experimental investigation and the analysis of the test results conducted in this investigation show that the collapse settlement of a strip footing constructed on collapsible soil and subjected to inundation can be reduced, significantly, by partially replacing the collapsible soil by compacted sand with the inclusion of geotextile layer at the interface between the two soil layers. The deformed shape has a great influence on the performance of the foundation system and the settlement the strip footing goes through. Figure (5-1) presents a photo for the deformed shape obtained from tests and a simplified sketch is given in Figure (5-2).

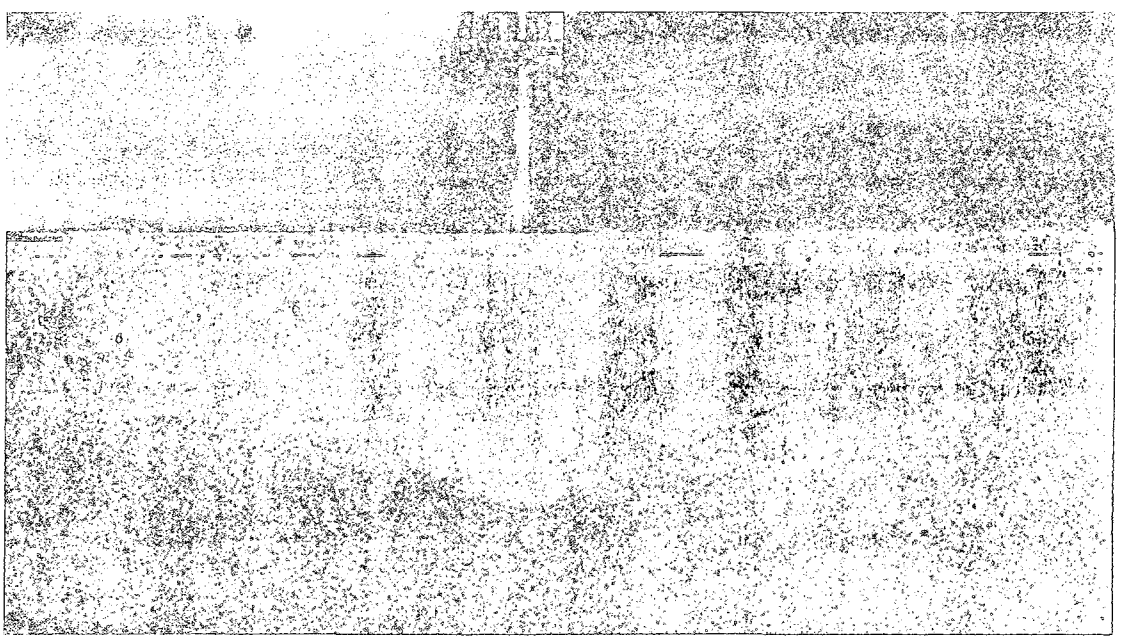

Figure (5-1): Geotextile deformed shape after collapse

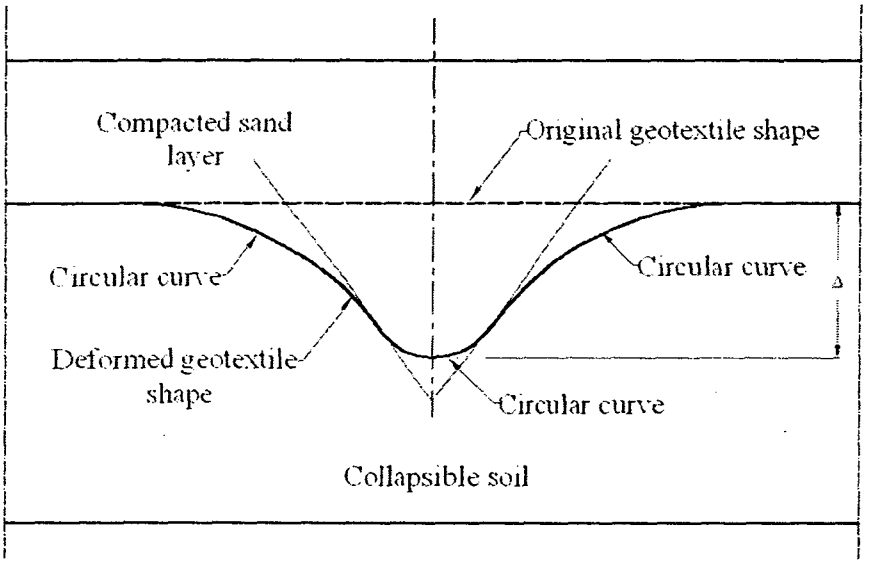

Figure (5-2): Simplified geotextile deformed shape after collapse

An empirical model will be introduced to determine the amount of collapse settlement that the strip footing will experience when collapsible soil is inundated, reaching the full saturation status in case of homogeneous collapsible soil as well as the case of partially replaced collapsible soil by compacted sand having various thickness with / without geotextile layer at the interface between the two soil layers.

An analytical model will be introduced to determine the strain developed in the geotextile layer in the case of partially replaced collapsible soil with sand thickness equal to the footing width, which was proved to be the most suitable, economical and effective thickness on reduction of collapse settlement. That will give the geotechnical engineer the limitations of the product that will be chosen for a specific job.

A third model will be introduced for estimating and determining the detailed geometry of the deformation after collapse for the same case of replacement equal to the footing width.

The trend of these models is based on the experimental investigation that was carried out in this research; also, the results obtained from the various tests were used to obtain the constants in the formulas.

5.2. EMPIRICAL MODEL TO PREDICT THE COLLAPSE SETTLEMENT

Utilizing the results from the laboratory tests carried out in this investigation, an empirical model was developed in case of homogeneous collapsible soil, (section 4-2), to determine the amount of collapse settlement a strip footing experiences when the collapsible soil is subjected to inundation under different applied stresses, various collapsible soils and various soil depths, (Formula 4-3):

$$\frac{\varepsilon_c}{Log\sigma} = 0.0005C_p + 0.296$$

This formula can be used to calculate the settlement:

$$\epsilon_c = Log\ \sigma\ (0.0005C_p + 0.296)$$

$$\frac{\Delta_h}{d_c} = Log\ \sigma\ (0.0005C_p + 0.296)$$

$$\Delta_h = d_c\ Log\ \sigma\ (0.0005C_p + 0.296) \quad \text{..... (5-1)}$$

Where

(Δ_h) collapse settlement for homogeneous collapsible soil

(d_c) collapsible soil depth

(σ) stress acting on the footing in kPa, and

(C_p) soil collapse potential measured at $\bar{\sigma}$ equal to 200 kPa.

In case of the partial replacement of the collapsible soil by compacted sand with or without the inclusion of geotextile layer at the interface between the two soil layers, (*CSRF*) was introduced (section 4-3) that shows the improvement (reduction) in the settlement of the strip footing due to the application of sand replacement with / without geotextile, (Formula 4-4):

$$CSRF = \frac{\Delta_h - \Delta}{\Delta_h}$$

Where,

CSRF = collapse settlement reduction factor

Δ_h= Collapse settlement of homogeneous soil.

Δ = Collapse settlement of partially replaced collapsible soil with / without reinforcements.

$$CSRF = \frac{\Delta_h - \Delta}{\Delta_h} = 1 - \frac{\Delta}{\Delta_h}$$

$$\frac{\Delta}{\Delta_h} = 1 - CSRF$$

$$\therefore \Delta = (1 - CSRF)\Delta_h \quad \text{.....(5-2)}$$

From equations (5-1) and (5-2) the settlement the strip footing experiences when the collapsible soil is partially replaced by compacted sand with / without the inclusion of geotextile layer at the interface between the two soil layers can be determined as follows:

$$\Delta = (1 - CSRF)\left[d_c \, Log\, \sigma \left(0.0005 C_p + 0.296\right)\right] \quad \text{(5-3)}$$

Or

$$\Delta = (RF)\left[d_c \, Log\, \sigma \left(0.0005 C_p + 0.296\right)\right] \quad \text{(5-4)}$$

Where

RF is Reduction factor that equals $(1 - CSRF)$

From the test results of series (III) and following the analysis presented in section (4-3) and shown in Figure (4-19), it can be concluded that for the range of sand replacement ratio (d_s / B) between 1 and 3, $(1 \leq \frac{d_s}{B} \leq 3)$, the $CSRF$ will have the relation with (d_s / B) as shown in Figure (5-3) which is represented by the following formula;

$$CSRF = -a\frac{d_s}{B} + b \quad \text{(5-5)}$$

Where,

a and b = constants

Given that:

$a \rightarrow f(C_p, E_t)$

$b \rightarrow f(E_t)$

Where,

C_p = Soil's collapse potential

E_t = Geotextile modulus of elasticity

$\frac{d_s}{B}$ = Sand replacement thickness ratio

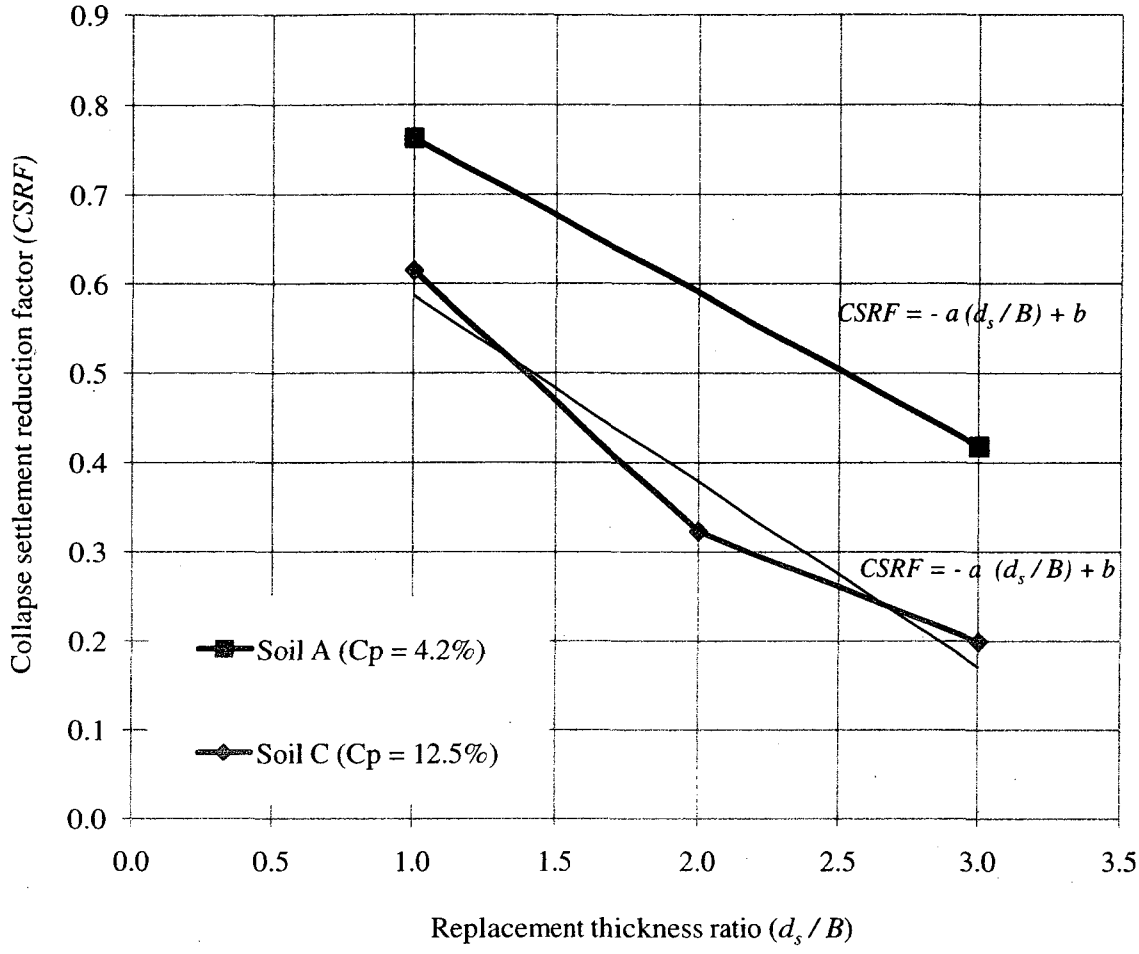

Figure (5-3): Relationship between collapse settlement reduction factor and replacement thickness ratio

Hence, Formula (5-5) can be written in the following form,

$$CSRF = -\frac{d_s}{B}(a_1 C_p + a_2 E_t + a_3) + (a_4 E_t + a_5) \quad \text{(5-6)}$$

Formula (5-6) can be rewritten as:

$$CSRF = -\frac{d_s}{B}(a_1 C_p + a_3) + E_t\left(a_4 - \frac{d_s}{B} a_2\right) + a_5 \quad \text{(5-7)}$$

$a_1, a_2 \ldots\ldots a_5$ are Constants

From experimental investigation and by performing back calculations, the following values for the various constants were obtained as:

$a_1 = 0.002,$ $a_2 = 7.6 * 10^{-6},$ $a_3 = 0.03$

$a_4 = 1.6 * 10^{-6},$ $a_5 = 0.19$

Accordingly, formula (5-7) takes the following form,

$$CSRF = -\frac{d_s}{B}(0.002C_p + 0.03) + E_t * 10^{-6}\left(1.6 - 7.6\frac{d_s}{B}\right) + 0.19 \quad \text{..... (5-8)}$$

$$\therefore RF = \left\{1 - \left[-\frac{d_s}{B}(0.002C_p + 0.03) + E_t * 10^{-6}\left(1.6 - 7.6\frac{d_s}{B}\right) + 0.19\right]\right\} \text{.. (5-9)}$$

$$\therefore \Delta = \{RF\}\left[d_c \, Log\, \sigma\, (0.0005C_p + 0.296)\right] \quad \text{..... (5-10)}$$

Comparison between values of the strip footing collapse settlement measured in the experimental investigation and the one obtained from Formula (5-10) is presented in Figure (5-4) and it shows good agreement between these values.

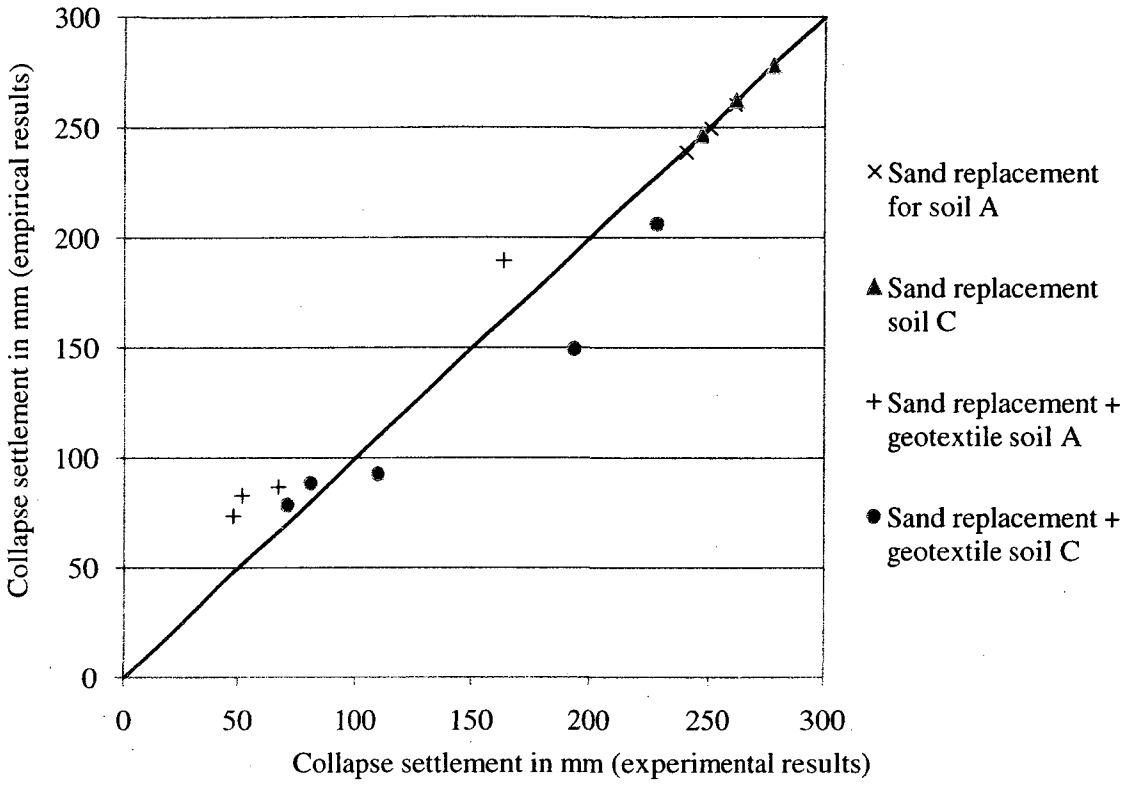

Figure (5-4): Experimental versus empirical values of the strip footing collapse settlement

As in section 4-3 and presented in Figure (4-19), the collapse settlement of strip footing is divided into different cases shown as sections. Calculation of the footing settlement will be according to the corresponding section that applies to each specific case. In this model, sections I ($d_s / B = 0$, which is the case of homogeneous collapsible soil) and section III ($1 \leq \frac{d_s}{B} \leq 3$, which is the case of partial replacement of collapsible soil with compacted sand with thickness ratio between 1 and 3) are the ones that will be analyzed. Section II was not applicable in the experimental work and section IV is not economical or practical solution to perform.

This leads to the conclusion that the settlement of a strip footing constructed on collapsible soils can be determined for various cases as follow:

1. For homogeneous collapsible soils:

$$\Delta_h = d_c \, Log \, \sigma \left(0.0005 C_p + 0.296\right) \quad \text{(5-11)}$$

2. For partially replaced collapsible soil with compacted sand with or without the inclusion of geotextile layer at the interface between the two soil layers with sand thickness ratio in the range of $1 \leq \frac{d_s}{B} \leq 3$

$$\Delta = \{RF\}\left[d_c \, Log \, \sigma \left(0.0005 C_p + 0.296\right)\right] \quad \text{(5-12)}$$

Where *RF* is equal to

$$RF = \left\{1 - \left[-\frac{d_s}{B}\left(0.002 C_p + 0.03\right) + E_t * 10^{-6}\left(1.6 - 7.6\frac{d_s}{B}\right) + 0.19\right]\right\} \quad \text{(5-13)}$$

Graphs are presented to obtain the required value for the (*RF*) according to the variation of the sand replacement thickness ratio (d_s / B), the modulus of elasticity (E_t) of the geotextile material and for different collapse potential values (C_p).

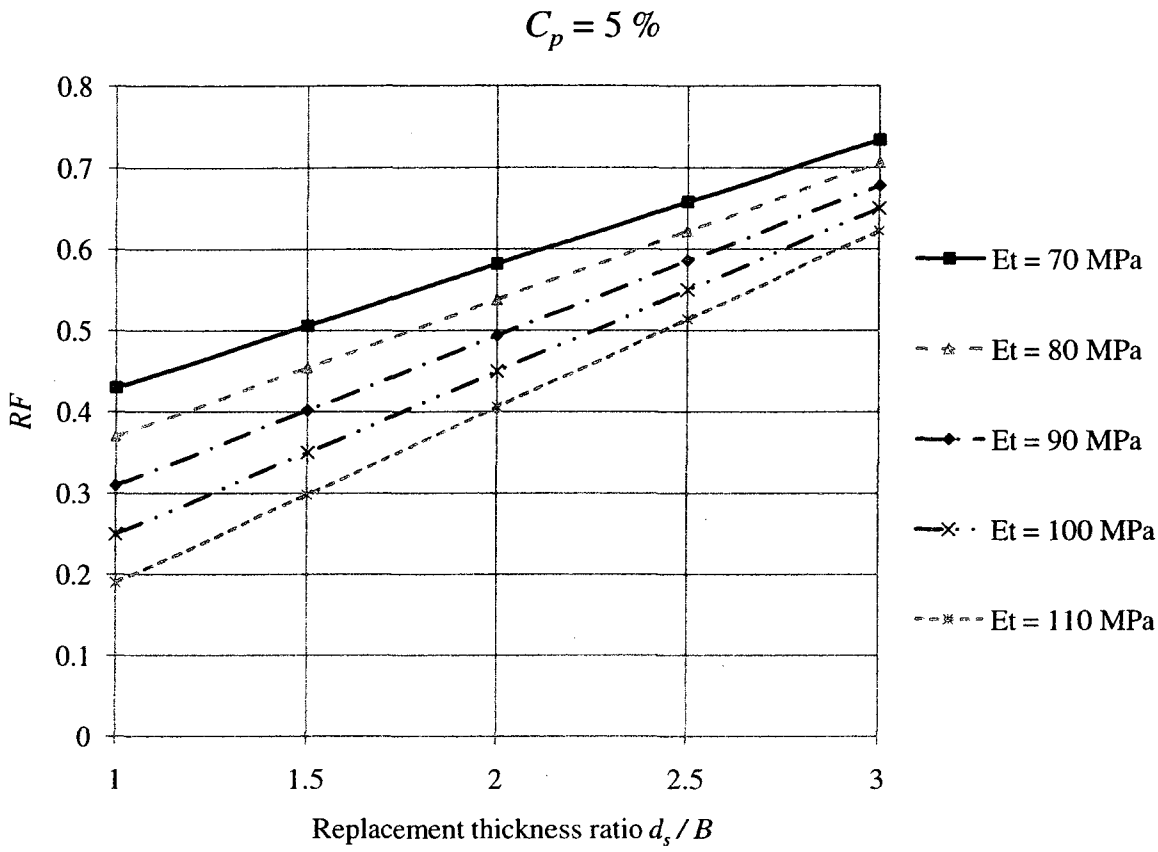

Figure (5-5): Reduction factor versus replacement thickness ratio for different geotextile types ($C_p = 5\%$)

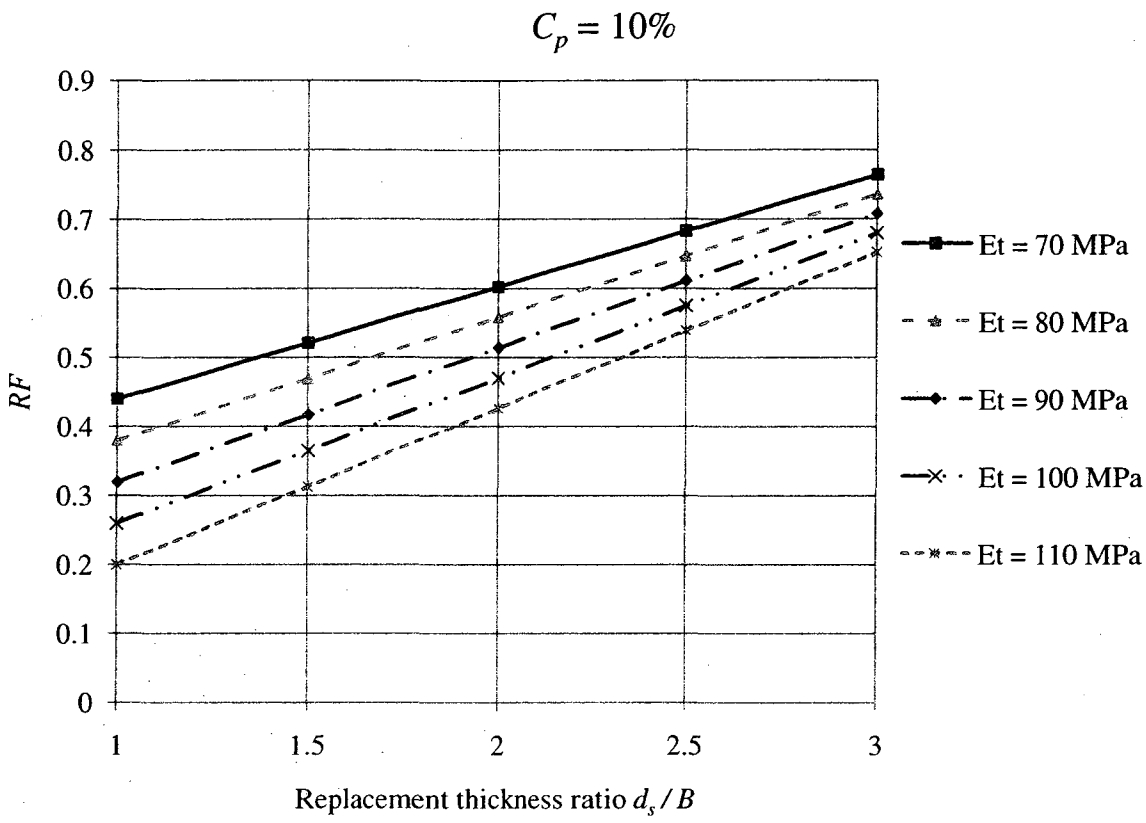

Figure (5-6): Reduction factor versus replacement thickness ratio for different geotextile types (C_p = 10%)

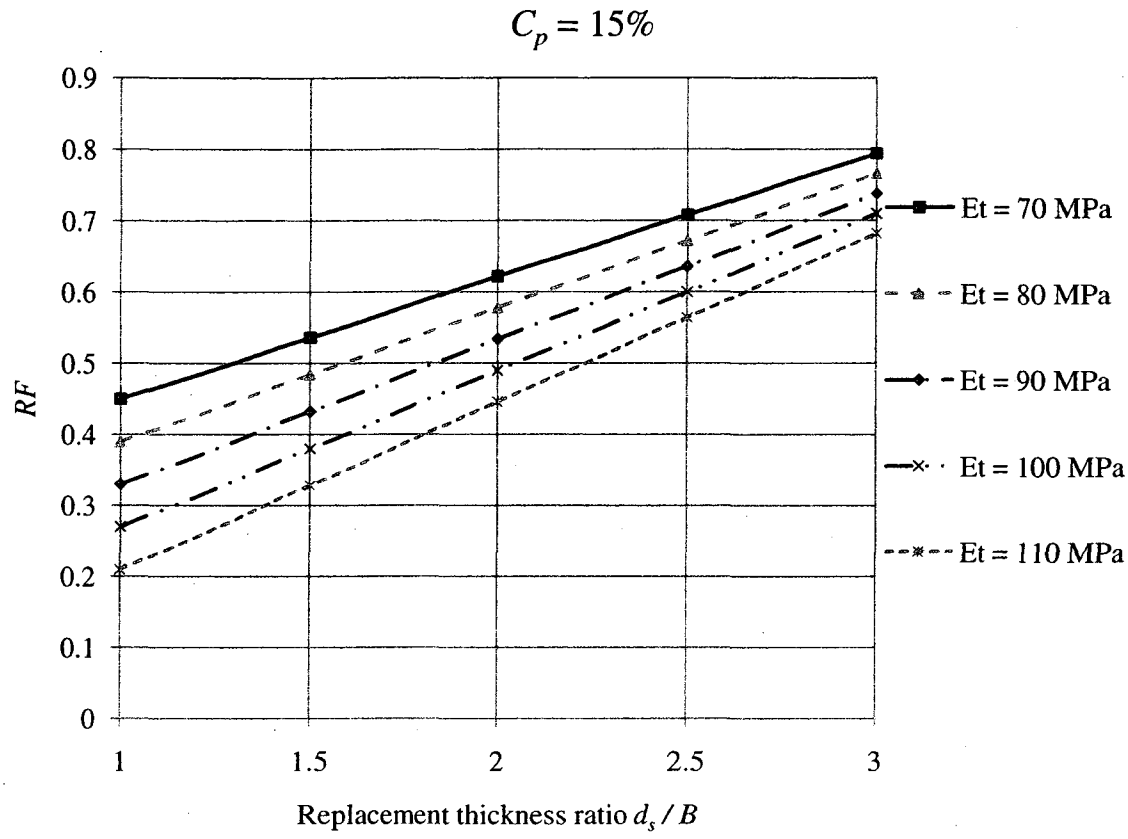

Figure (5-7): Reduction factor versus replacement thickness ratio for different geotextile types ($C_p = 15\%$)

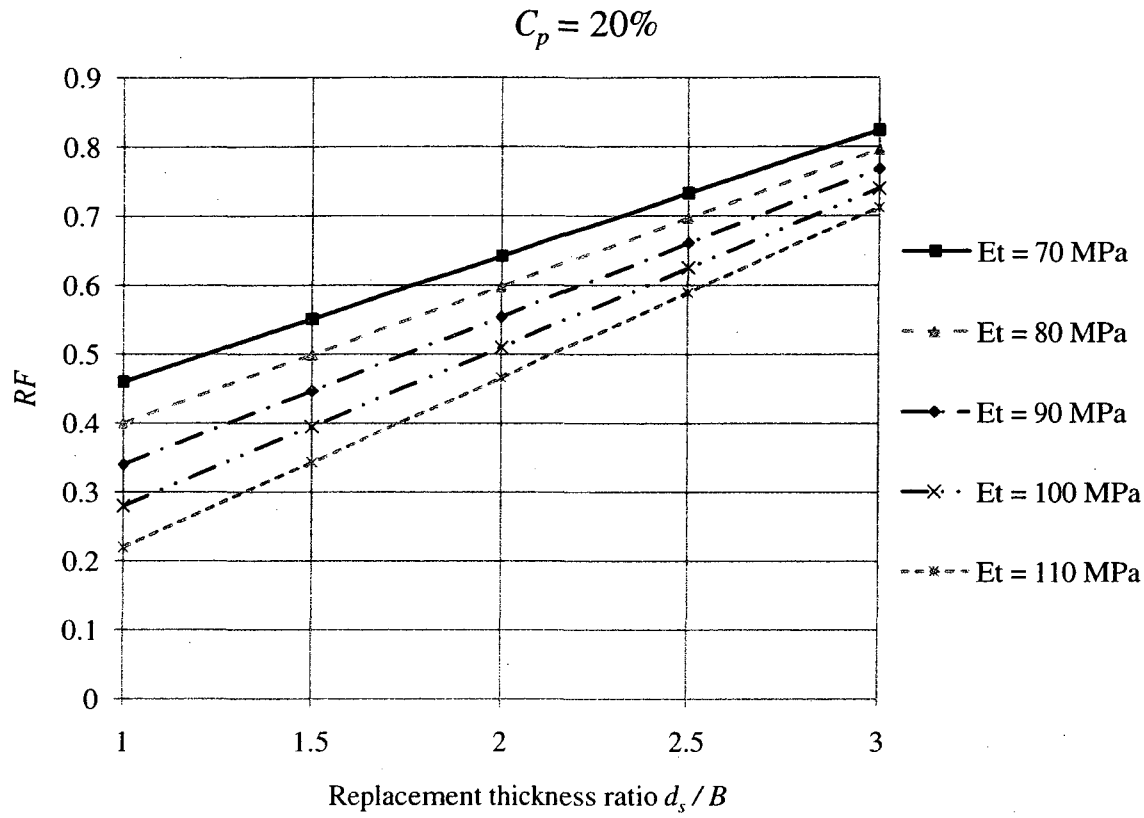

Figure (5-8): Reduction factor versus replacement thickness ratio for different geotextile types (C_p = 20%)

5.3. ANALYTICAL MODEL TO PREDICT STRAIN DEVELOPED IN THE GEOTEXTILE AT COLLAPSE

By idealization of the deformed shape of the geotextile layer at the interface between the two soil layers during loading and inundation, Figure (5-9) shows the deformed shape of the geotextile layer at collapse. Figure (5-10) presents photos for the deformed shape obtained from the test results, where it can be noted that the surface of the geotextile deformed beneath the footing forming almost a circular curve (concave) and from the two

sides from this curve almost two circular curves are formed (convex) and the tangent surface for these two curves is at the level of separation between the two soil layers (the level of the geotextile layer). This type of deformation occurred in tests carried out on soil C and is considered as case (1).

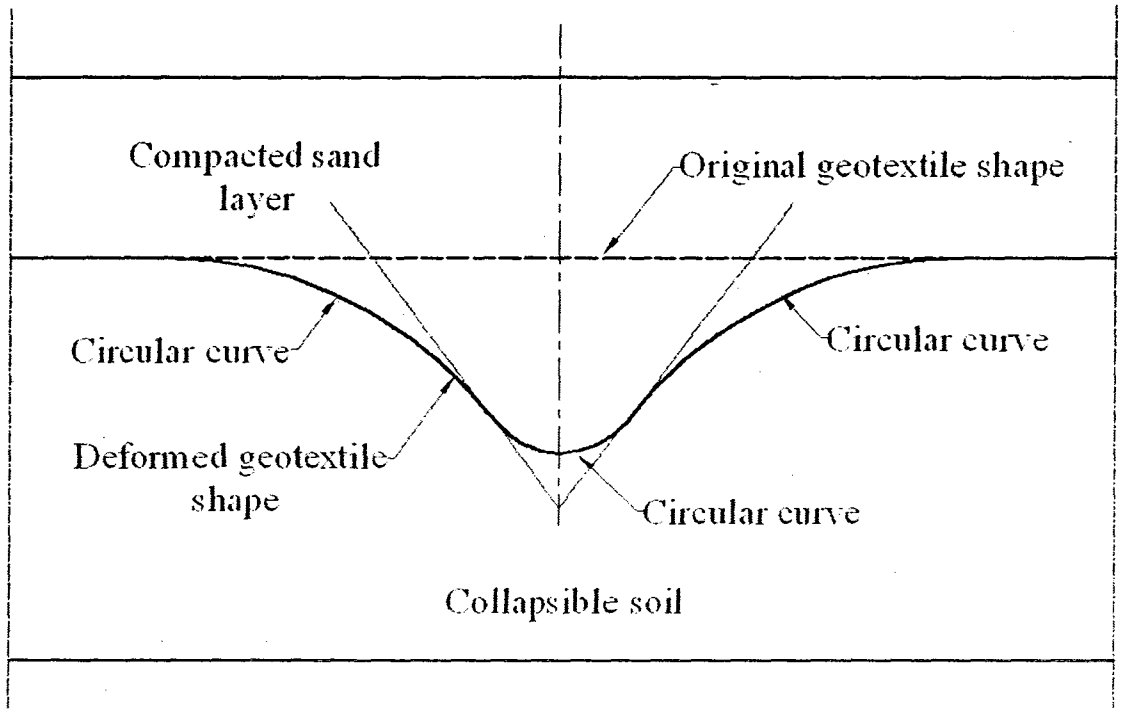

Figure (5-9): Idealized deformed shape of geotextile layer at collapse (case 1)

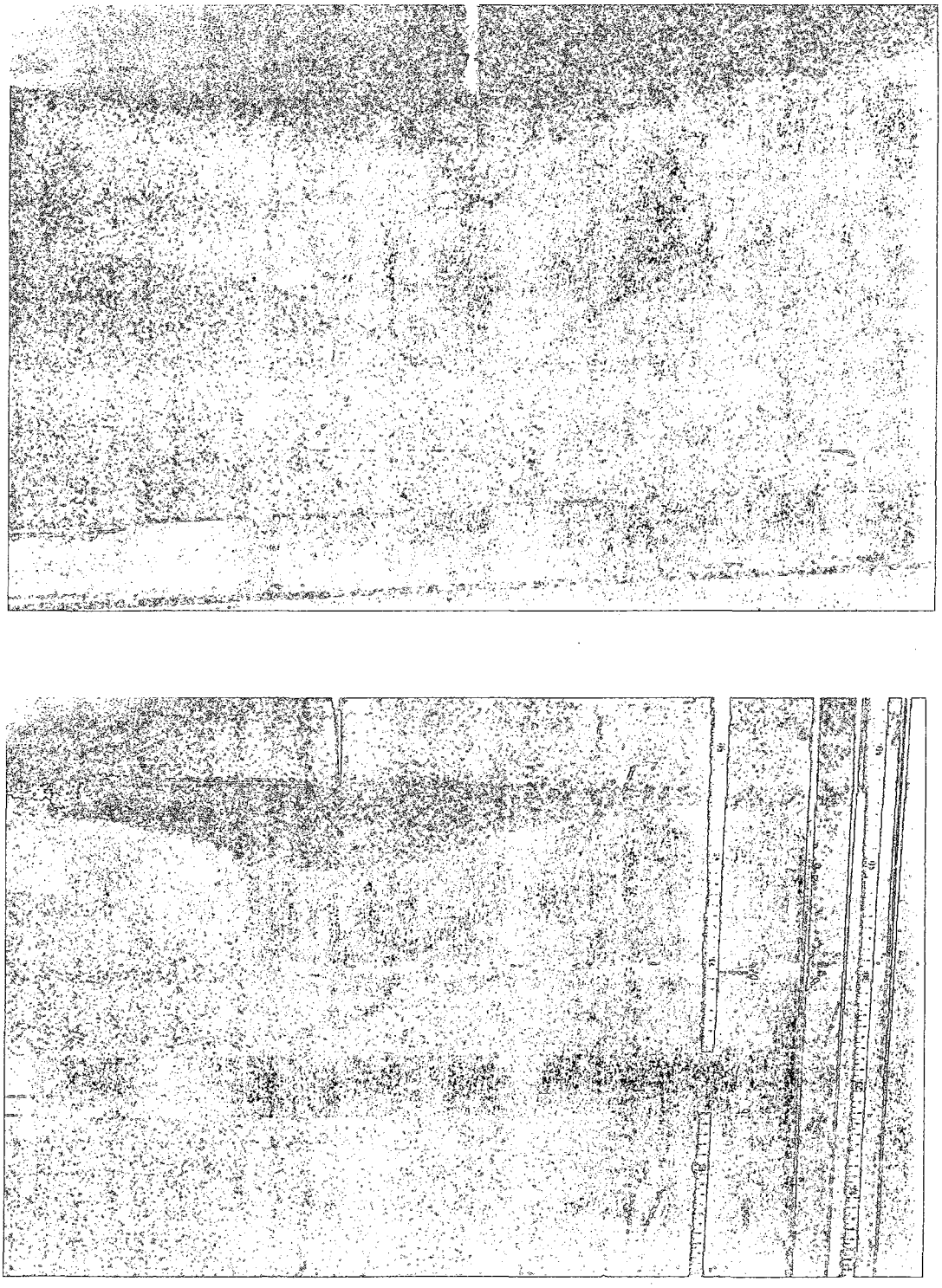

Figure (5-10): Geotextile deformed shape at inundation (case 1)

On the other hand, for tests carried out on soil A, the deformed surface was a little different. The geotextile under the footing was deformed like case (1) forming almost a concave circular curve and two convex curves but the tangent surface for these two curves is not at the level of separation between the two soil layers, but a line with an upward angle (δ_2) with the geotextile level. The collapsible soil is deformed and pushed upward pushing the geotextile layer upward as well. This case of deformation is idealized and presented in Figure (5-11), while Figure (5-12) presents pictures for test results carried out on soil A where this deformed shape is obtained and is considered as case (2).

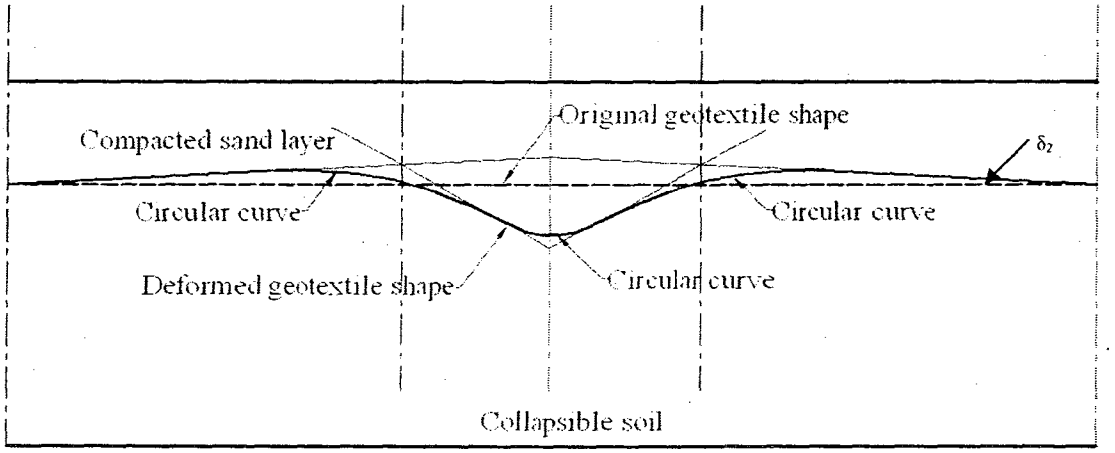

Figure (5-11): Idealized deformed shape of geotextile layer at collapse (case 2)

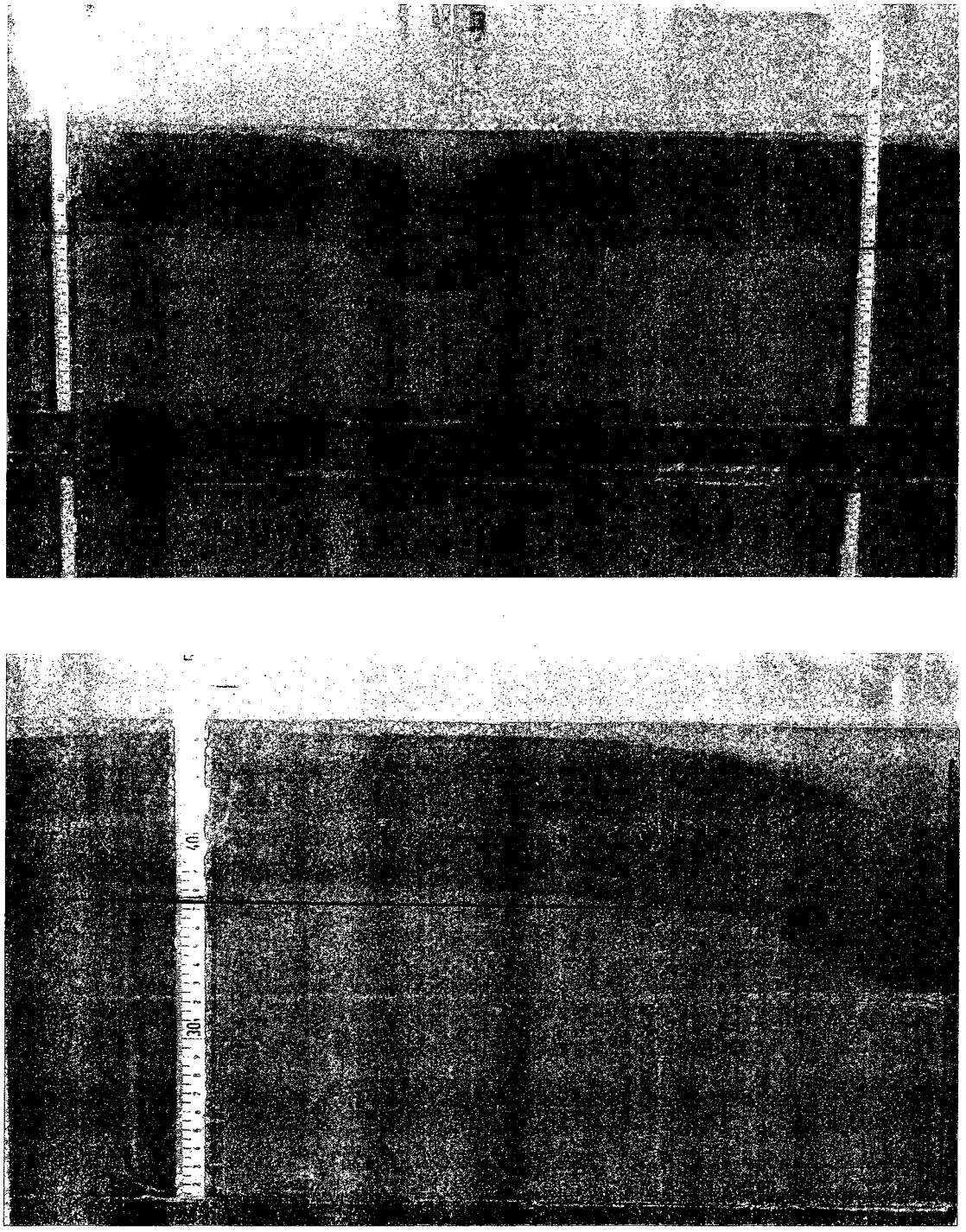

Figure (5-12): Geotextile deformed shape at inundation (case 2)

Analyzing the deformed shape of the geotextile at collapse is of great importance in determining the strain developed in the geotextile material, i.e. the type of geotextile to be used, and to fully determine the deformed shape and the length of geotextile needed for each job.

The main difference between the two cases is that in case (1) no upward movement of the geotextile and the collapsible soil beneath and the tangent points between the formed curves and the straight part of the geotextile are at the two soils interface level, while in case (2) these tangent points are pushed upwards above the original interface level with an upward angle of (δ_2) with the geotextile level.

The strain developed in the geotextile from case (2) will be determined and for the same measurements of the deformed shape it will be assumed that it took the profile as in case (1) and comparison will be carried out to determine the difference on the developed strain between the two cases.

Certain assumptions and facts have to be clarified prior to the analysis of the idealized deformation shape of the geotextile, which are as follows:

1. The geotextile deformation is symmetrical about the centerline of the footing.
2. The deformed profile is assumed to consist of a part of a circle having a concave shape connected from both sides with two parts of circles having convex shapes.
3. The connection between the concave and the convex curves through reflection points and the tangent for the two curves passes through this point inclined with the horizontal at an angle θ.

4. The part of the concave circle has a radius R_1 and curve length l_1 with a corresponding horizontal length before deformation equals to L_1, which is equal to the footing width (B) in all cases.
5. The two parts of the convex circles on each side of the center of the footing have a radius R_2 and curve length l_2 / 2 each with a corresponding horizontal length before deformation equals to L_2 / 2.
6. The total length of deformed geotextile equals to l_1 + l_2 corresponding to horizontal length of L before deformation.
7. Friction between the geotextile layer and the soils is not a part of this analysis and it is assumed, according to the range of the applied load on the footing that no slippage will occur between the soil and the geotextile.

The details of these assumptions and parameters are shown in Figure (5-13).

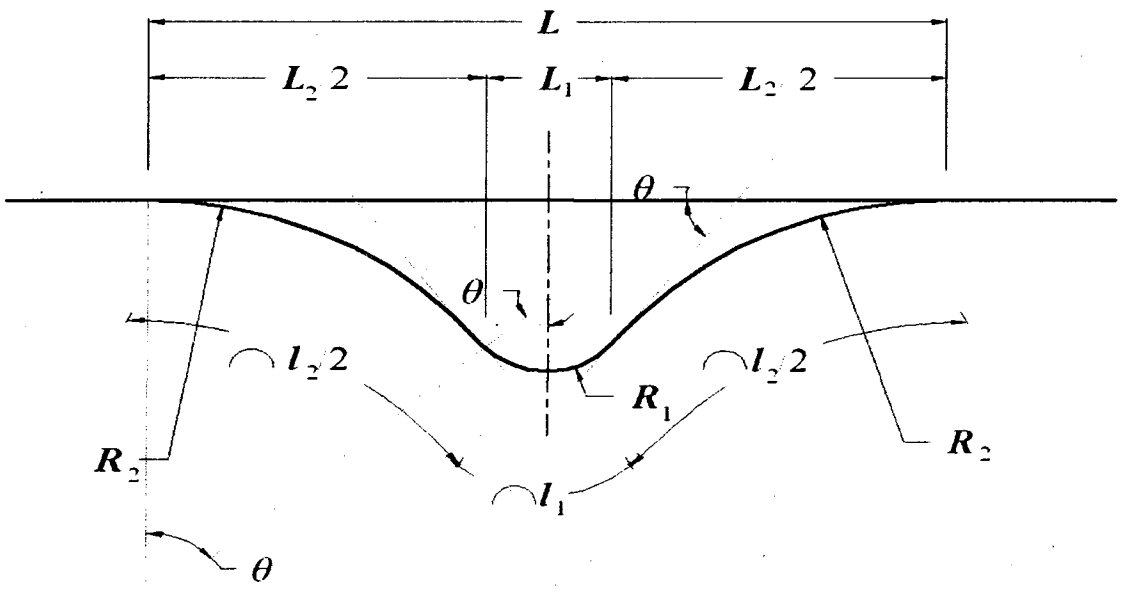

Figure (5-13): Details of geotextile deformed profile

The strain developed in the geotextile can be determined by analyzing the deformation profile as follow:

$$\sin\theta = \frac{L_1}{2R_1} \qquad \therefore R_1 = \frac{L_1}{2\sin\theta} \quad \text{..... (5-14)}$$

$$\frac{l_1}{2} = 2\pi R_1\left(\frac{\theta}{360}\right) \qquad \therefore l_1 = \pi R_1\left(\frac{\theta}{90}\right) \quad \text{..... (5-15)}$$

Similarly,

$$\sin\theta = \frac{L_2}{2R_2} \qquad \therefore R_2 = \frac{L_2}{2\sin\theta} \quad \text{..... (5-16)}$$

$$\frac{l_2}{2} = 2\pi R_2\left(\frac{\theta}{360}\right) \qquad \therefore l_2 = \pi R_2\left(\frac{\theta}{90}\right) \quad \text{..... (5-17)}$$

From (14) *and* (15)

$$l_1 = \frac{\pi L_1}{2\sin\theta}\left(\frac{\theta}{90}\right) = \frac{\pi L_1}{180}\left(\frac{\theta}{\sin\theta}\right) \quad \text{..... (5-18)}$$

From (16) *and* (17)

$$l_2 = \frac{\pi L_2}{2\sin\theta}\left(\frac{\theta}{90}\right) = \frac{\pi L_2}{180}\left(\frac{\theta}{\sin\theta}\right) \quad \text{..... (5-19)}$$

The elongation occurs in the geotextile (δ) can be calculated as follows:

$$\delta = [l_1 + l_2] - [L_1 + L_2] \quad \text{..... (5-20)}$$

Substituting the values of l_1 and l_2 from formulas (5-18) and (5-19) into formula (5-20), the value of the developed elongation in the geotextile can be written as:

$$\delta = \left[\frac{\pi L_1}{180}\left(\frac{\theta}{\sin\theta}\right) + \frac{\pi L_2}{180}\left(\frac{\theta}{\sin\theta}\right)\right] - [L_1 + L_2]$$

$$\delta = \left[\frac{\pi L_1}{180}\left(\frac{\theta}{\sin\theta}\right) - L_1\right] + \left[\frac{\pi L_2}{180}\left(\frac{\theta}{\sin\theta}\right) - L_2\right]$$

$$\delta = L_1\left[\frac{\pi}{180}\left(\frac{\theta}{\sin\theta}\right) - 1\right] + L_2\left[\frac{\pi}{180}\left(\frac{\theta}{\sin\theta}\right) - 1\right]$$

$$\delta = (L_1 + L_2)\left[\frac{\pi}{180}\left(\frac{\theta}{\sin\theta}\right) - 1\right] \quad \text{..... (5-21)}$$

$$\varepsilon_t = \frac{\delta}{L_1 + L_2} \quad \text{..... (5-22)}$$

From (21) *into* (22)

$$\varepsilon_t = \frac{(L_1 + L_2)\left[\frac{\pi}{180}\left(\frac{\theta}{\sin\theta}\right) - 1\right]}{(L_1 + L_2)}$$

$$\therefore\ \varepsilon_t = \left[\frac{\pi}{180}\left(\frac{\theta}{\sin\theta}\right) - 1\right] \quad \text{..... (5-23)}$$

The general shape of deformation after collapse in case (2) is presented in Figure (5-14). To make the necessary calculations for the strain developed in the geotextile, the deformed shape will be divided into three parts. Part (1) is shown in Figure (5-15) and it is the part directly under the footing.

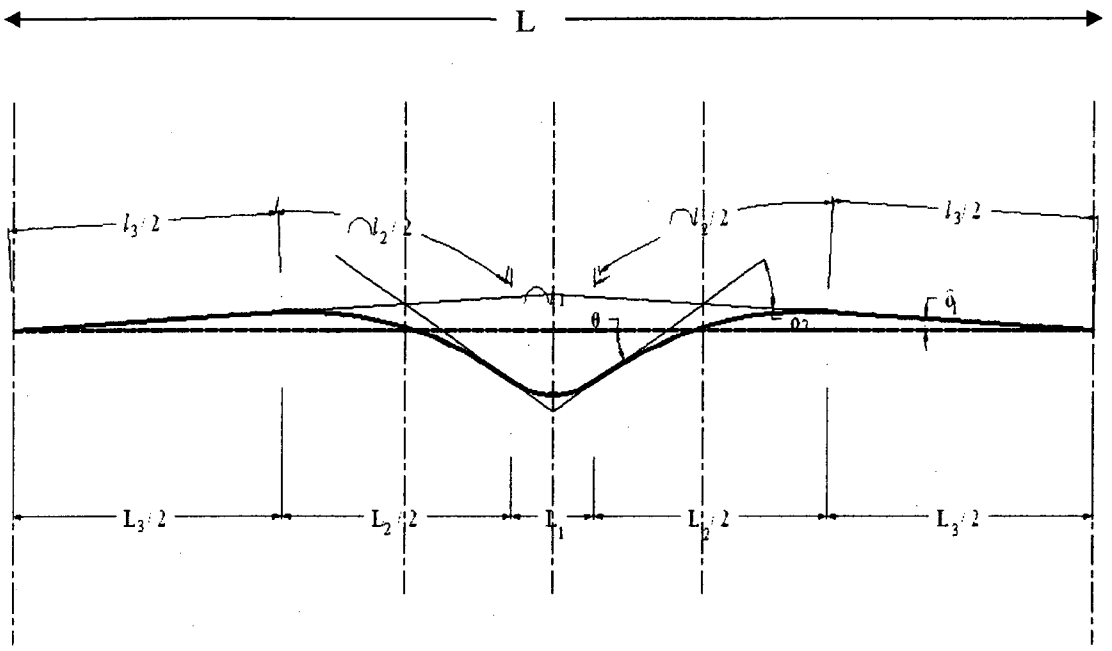

Figure (5-14): Detailed idealized deformed shape in case (2)

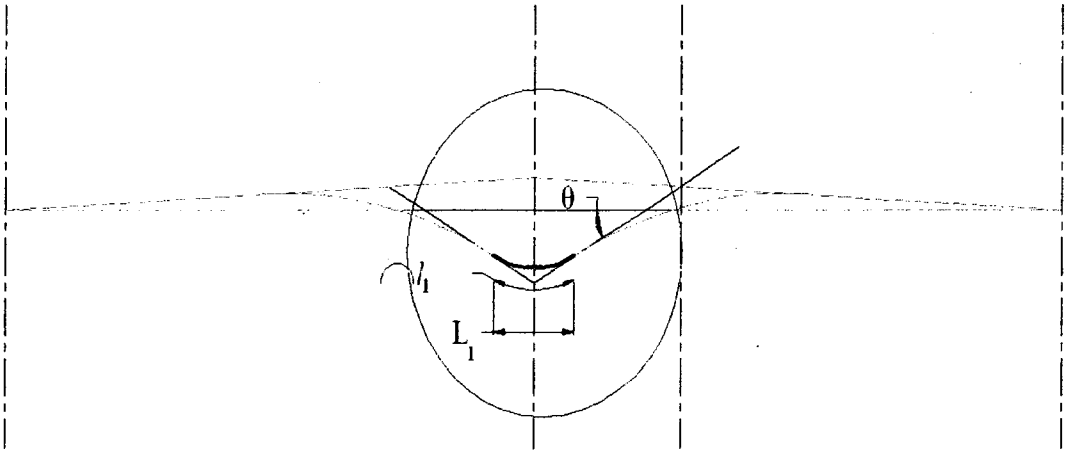

Figure (5-15): Details of part (1) in the deformed shape in case (2)

The original length of the geotextile at that part is equal to L_1 and the deformed length is equal to l_1. Following the assumptions for the idealized deformed shape, where $L_1 = B$, the following Formulas can be obtained,

$$l_1 = \frac{\pi B}{180}\left(\frac{\theta}{sin\theta}\right) \quad \text{(5-24)}$$

And

$$L_1 = B \quad \text{(5-25)}$$

Part (2) in the deformed shape is shown in Figure (5-16) that connects part (1) with part (3) and consists of a concave circular curve with length $l_2 / 2$.

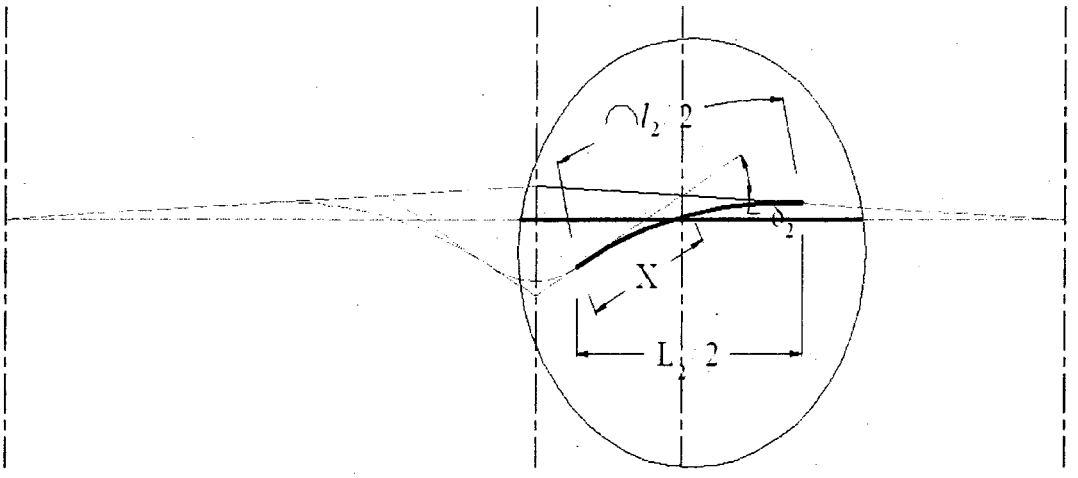

Figure (5-16): Details of part (2) in the deformed shape in case (2)

To determine the length $l_2 / 2$ with the knowledge of the tangent length (X) and the intersection angle (δ_2), as shown in Figure (5-16), the following formulas can be deduced:

$$X = R\tan\frac{\delta_2}{2} \text{ ..... And} \qquad R = \frac{\frac{l_2}{2}*180}{\delta_2\pi}$$

$$\therefore \frac{l_2}{2} = \frac{X\pi\delta_2}{180\ tan\frac{\delta_2}{2}} = \frac{X\pi}{180}\left(\frac{\delta_2}{\tan\frac{\delta_2}{2}}\right) \text{ ..... (5-26)}$$

Part (3) of the deformed shape is shown in Figure (5-17) and it is a straight part of the geotextile that is pushed upward with an angle (δ_1) with the horizontal.

$$\frac{l_3}{2} = \frac{\frac{L_3}{2}}{\cos\delta_1} = \frac{L_3}{2\cos\delta_1} \text{ ..... (5-27)}$$

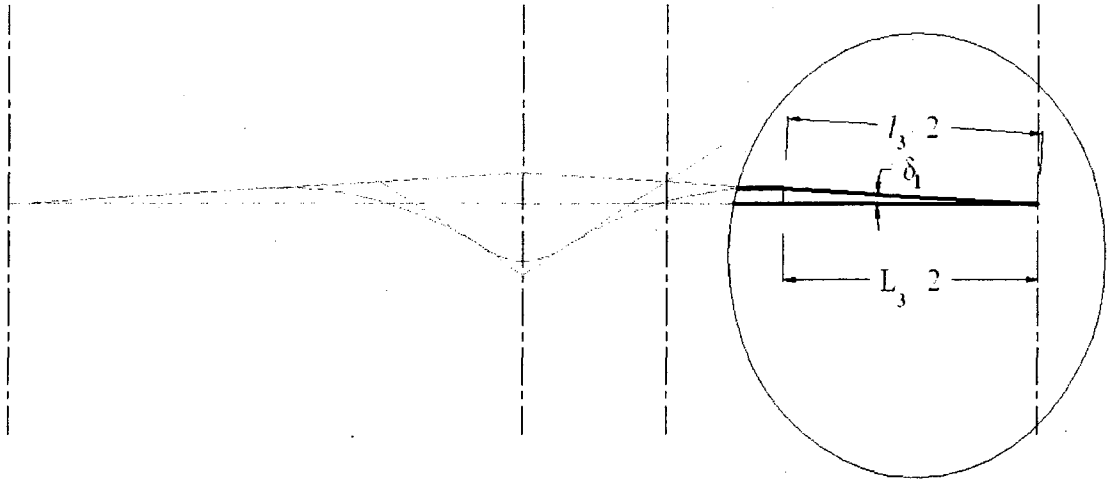

Figure (5-17): Details of part (3) in the deformed shape in case (2)

From Formulas (5-24), (5-26) and (5-27), the deformed length of the geotextile (l) will be equal to:

$$l = l_1 + \frac{2l_2}{2} + \frac{2l_3}{2}$$

$$l = \frac{\pi B}{180}\left(\frac{\theta}{sin\theta}\right) + \frac{2X\pi}{180}\left(\frac{\delta_2}{\tan\frac{\delta_2}{2}}\right) + \frac{2L_3}{2\cos\delta_1} \quad \text{.....(5-28)}$$

And,

$$L = L_1 + \frac{2L_2}{2} + \frac{2L_3}{2} \quad \text{.....(5-29)}$$

$$\delta = l - L \quad \text{.....(5-30)}$$

Where,

δ = Elongation

l = Total deformed length

L = total original length

And

$$\varepsilon_t = \frac{\delta}{L} \quad \text{.....(5-31)}$$

Where,

ε_l = Strain developed in the geotextile

Applying the results obtained by observations from tests carried out in soils that gave deformed shape according to case (2) (tests on soil A) and calculating the total deformed length (l) (Formula 5-28), and total original length (L) (Formula 5-29), the elongation on

the geotextile can be obtained (Formula 5-30) and hence, the strain developed in the geotextile (ε) (Formula 5-31).

Considering the same case but assuming that there is no upward movement for the soil (the geotextile), which means:

$\delta_1 = 0$ and accordingly

$\delta_2 = \theta$

Applying the same test results on Formulas developed for case (1), the strain developed in the geotextile in this case (ε) can be calculated.

To illustrate this, the data of the test carried out on soil A with partial replacement of the collapsible soil by thickness equal to $1B$ and with inundation stress of 125 kPa (test III-1), will be used to calculate the geotextile strain in both abovementioned cases. The obtained data was as follows:

$\theta = 28^{\circ}$, $\delta_1 = 2^{\circ}$, $\delta_2 = 30^{\circ}$, $X = 9.5$ cm, $(L_3/2) = 30$ cm, $L = 83.0$ cm

The calculated geotextile strain considering case (2) was equal to 3.58%, while it was equal to 4.2% if calculating considering the deformed shape as if in case (1).

This leads to the conclusion that the variation of the calculated geotextile strain between the two cases was 14.76% and that case (1) was more on the conservative side. Similarly, other comparisons were carried out and the variations were between 10% and almost 15%. Accordingly, the idealized deformed shape developed in case (1) can be used in the analysis and in the determination of the detailed geometry of the deformed

geotextile shape carried out in this research and equation (5-23) can be used to determine the value of the strain developed in the geotextile, which depends on the angle of deformation θ, which leads us to the determination of the deformation angle θ and the geometry of the deformed shape at collapse.

5.4. EMPIRICAL MODEL TO DETERMINE GEOMETRY OF DEFORMED SHAPE AT COLLAPSE:

The detailed deformed shape in Figure (5-13) shows that the main parameters that control the profile of the deformed shape are the deformation angle (θ), the deformed length (L) and the curvature radii (R_1 and R_2). The determination of these parameters will be discussed in the following sections.

Recent research was carried out by Al-Adili et al. (2009) to obtain the deformed shape of geosynthetics reinforcement and determine the settlement of a strip footing resting on reinforced granular bed on soft soil. In this research, the Finite Element Method was used and a computer program PLAXIS-8 was employed for this case. The main objective was to determine the settlement of the footing when slip of reinforcement is considered and compare it to the case when it is not allowed.

It is an interesting subject to investigate, but there are some concerns about the modelling itself and especially the boundaries for the model. The horizontal extent for the model was taken equal to 1.5 the footing width from each side of centerline of the footing and the vertical extent was taken equal to 1.75 the footing width. With these dimensions of the model, it is believed that there will be boundary effect on the obtained results.

The results from this investigation are presented herein to demonstrate the trend of the performance of the geosynthetics reinforcement, the soil layers and the deformed shape of the reinforcement layer. Results are shown in Figures (5-18) and (5-19) for the case of 1 layer of geogrid and when considering a phreatic surface respectively.

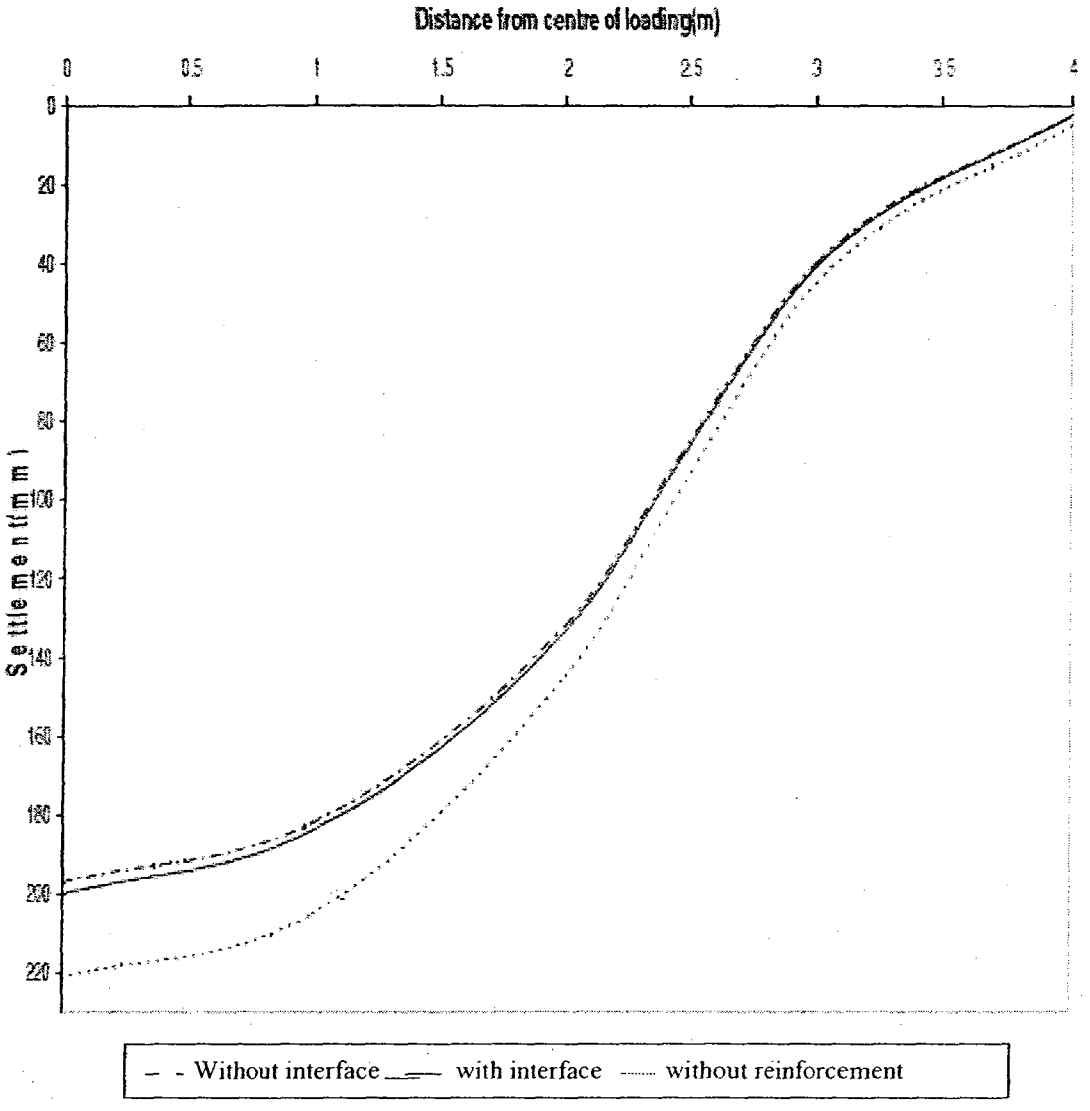

Figure (5-18): settlement profile for 1-layer of geogrid (Al-Adili et al., 2009)

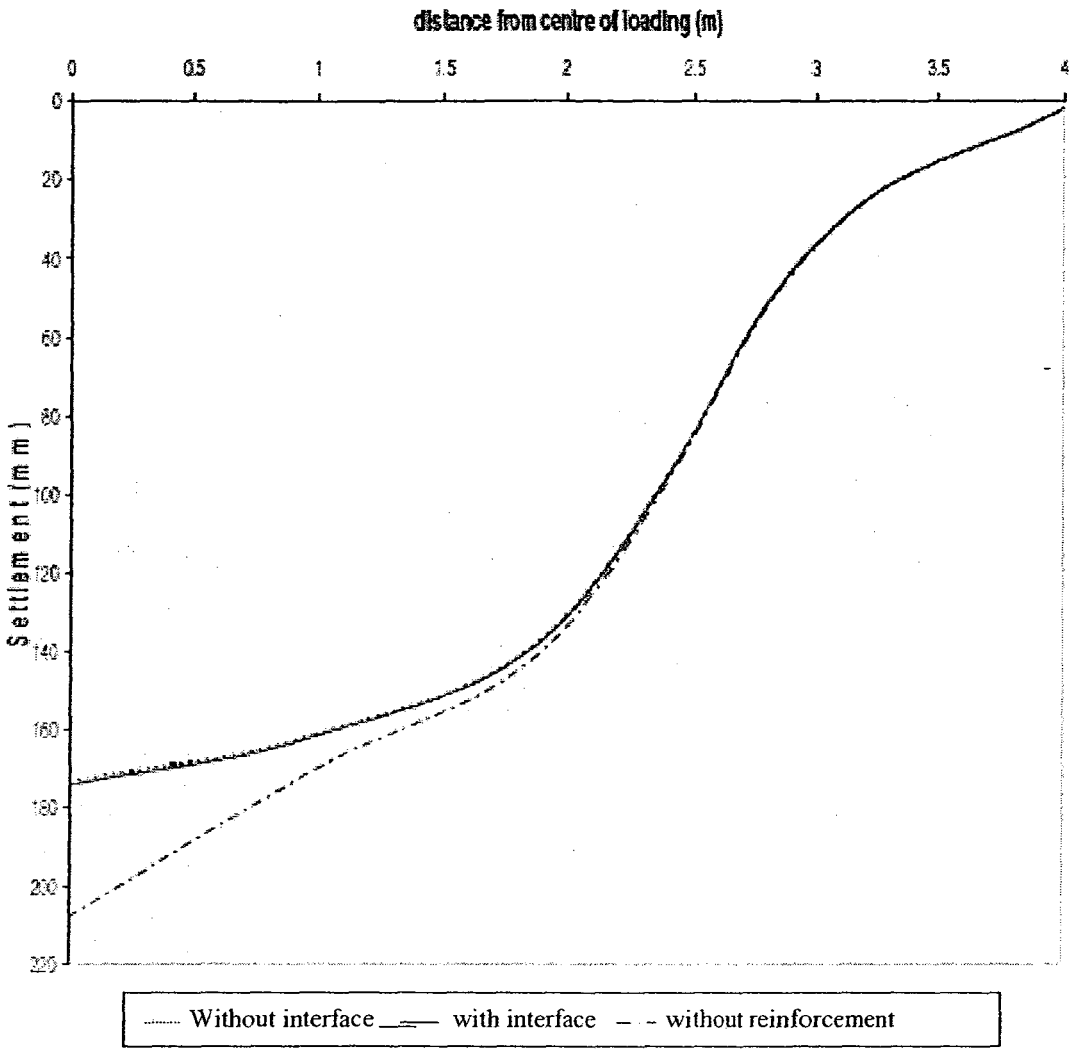

Figure (5-19): settlement profile for a load of 52.6 kN/m^2 for cases including a phreatic surface (Al-Adili et al., 2009)

Figures (5-18) and (5-19) show that the deformed shapes (settlement profiles) obtained by Al-Adili et al. (2009) when using reinforcement is similar to the ones obtained from the experimental tests carried out in this investigation and the idealized ones shown in Figures (5-9) and (5-11). According to this, in addition to the observations

while conducting the experimental tests, the obtained deformed shapes will be used in the following analysis.

Angle of deformation, θ, is affected by factors related to the footing (applied stress), factors related to collapsible soil (the collapse potential value) in addition to factors related to the geotextile material (modulus of elasticity). The relations between the tangent of deformation angle ($tan\ \theta$) and these factors are:

$$tan\ \theta \propto \sigma \quad \text{(5-32)}$$

$$tan\ \theta \propto C_p \quad \text{(5-33)}$$

$$tan\ \theta \propto \frac{1}{E_t} \quad \text{(5-34)}$$

From test results on soils with different collapse potentials, a relationship between the applied stress (σ) and the tangent of deformation angle ($tan\ \theta$) is obtained and shown in Figure (5-20). As the tests in this experimental research were carried out under minimum value of applied stress equals to almost $q_u / 4$ that is equal to 60 kPa. The value of applied stress, σ, in the following analysis will be replaced by the value (σ - 60). In Figure (5-20) the vertical axis will be shifted and the zero point for horizontal axis will be (σ - 60) as well.

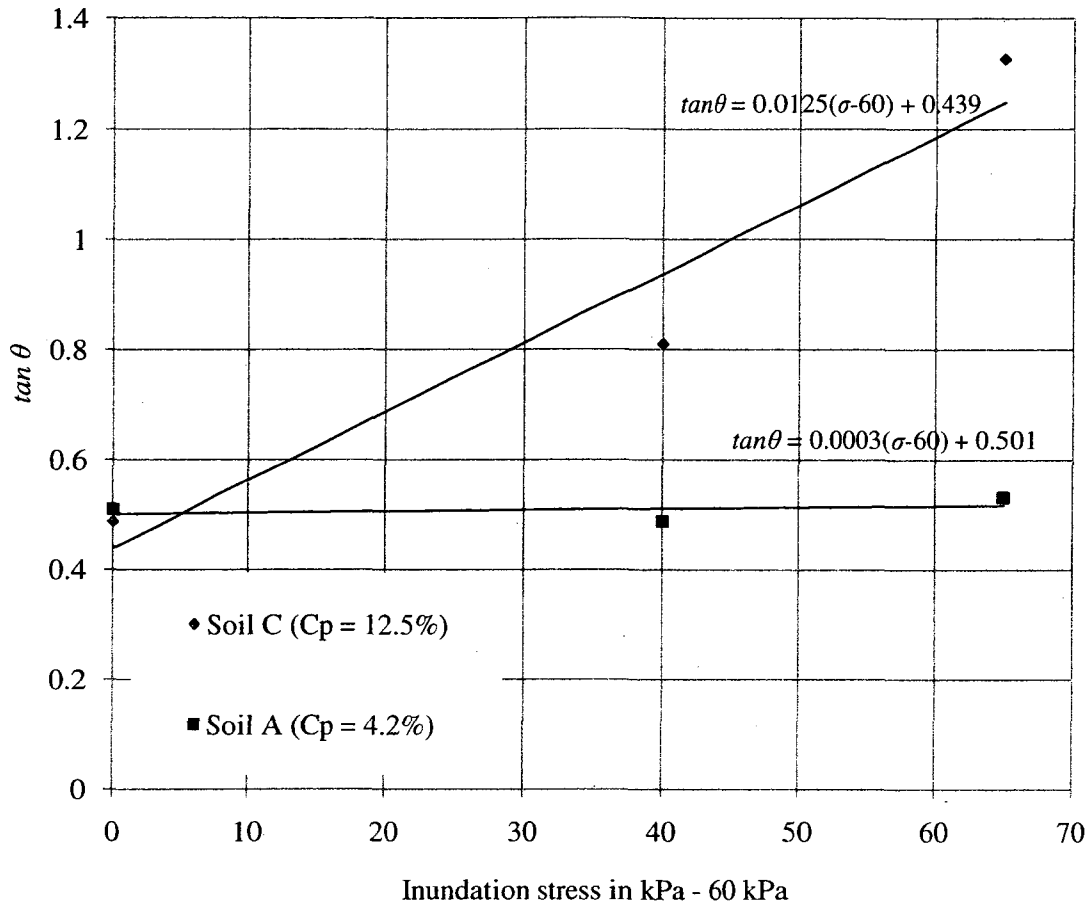

Figure (5-20): Angle of deformation versus inundation stress for different collapsible soils

It can be seen from Figure (5-20) that the formula (5-32) can be given in a general form of

$$tan\,\theta = a(\sigma - 60) + b \quad \text{..... (5-35)}$$

From Figure (5-20), the value of constant (a) varies with different collapsible soil types i.e. with the value of C_p. By analyzing Figure (5-20) and engineering judgement, it can be concluded that the variation of (a) with (C_p) can be assumed linear as in Figure (5-21) based on the best fitting for the experimental results.

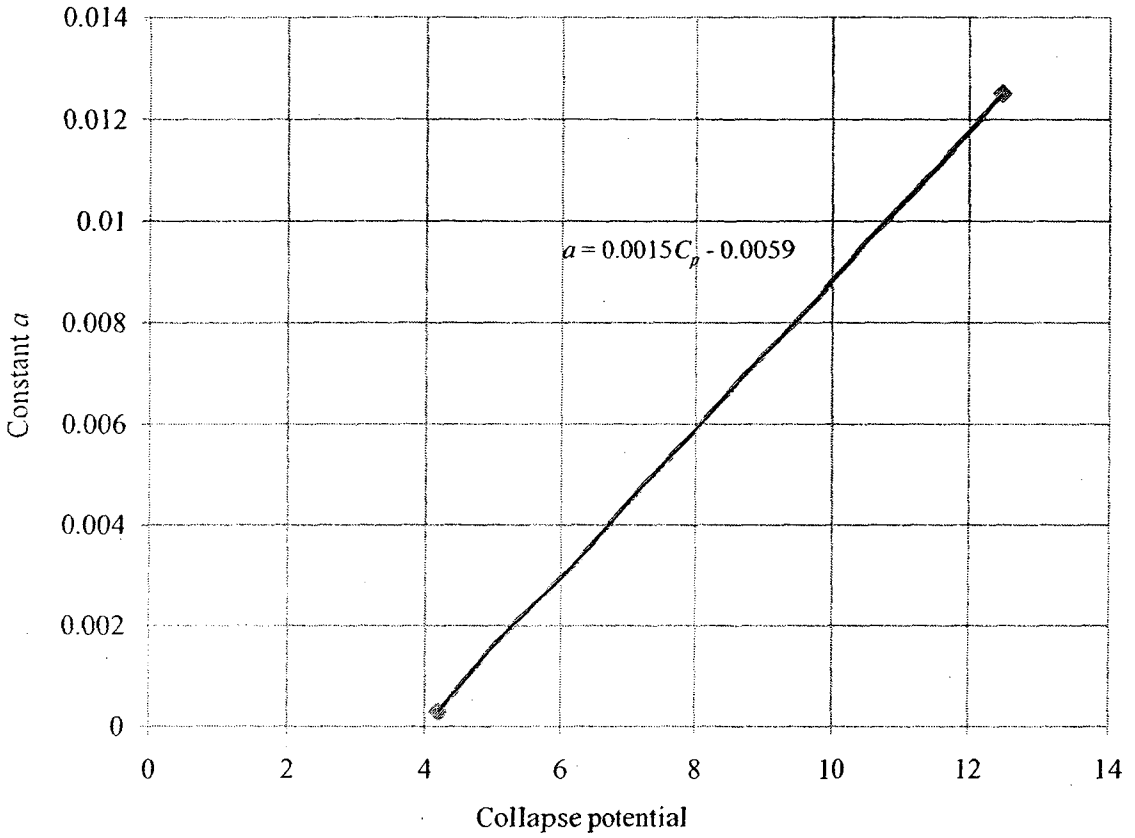

Figure (5-21): Variation of constant (a) with collapse potential

The trend of variation of constant (a) with the collapse potential can be represented by the following formula:

$$a = 0.0015C_p - 0.0059 \quad \text{(5-36)}$$

The value of constant (b) in formula (5-35) will be taken as the average value of the two equations obtained for soil A and C and that will give a value of constant (b) of 0.47 thus, formula (5-35) will be:

$$tan\ \theta = a(\sigma - 60) + 0.47 \quad \text{(5-37)}$$

The value of constant (a) can be calculated for different values of collapse potential using formula (5-36).

From the relation (5-33), the variation of the tangent of deformation angle ($tan\ \theta$) with the collapse potential value will take the form:

$$tan\ \theta = cC_p + d \quad \text{(5-38)}$$

Where c *and* d are constants

Also, from formula (5-34), the variation of the tangent of deformation angle ($tan\ \theta$) with the geotextile modulus of elasticity (E_t) will take the form:

$$tan\ \theta = \frac{e}{E_t} \quad \text{(5-39)}$$

Where e is a constant

Combining formulas (5-37), (5-38), and (5-39), the obtained equation is:

$$tan\ \theta = \frac{KC_p[a(\sigma-60)+0.47]}{E_t} \quad \text{(5-40)}$$

Where,

K constant

C_p soil's collapse potential in percentage

a variable depends on C_p and can be calculated from formula (5-36)

σ applied stress in kPa

E_t modulus of elasticity for the geotextile material in kPa

Using the results obtained from the tests on soils A and C (C_p = 4.2% and 12.5%), values for constant K can be obtained. As the variation between the collapse potential value and the constant K is expected to be linear, the results obtained for soils A and C will be connected in a linear relationship and a formula for this type of variation is obtained. This relationship is shown in Figure (5-22) and the formula representing this relationship is shown below (Formula 5-41).

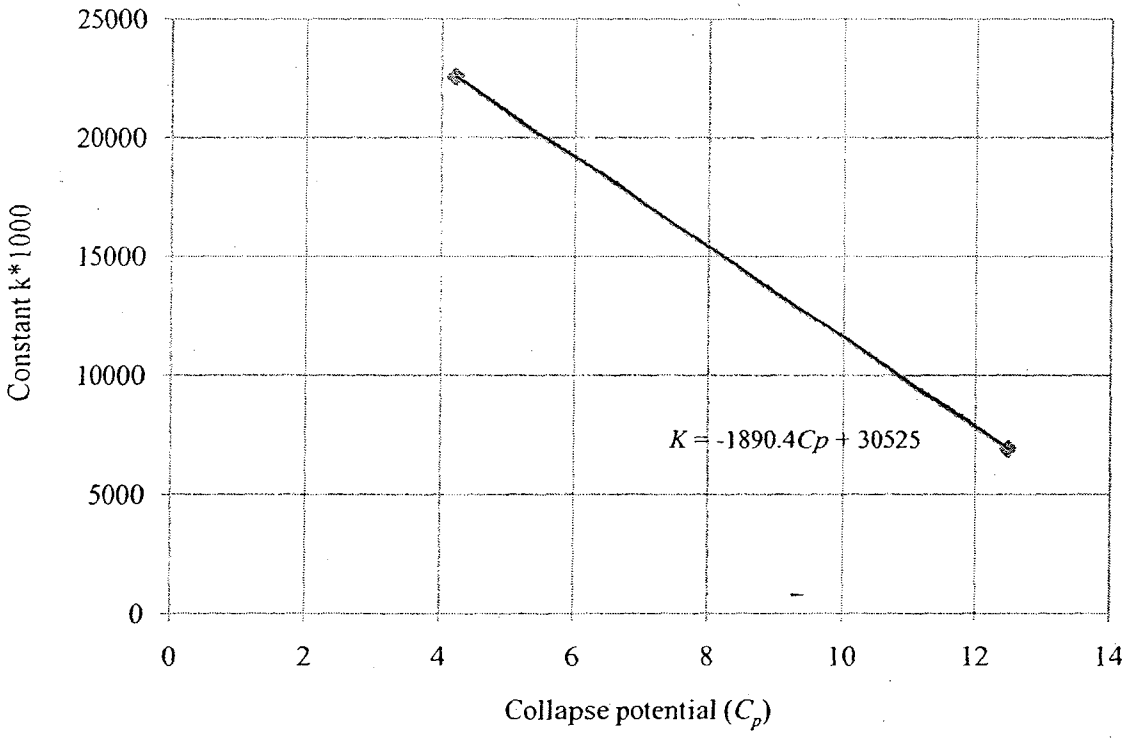

Figure (5-22): Variation of constant K with collapse potential

$$K = -1890.4C_p + 30525 \quad \text{(5-41)}$$

From Formula (5-40) where:

$$\tan\theta = \frac{KC_p[a(\sigma - 60) + 0.47]}{E_t}$$

and

$$a = 0.0015C_p - 0.0059 \quad \textit{and} \quad K = -1890.4C_p + 30525$$

Values of angles of deformation are determined.

Figure (5-23) shows a comparison between the values of the tangent of the deformation angle ($\tan\theta$) obtained from the empirical model and the experimental results; it can be noted that they are in good agreement.

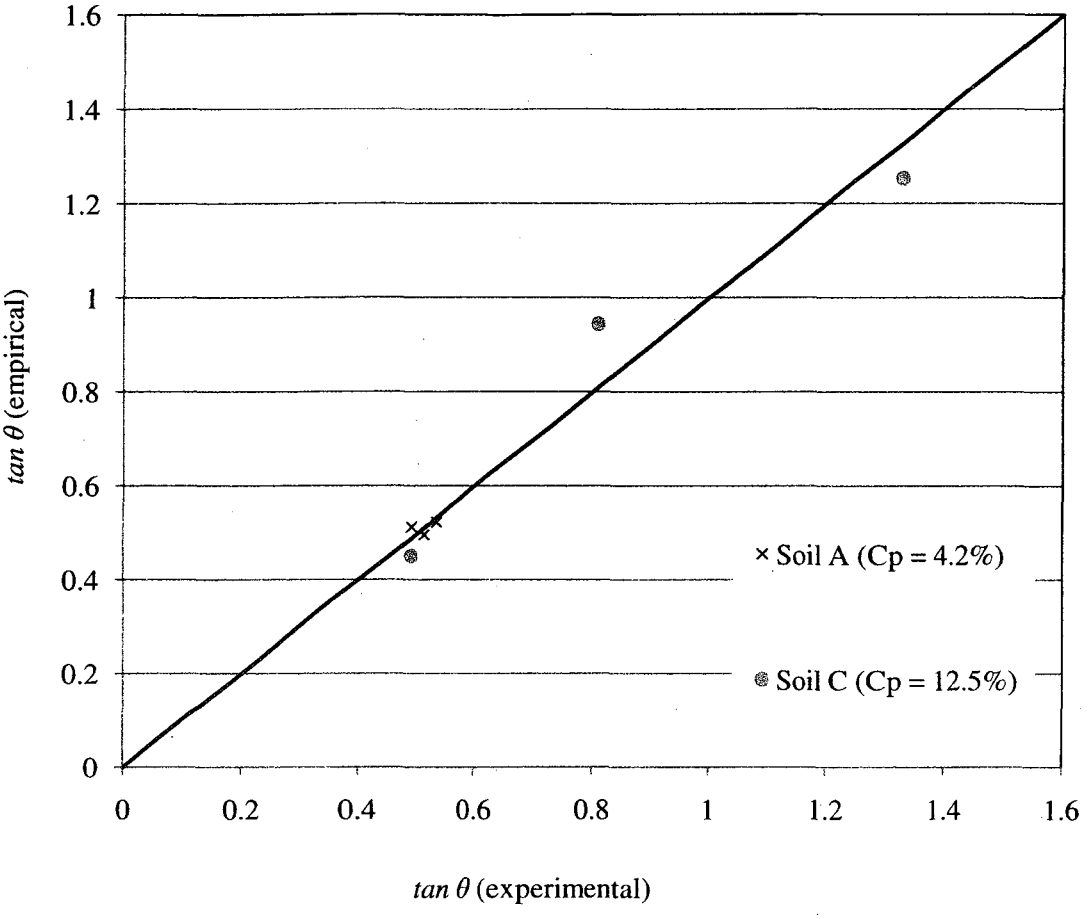

Figure (5-23): Experimental versus empirical values of the geotextile deformation angle (*tan* θ)

The determination of the deformed length extension, (L), with the deformation angle (θ), is essential to facilitate and establish the geometry of the deformed shape of the geotextile. The idealized deformed shape of the geotextile and its component obtained from experimental tests carried out in this investigation is shown in Figure (5-24).

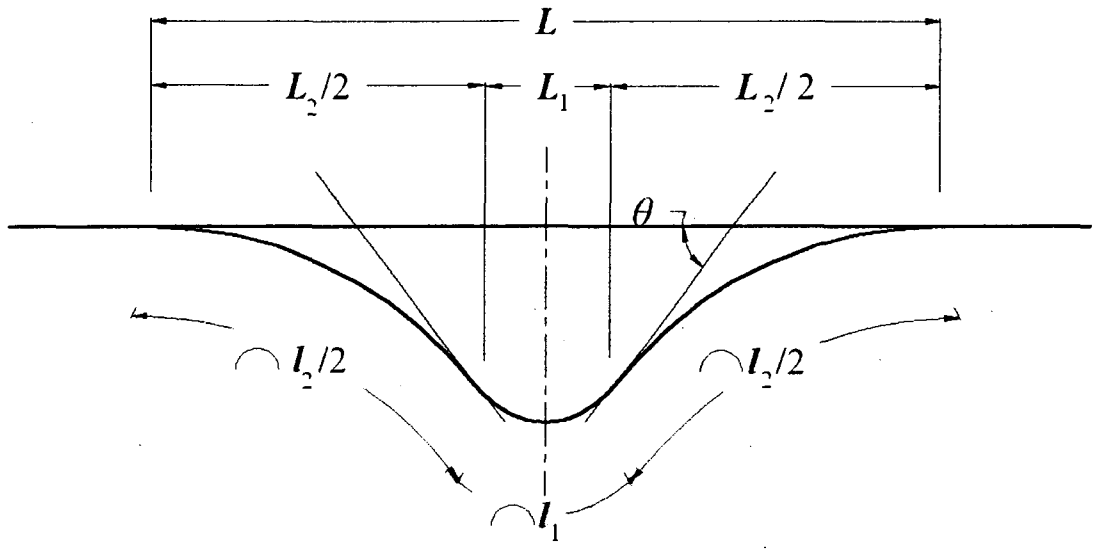

Figure (5-24): Idealized geotextile deformed shape

From tests carried out on soils A and C in this investigation with geotextile layer at the two soil layers interface with replacement thickness ratio (d_s / B) of 1, as it is the recommended replacement thickness ratio according to the results from this experimental investigation and from the observed deformed shape of the geotextile after inundation, it is noticed that the deformed length is function of the ratio of σ / E_t and the collapse potential (C_p).

$$L = a_1 \frac{\sigma}{E_t} + b \quad \text{..... (5- 42)}$$

Where (Figure 5-25)

a_1 = Assumed constant for different soil types under various stresses

$b \rightarrow f(C_p)$

$b = a_2 C_p + a_3$

$$\therefore L = a_1 \frac{\sigma}{E_t} + a_2 C_p + a_3 \quad \text{..... (5- 43)}$$

This conclusion is shown in Figure (5-25) after the vertical axis was shifted by 60 kPa in a way that the values of the stresses are presented as (σ-60) and Formula (5- 43) will be:

$$\therefore L = a_1 \frac{(\sigma - 60)}{E_t} + a_2 C_p + a_3 \quad \text{..... (5- 44)}$$

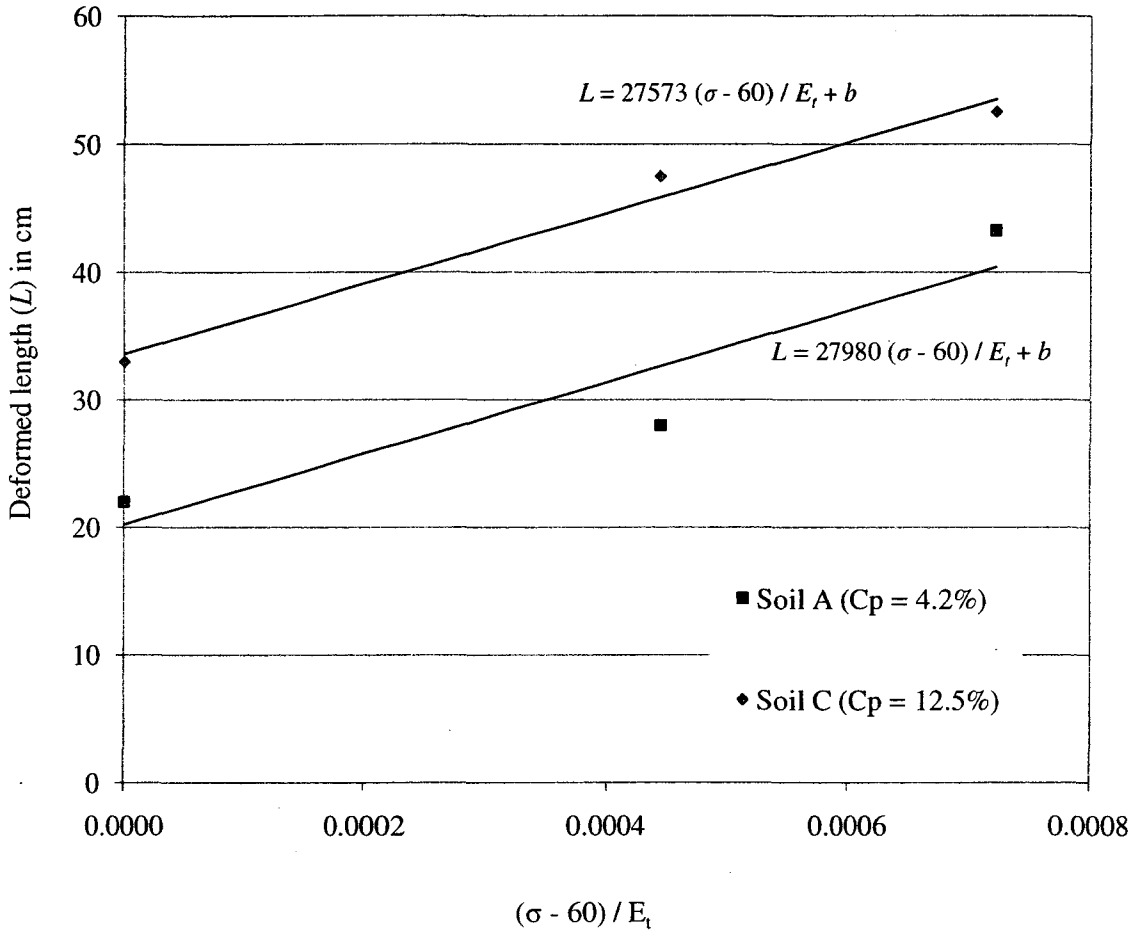

Figure (5-25): Relation between the geotextile deformed length (L) and ($\sigma - 60$) / E_t

From Figure (5-25) the value of constant a_1 slightly varies with C_p, accordingly, the assumption that a_1 is constant can be assumed valid for various collapsible soils.

Solving Formula (5-44) for constants a_2 and a_3 and assuming a_1 has an average value for the two types of collapsible soils used in these tests, the following values are obtained:

$a_1 = 2.8 * 10^4$, $a_2 = 1.6$, $a_3 = 13.6$

Formula (5-44) will become as follows:

$$L = 2.8 * 10^4 \frac{(\sigma - 60)}{E_t} + 1.6\, C_p + 13.6 \quad \text{..... (5- 45)}$$

Comparison of the results obtained from the experimental tests and the ones using Formula (5-45), indicates that they are in good agreement as shown in Figure (5-26).

After the determination of the geotextile deformed length (L) and to be able to define the geometry of the deformed geotextile shape after collapse, the radii R_1 and R_2 should be determined. The details of the deformed shape was shown in Figure (5-13) and following the assumptions stated in section 5-3, the determination of R_1 and R_2 will be as follows:

From Formula (5-14),

$$\sin\theta = \frac{L_1}{2R_1} \qquad \therefore R_1 = \frac{L_1}{2\sin\theta}$$

Following the assumptions and the observations from the experimental investigation as well where $L_1 = B$

$$\therefore R_1 = \frac{B}{2\sin\theta} \quad \text{..... (5-46)}$$

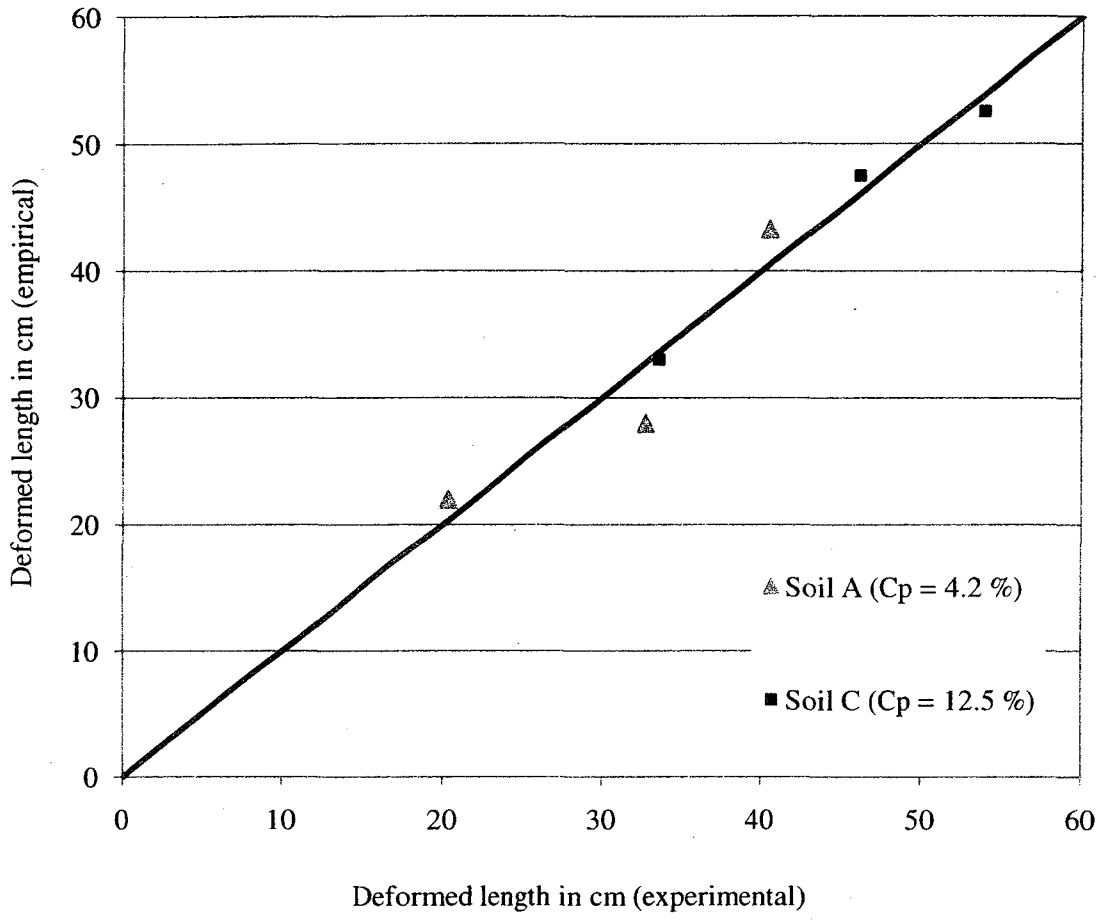

Figure (5-26): Experimental versus empirical values for deformed geotextile lengths (L)

Knowing the value of the footing width and the value of the deformation angle (θ), which can be determined from Formula (5-40), R_1 can be determined.

From Formula (5-16)

$$\sin\theta = \frac{L_2}{2R_2} \qquad \therefore R_2 = \frac{L_2}{2\sin\theta}$$

$$L_2 = L - L_1 = L - B \quad \text{(5-47)}$$

L is calculated from Formula (5-45) and B is the footing width, so, the value of L_2 can be determined and R_2 will be:

$$R_2 = \frac{L-B}{2\sin\theta} \quad \text{(5-48)}$$

By determining the values of the deformation angle (θ) from Formula (5-40), the deformed length (L) from Formula (5-45), the curvature radius (R_1) from formula (5-46) and the curvature radius (R_2) from Formula (5-48), the geometry of the deformed shape is fully defined.

5.5. DESIGN PROCEDURE

The analytical and empirical models developed in this chapter can be used to determine the settlement that a strip footing would experience if it is constructed on homogeneous collapsible soil or on partially replaced collapsible soil by compacted sand with / without the inclusion of geotextile layer at the interface between the two soil layers. From the experimental investigation carried out in this research, the most effective sand replacement thickness is equal to the footing width and in this case the strain developed in the geotextile in addition to the geometric profile for the deformed shape after collapse can be also determined.

The following are the design procedures recommended to be followed:

1. Calculations of the load that the strip footing will be carrying (σ).
2. Determination of the collapsible soil depth (d_c) from site investigation.

3. Determination of the soil's collapse potential from the conventional laboratory oedometer test or following formulas like the ones provided by Adnan and Erdil (1992) or by Ayadat and Hanna (2007).
4. Applying Formula (5-11) to calculate the expected collapse settlement in case of constructing on the homogeneous collapsible soil.

$$\Delta_h = d_c \, Log \, \sigma \left(0.0005 C_p + 0.296\right)$$

5. Compare the calculated settlement with the allowable according to the nature of the structure to be supported by the strip footing.
6. If the calculated settlement from step (4) is higher than the allowable values, partial replacement for the collapsible soil by compacted sand with / without the inclusion of geotextile layer at the interface should be carried out.
7. The expected settlement after applying the method mentioned in step (6) can be determined from Formula (5-12)

$$\Delta = \{RF\}\left[d_c \, Log \, \sigma \left(0.0005 C_p + 0.296\right)\right]$$

The values for *RF* can be determined from formula (5-13)

$$RF = \left\{1 - \left[-\frac{d_s}{B}\left(0.002 C_p + 0.03\right) + E_t * 10^{-6}\left(1.6 - 7.6\frac{d_s}{B}\right) + 0.19\right]\right\}$$

RF can be also determined from charts given in Figures (5-4) to (5-7) according to the collapse potential value, replacement thickness and the geotextile's modulus of elasticity.

8. By the variation of the geotextile type and / or the replacement thickness, the corresponding settlement can be determined till it is within the allowable limits.

9. The most effective replacement thickness was found to be equal to the footing width, consequently, the strain developed in the geotextile material can be determined using Formula (5-23)

$$\varepsilon = \left[\frac{\pi}{180}\left(\frac{\theta}{\sin\theta}\right) - 1\right]$$

10. The value of the angle of deformation can be determined from formula (5-40)

$$tan\,\theta = \frac{KC_p[a(\sigma-60)+0.47]}{E_t}$$

Where values of constants a and K can be determined from formulas (5-36) and (5-41) respectively

$$a = 0.0015C_p - 0.0059 \quad and \quad K = -1890.4C_p + 30525$$

11. The detailed deformed shape can be obtained by the determination of the deformed length (L) from formula (5-45)

$$L = 2.8 * 10^4 \frac{(\sigma-60)}{E_t} + 1.6\,C_p + 13.6$$

And the determination of the curvature radii (R_1 and R_2) from formula (5-46) and formula (5-48) respectively

$$R_1 = \frac{B}{2\sin\theta} \qquad \text{and} \qquad R_2 = \frac{L-B}{2\sin\theta}$$

CHAPTER 6

CONCLUSIONS AND RECOMMENDATIONS

6.1. CONCLUSIONS

Results obtained from this experimental investigation for surface rigid strip footing on homogeneous collapsible soil, partially replaced collapsible soil, partially replaced reinforced collapsible soil subjected to inundation due to the rise of ground water table lead to the following conclusions;

1. Collapse settlement for surface strip footing constructed on homogeneous collapsible soil and subjected to inundation depends on the collapsible soil depth, inundation stress and collapse potential value.
2. Partial replacement of collapsible soil with various thicknesses of compacted sand alone has slight effect on reducing the collapse settlement of the strip footing.
3. For collapsible soil with collapse potential of 4.2% (soil A in this investigation), collapse settlement reduction factors (*CSRFs*) of 14.5%, 10.8% and 6.9% were obtained when partially replacing the collapsible soil with compacted sand with thicknesses $1B$, $2B$ and $3B$, respectively, where B is the footing width. On the other hand, values for *CSRFs* for collapsible soil with 12.5% collapse potential were 13.4%, 8%, and 2.1% for the same replacement thicknesses. Thus, the most effective replacement thickness, within the tested range, was found to be equal to the footing width.
4. For the case of partially replaced collapsible soil reinforced with geotextile layer at the interface between the two soil layers, the most effective replacement

thickness, within the tested range, was found to be equal to the footing width as well. *CSRFs* of 76.3% for soil A and 61.5% for soil C were obtained for this case.

5. Using replacement thickness of $2B$ with geotextile layer at the interface, a *CSRF* of 32.3% was obtained for soil C while when using replacement thickness of $3B$, *CSRFs* of 41.8% and 19.9% were obtained for soils A and C respectively.
6. In case of partially replacing collapsible soil (C) with thickness of $1B$ and geotextile layer at the interface between the two soil layers, there is no significant effect on the collapse settlement when adding a geogrid layer at different depths. Placing a geogrid layer at a depth of $0.3B$ the *CSRF* obtained was 63.1% while it was 62.9% when placing the geogrid at depth of $0.7B$ compared to 61.5% without geogrid.
7. For replacement thickness of $1B$ for soil C and using 2 layers of geogrid within the compacted sand spaced at the third of the total replacement thickness, a *CSRF* of 65.4% was obtained while this value was 61.5% with geotextile alone.
8. The geogrid reinforcement has significant effect on increasing the *CSRF* when the replacement thickness is increased beyond $1B$, while keeping the geogrid spacing constant at the third of the total replacement thickness.
9. For replacement thickness of $2B$ for soil C and using 2 layers of geogrid within the compacted sand spaced at the third of the total replacement thickness, a *CSRF* of 74.4% was obtained while this value was 32.3% with geotextile alone.
10. For replacement thickness of $3B$ for soil C and using 2 layers of geogrid within the compacted sand spaced at the third of the total replacement thickness, a *CSRF* of 72.7% was obtained while this value was 19.9% with geotextile alone.

11. The most effective method to increase the *CSRF* for soil having high collapse potential (soil C where C_p = 12.5%) is to partially replace the collapsible soil with compacted sand with thickness equal to 2 times the footing width, geotextile layer at the interface and with the placement of 2 geogrid layers within the compacted sand. The *CSRF* obtained in this case is 74.4%. On the other hand, partially replacing collapsible soil (Soil C where C_p = 12.5%) with compacted sand with thickness equal to the footing width with geotextile layer at the interface will result in *CSRF* of 61.5%.
12. From the *CSRF* values obtained from the results, partially replacing the collapsible soil with compacted sand with thickness equal to the footing width with geotextile layer at the interface between the two soil layers is an effective and economical method to reduce, significantly, the collapse settlement of collapsible soils.
13. Empirical models were introduced that allow geotechnical engineers to predict the collapse settlement for rigid surface strip footing on homogeneous collapsible soils in addition to partially replaced collapsible soils, with replacement thickness in the range of 1 till 3 times the footing width, with / without geotextile layer at the interface between the two soil layers.
14. The strain developed in the geotextile layer, in case of replacement thickness of 1*B*, which was proved to be the most effective and economical method, can be determined by using the analytical model developed in this research. This allows the geotechnical engineer to select the suitable geotextile material for the project considered.

15. The detailed geometry of the deformed shape can be determined with the aid of a simple empirical model from which deformation on the geotextile can be obtained.

6.2. LIMITATIONS:

Results obtained in this investigation were from model tests, full scale tests are required to investigate the scale effect on these results.

6.3. RECOMMENDATIONS:

1. Conducting numerical modeling study on the collapse settlement of a strip footing considering the homogeneous and the partially replacement case, which will allow the study of additional parameters such as various replacement materials, various reinforcement materials placement and configurations etc.
2. Investigating the effect of different footings shape (square, rectangular and circular).
3. Examining the effect of friction between the geotextile layer and the soils on the collapse settlement of the footing.
4. Developing analytical and empirical models that allow the determination of collapse settlement in case of using geogrid reinforcement within the replacement layer

REFERENCES

Abdrabbo, F. M., Gaaver, K. E. and Elwakil. A. Z., 2004, "Behavior of square footings on single reinforced soil", Geotechnical Special Publication, n 124, pp. 1015-1026.

Adams, M. T. and Collin, j. G. 1997, "Large model spread footing load tests on geosynthetic reinforced soil foundations", Geotechnical and Geoenvironmental Engineering, ASCE, Vol. 123, No. 1 pp. 66-72.

Adnan, B., A., and Erdil, T., R., 1992, "Evaluation and control of collapsible soils", Journal of Geotechnical Engineering, ASCE, Vol. 118, No. 10, pp. 1491-1504.

Akiinmusuru, J.O., and Akinbolade, J. A., 1981, "Stability of loaded footings on reinforced soil", Geotechnical Engineering, ASCE, Vol. 107, No. GT6, pp. 819-827.

Al-Adili, A., Chandra, S. and Sivakugan, N., 2009, "Slippage effect on the settlement response of a granular soft soil system", Proceedings of the 17th International Conference on soil Mechanics and geotechnical engineering, Alexandria, Egypt, pp: 853-856

Alawaji, H. A., 2001, "Settlement and bearing capacity of geogrid reinforced sand over collapsible soil", Geotextiles and Geomembranes, Vol. 19, pp. 75-88.

Andrawes, K. Z., McGown, A., and Wilson-Fahmy, R. F., 1983, "The behaviour of a geotextile reinforced sand loaded by a strip footing", Proc. the 8th European conference on soil mechanics and foundation Engineering, Helsinki, pp. 329-334.

Annual Book of ASTM Standards Designation: D 5333-03 (2003). *Standard test method for measurement of collapse potential of soils, Vol. 04.09*

Ata, A. and Vipulanandan, C., 1998, "Cohesive and adhesive properties of Silicate grout on grouted sand behavior", Geotechnical and Geoenvironmental Engineering, ASCE, Vol. 124, No. 1, pp. 38-44.

Ata, A. and Vipulanandan, C., 1999, "Factors affecting mechanical and creep properties of Silicate grouted sands", Geotechnical and Geoenvironmental Engineering, ASCE, Vol. 125, No. 10, pp. 868 - 876.

Ayadat, T. and Hanna, A. M., 2005, "Encapsulated stone columns as a soil improvement technique for collapsible soil", Ground Improvement, 9, No. 4, pp. 137 – 147.

Ayadat, T. and Hanna, A. M., 2007, "Prediction of collapse behavior in soil", European Journal of Civil Engineering, 9, No. 5, pp. 603 - 619.

Badeev, S. Yu., Soshin, M. V., Kuzin, B. N. and Isaev, B. N., 1987, "Experience in chemical stabilization of loess at the base of bored injection piles", Soil Mechanics and Foundation Engineering, Vol. 24, No. 2, pp. 72 – 75.

Bara, J., P., 1976, "Collapsible soils," presented at the ASCE Annual Convention and Exposition, held at Philadelphia, USA.

Basudhar, P. K., Dixit, P. M., Gharpure, A, and Deb, K., 2008, "Finite element analysis of geotextile-reinforced sand-bed subjected to strip loading", Geotextiels and Geomembranes, Vol. 26, pp. 91 – 99

Basudhar, P.K., Saha, S., and Deb, K. (2007). "Circular footings resting on geotextile reinforced sand bed." Geotextiels and Geomembranes, Vol. 25, pp. 377 – 384.

Binquet, J., and Lee, K. L., 1975 a, "Bearing capacity tests on reinforced earth slabs", Geotechnical Engineering division, ASCE, Vol. 101, No. GT12, pp. 1241-1255.

Binquet, J., and Lee, K. L., 1975 b, "Bearing capacity tests on reinforced earth slabs", Geotechnical Engineering division, ASCE, Vol. 101, No. GT12, pp. 1257-1275.

Boushehrian, J. H. and Hataf, N., 2003, "Experimental and numerical investigation of the bearing capacity of model circular and ring footings on reinforced sand", Geotextiles and Geomembranes, Vol. 21, pp. 241-256.

Bowles, J.E., 1984, "Physicals and Geotechnical properties of soils", McGraw-Hill, Inc.

Burd, H. J., and Frydman, S., 1997, "Bearing capacity of plane-strain footings on layered soils", Canadian Geotechnical Journal, Vol. 34, pp. 241-253.

Burd, H.J., 1995, "Analysis of membrane action in reinforced unpaved roads", Canadian Geotechnical Journal, Vol. 32, pp. 946-956.

Chen, Q., Abu-Farsakh, M.Y., Sharma, R., and Zhang, X. 2007, "Laboratory investigation of behavior of foundations on geosynthetic reinforced clayey soil." Transportation research record, pp. 28 – 38.

Das, B. M., 1988, "Shallow foundation on sand underlain by soft clay with geotextile interface", Geotechnical Special Publication, n 18, pp. 112-126.

Das, B. M., khing, K. H., and Shin, E. C., 1998, "Stabilization of weak clay with strong sand and geogrid at sand clay interface", Transportation Research Record, No. 1611, pp. 55-62.

Day, Robert,W., 2006, "Foundation engineering handbook : design and construction with the 2006 international building code", New York : McGraw-Hill, 2006.

Dembicki, E., Jermolowicz, P., and Niemunis, A., 1986, "Bearing capacity of strip foundation on soft soil reinforced by geotextile", Proc., Third International Conference on Geotextiles, Vienna, Austria, pp. 205-209.

El-Naggar, M. E., Kennedy, J. B., and Ibrahim, E. M., 1997, "Mechanical properties of reinforced soil", Composites Part B: Engineering, vol. 28, No. 3, pp. 275-286

Evstatiev, D., 1988, "Loess improvement methods", Engineering Geology, Vol. 25, pp. 341 – 366.

Fragaszy, R. J., and Lawton, E., 1984, "Bearing capacity of reinforced sand subgrades", Geotechnical Engineering, ASCE, Vol. 110, No. GT10, pp. 1500-1507.

Fragaszy, R., Lawton, E. and Asgharzadeh-Fozi, Z., 1983, "Bearing capacity of reinforced sand", Proc. 8th European Conference of SMFE, Helsinki.1, pp. 357-360.

Guido, V. A., Biesiadecki, G. L., and Sullivan, M. J., 1985, "Bearing capacity of a geotextile reinforced foundation", proceedings of the 11th International Conference on Soil Mechanics and foundation Engineering, San Francisco, Vol. 3, pp. 1777-1780.

Guido, V. A., Chang, D. K., and Sweeny, M. A., 1986, "Comparison of geogrid and geotextile reinforced slab", Canadian Geotechnical Journal, Vol. 23, No. 4, pp. 435-440.

Guido, V. A., Knueppel, J. D. and Sweeny, M. A., 1987, "Plate loading tests on geogrid-reinforced earth slabs", geosynthetic 1987 Conference, New Orleans, USA, pp. 216-225.

Haeri, S. M., Noorzad, R., and Oskoorouchi A. M., 2000, "Effect of geotextile reinforcement on the mechanical behavior of sand", Geotextiles and Geomembranes, Vol. 18 pp. 385-402.

Hepworth, R. C., and Langfelder, J., 1988, "Settlement and repairs to cement plant in central Utah", Int. Conf. On Case Histories in Geotech. Engrg., Univ. of Misouri-Rolla, Rolla, Mo., pp. 1349 – 1354.

Hirao, K., Yasuhara, K., Takaoka, K., Nishimura, J. and Tanabashi, Y., 1992, "Laboratory model tests on the application of composite fabrics to soft clay ground", Proc., Earth Reinforcement Practice, Balkema, Fukuoka, Kyushu, Japan, pp. 601-606.

Houston, S. L., and Houston, W. N., 1997, "Collapsible soil engineering," Unsaturated Soil Engineering Practice, Geotechnical Special Publication No. 69, ASCE, pp. 199-232.

Houston, S. L., Houston, W. N. and Lawrence, C. A., 2002, "Collapsible soil engineering in highway infrastructure development", Journal of Transportation Engineering, Vol. 128, No. 3, pp. 295 – 300.

Houston, S. L., Houston, W. N., Zapata, C. E., and Lawerence, C., 2001, "Geotechnical engineering practice for collapsible soils," Journal of Geotechnical and Geological Engineering, Vol. 19, pp. 333-355.

Houston, W. N. and Houston, S. L., 1989, "State of the practice: Mitigation measures for collapsible soil sites", Footing Engineering: Current Principles and Practices, Evanston, IL, USA, pp. 161 – 175.

Huang, C. C. and Tatsuoka, F., 1990, "Bearing capacity of reinforced horizontal sandy ground" Geotextiles and Geomembranes, Vol. 9, pp. 51-82.

Ishihara, K., and Harada, K., 1994, "Cyclic behavior of partially saturated collapsible soils subjected to water permeation", Geotechnical Special Publication, n 44, Ground failures under seismic, pp. 34 - 50.

Ismail, I. And Raymond, G. P., 1995, "Influence of geosynthetic reinforcement on granular soils", Transportation Research Record, No. 1474, pp. 96-101.

Jefferson, I., Evstatiev, D. and Karastanev, D., 2008, "The treatment of collapsible loess soils using cement materials", Geotechnical Special Publication 178: 662-669, 2008, Proceedings of session of GeoCongress 2008 - GeoCongress 2008: Geosustainability and Geohazard Mitigation, GSP 178

Jennings, J. E., and Knight, K., 1975, "A guide to construction on or with materials exhibiting additional settlement due to 'collapse' of grain structure," Sixth Regional Conference For Africa on Soil Mechanics and Footing Engineering, Sept., 1975, pp. 99-105.

Kazimierowicz-Frankowska, K., 2007, "Influence of geosynthetics reinforcement on the load settlement characteristics of two layer subgrade", Geotextiles and Geomembranes, Vol. 25, pp. 366 –376.

Khing, K., H., Das, B., M., Puri, V., K., Yen, S., C., and Cook, E., E., 1994, "Foundation on strong sand underlain by weak clay with geogrid at the interface", Geotextiles and Geomembranes, Vol. 13, pp. 199-206.

Kim, S. I. And Cho, S. D., 1988, "An experimental study on the contribution of geotextiles to bearing capacity of footings on weak clays", International Geotechnical Symposium on Theory and Practice of Earth Reinforcement / Fukuoka Japan pp. 215-220.

Kumar, A., 1997, "Interaction of footings on reinforced earth slab", Ph. D. Thesis, University of Roorkee, Roorkee (UP), India.

Kumar, A., Ohri, M. L., and Bansal, R. K., 2007, "Bearing capacity tests of strip footings on reinforced layered soil", Geotechnical and geological Eng., Vol. 25, pp. 139-150.

Kumar, A., Walia, B. S. and Saran, S., 2005, "Pressure-settlement characteristics of rectangular footings on reinforced sand", Geotechnical and Geological Engineering, Vol. 23, pp. 469 – 481.

Kurian, N. P., Beena, K. S., and Kumar, R. K., 1997, "Settlement of reinforced sand in foundations", Geotechnical and Geoenvironmental Engineering, ASCE, Vol. 123, No. 9 pp. 818-827.

Lawton, E.C., Fragaszy, R.J., Hetherington, M.D., 1992, "Review of wetting-induced collapse in compacted soil", Journal of Geotechnical Engineering, ASCE, Vol. 118, No. 9, pp. 1376 – 1394.

Lee, K. M., Manjunath, v. R. and Dewaikar, d. M., 1999, "Numerical and model studies of strip footing supported by a reinforced granular fill-soft soil system", Canadian Geotechnical Journal, Vol. 36, pp. 793-806.

Lizuka, A., and Ohta, H., 1987, "A determination procedure of input parameters in elasto-viscoplastic finite element analysis", Soils and Foundation, Vol. 27, No. 3, pp. 71-87.

Makiuchi, K., and Minegishi, K., 1992, "An estimation of improvement effects of geotextile on bearing capacity of soft ground", Proc., Earth Reinforcement Practice, Balkema, Fukuoka, Kyushu, Japan, pp. 637-640.

Mandal, J. N. and Manjunath, V. R., 1990, "Bearing capacity of single layer of geosynthetic sand subgrade", Proc. Indian Geotechnical conference, pp.7-10.

Mashhour, M., Saad, M., Aly, A. and El-Bahhi, E. (1999). "Experimental study of a strip footing on collapsible soil." Proceedings of the 12th Regional Conference For Africa on Soil Mechanics and Geotechnical Engineering: 189-193.

Meyerhof, G. G., and Hanna, A., M., 1978, "Ultimate bearing capacity of foundations on layered soil under inclined load", Canadian Geotechnical Journal, Vol. 15, No. 4, Paper no. 4.2.

Michalowski, R. L., 2004, "Limit loads on reinforced foundation soils", Geotechnical and Geoenvironmental Engineering, ASCE, Vol. 130, No. 4 pp. 381-390.

Michalowski, R. L., and Shi, L., 2003, "Deformation patterns of reinforced foundation sand at failure", Geotechnical and Geoenvironmental Engineering, ASCE, Vol. 129, No. 5 pp. 439-449.

Miller, H., Djerbib, Y, Jefferson, I.F., and Smalley, I.J., 1998, "modeling the collapse of metastable loess soils", Proceedings of the 3rd International Conference on Geo-Computation, University of Bristol, United Kingdom, 17-19 September 1998.

Otani, J., Ochiai, H., Yamamoto, K., 1998, "Bearing capacity analysis of reinforced foundations on cohesive soils", Geotextiles and Geomembranes, Vol. 16, pp. 195-206.

Patel, N. M., 1988, "Reinforcing with geotextile layer and covering pad", Proc., First Indian Geotextiles Conference on Reinforced Soil and Geotextiles, Bombay, India, pp. B.3-B.8.

Prakash, S., Saran, S. and Sharan, U. N., 1984, "Footings and constitutive laws", Journal of Geotechnical Engineering, ASCE, Vol. 110, No. 10, pp. 1473 – 1487.

Rogers, C. D. F., 1995, "Types and distribution of collapsible soils", NATO ASI Series C: Mathematical and Physical Sciences, Vol. 468, Kluwer Academic Publisher, The Netherlands, pp. 1 – 16.

Rollins, K. M. and Rogers, G. W., 1994, "Mitigation measures for small structures on collapsible alluvial soils", Journal of Geotechnical Engineering, ASCE, Vol. 120, No. 9, pp. 1533 – 1553.

Romani, F. and Hick, B. A., 1989, "Collapsible soils in the Antelope Valley – California", Foundation Engineering: Current Principles and Practices, Evanston, IL, USA, pp. 135 – 142.

Sakti, J. p., Das, B. M., 1987, "Model tests for strip foundation on clay reinforced with geotextile layers", Transportation Research Record, No. 1153, pp. 40-45.

Samtani, N. C. and Sonpal, R. C., 1989, "Laboratory tests of strip footing on reinforced cohesive soil", Geotechnical Engineering, ASCE, Vol. 115, No. 9, pp. 1326-1330.

Samuel E. French 1999, "Design Of Shallow Foundations", ASCE Press, 1801 Alexander Bell Drive, Reston, Virginia, USA.

Semkin, V. V. and Ermoshin, V. M., 1986, "Chemical stabilization of loess soils in Uzbekistan to prevent building deformations", Soil Mechanics and Foundation Engineering, Vol. 23, No. 5, pp. 196 – 199.

Sharan, U. N., 1977, "Pressure-settlement characteristics of surface foundations from constitutive laws", Ph.D. Thesis, University of Roorkee, Roorkee (U.P.), India.

Shaw, D., and Johnpeer, G., 1985, "Ground subsidence study near Espanola and recommendations for construction on collapsible soils", New Mexico Geology, 7 (3), pp. 75 – 80.

Shin, E. C., Das, B. M., Puri, V. K., Yen, S. C. and Cook, E. E., 1993, "Bearing capacity of strip foundation on geogrid reinforced clay", Geotechnical Testing Journal, Vol. 16, No. 4, pp. 534-541.

Sokolovich, V. E. and Semkin, V. V., 1984, "Chemical stabilization of loess soils", Soil Mechanics and Foundation Engineering, Vol. 21, No. 4, pp. 149 – 154.

Som, N., 1988, "Geotextile overlay for improving bearing capacity of foundations on soft clay", Proc., First Indian Geotextiles Conference on Reinforced Soil and Geotextiles, Bombay, India, pp. A.3-A.10.

Soni, K. M., Varadarajan, A., Sharma, K. G., 1992, "Effect of reinforcement length on bearing capacity", Proc., Earth Reinforcement Practice, Balkema, Fukuoka, Kyushu, Japan, pp. 689-694.

Souza, A., Cintra, J. C. A. and Vilar, O. M., 1995, "Shallow foundations on collapsible soil improved by compaction", Proceedings of the First International Conference on Unsaturated Soils, UNSAT'95, Paris, France, pp. 1017 – 1021.

Sreekantiah, H. R., 1988, "Stability of loaded footings on reinforced sand". Proc., First Indian Geotextiles Conference on Reinforced Soil and Geotextiles, Bombay, India, pp. C.3-C.8.

Tanabashi, Y., Kamuro, K., Hirao, K., Takaoka, K., Nishimura, J. and Yasuhara, k., 1992, "Numerical analysis for bearing capacity improvement of soft clay ground reinforced with geotextiles", Proc., Earth Reinforcement Practice, Balkema, Fukuoka, Kyushu, Japan, pp. 701-706.

Unnikrishnan, N., Rajagopal, K. and Krishnaswamy, N., R., 2002, "Behavior of reinforced clay under monotonic and cyclic loading", Geotextiles and Geomembranes, Vol. 20, pp. 117-133.

Vesic, A. S., 1973, "Analysis of ultimate loads on shallow foundations", Journal of Soil Mechanics and Footing Division, ASCE, Vol. 99, No. SM1, pp. 45-73.

Winterkorn, Hans F., and Fang, Hsai-Yang, 1975, "Foundation Engineering handbook", Van Nostrand Reinhold Company, New York.

Yamamoto, K., and Otani, J., 2002, "Bearing capacity and failure mechanism of reinforced foundations based on rigid plastic finite element formulation", Geotextiles and Geomembranes, Vol. 20, pp. 367-393.

Yang, Z., 1972, "Strength and deformation characteristics of reinforced sand", Ph.D. Thesis, University of California, Los Angeles, USA.

Yetimoglu, T., Inanir, M. and Inanir O. E., 2005, "A study on bearing capacity of randomly distributed fiber reinforced sand fills overlying soft clay", Geotextiles and Geomembranes, Vol. 23, pp. 174 –183.

Yetimoglu, T., Wu, Jonathan T. H. and Saglamer, A., 1994, "Bearing capacity of rectangular footings on geogrid-reinforced sand", Geotechnical Engineering, ASCE, Vol. 120, No. 12, pp. 2083-2099.

Zhao, A., 1998, "Slip line analyses of geosynthetic reinforced strip footings", Geotechnical Special Publication, n 76, pp. 49-61.

Kumar, S., 2003, "Eccentrically and obliquely loaded footings on reinforced earth slab", Ph.D. Thesis, IIT Roorkee, Roorkee (UA), India.

APPENDIX

GEOSYNTHETIC MATERIALS PROPERTIES

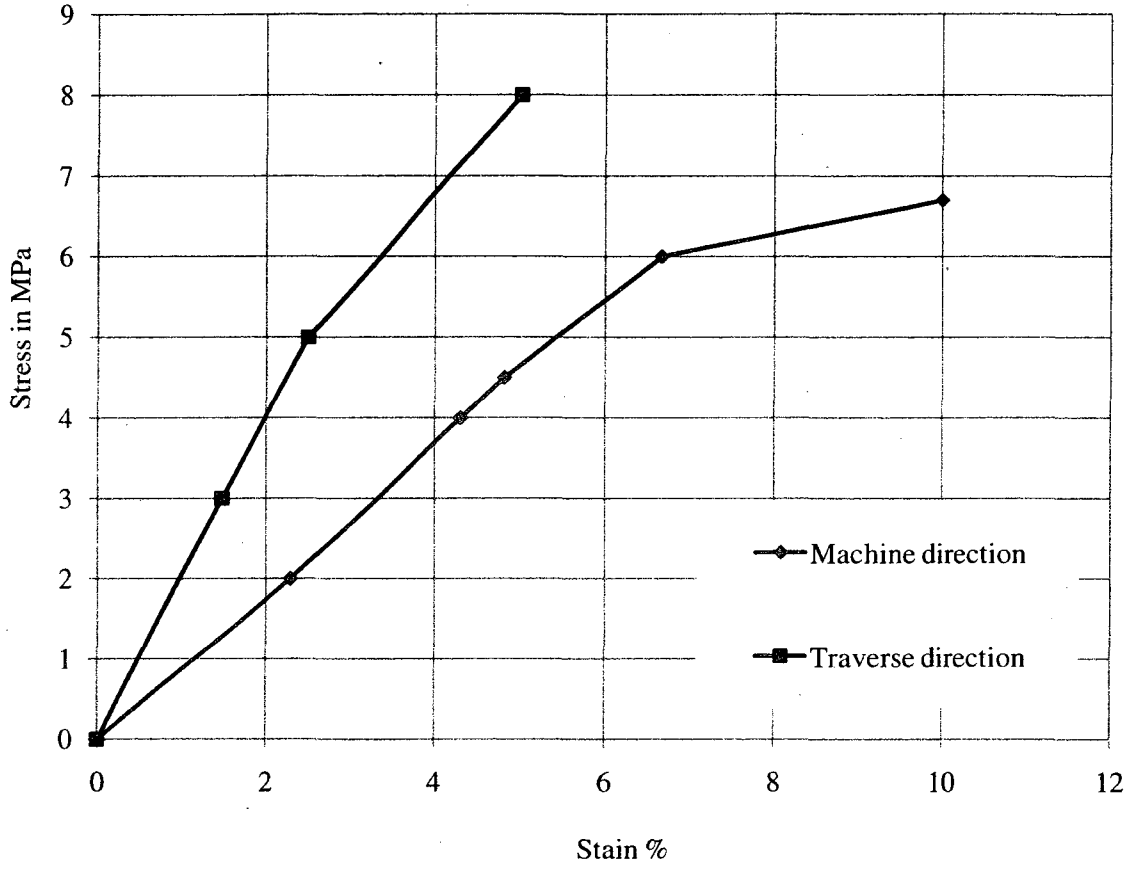

Figure (A-1): Stress-strain relationship for Geo-9

Table (A-1): Geotextile (Geo-9) technical data sheet

Texel

Technical Data Sheet

02291REV10-2005123

Product group:	TEXEL GEO-9
Product description:	GEO-9 04.00M PP GR 100M
Texel product code:	02291
Product type:	Needlepunched Nonwoven, Short staple fiber
Fiber composition:	Polypropylene
Reinforcement:	Polypropylene

	MIN	MAX	UNITS	METHOD	FREQUENCY
Thickness:	-	-	mm	ASTM D4632	Standard
Tensile strength (MD):	650	-	N	CGSB 148.1-7.3	Standard
Tensile strength (CD):	650	-	N	CGSB 148.1-7.3	Standard
Permeability:	1,3	-	10e-2 cm/s	CAN 148.1 No.4-94	Standard
FOS:	-	60	µ	CAN 148.1 No.10-94	Standard
Tensile strenght *(wide width method 200mm)*	11,0	-	kN/m	ASTM D4595-94	Standard
Tensile strenght *(after 5% of elongation))*	5,0		kN/m	ASTM D4595-94	Standard
Mullen:	2600	-	KPA	CGSB 4.2-11.1	Standard

	8 kPa	20 kPa	50 kPa	150 kPa	
Gradient : 0.1					
Average (m^2/s)	7,4 x 10e-6	4.3 x 10e-6	2.0 x 10e-6	7.8 x 10e-7	
C.V. (%)	15,20	10,00	27,50	16,50	
Gradient : 1.0					
Average (m^2/s)	7,9 x 10e-6	4.1 x 10e-6	1.9 x 10e-6	7.3 x 10e-7	
C.V. (%)	9,50	14,80	12,10	22,80	

Table (A-2): Geogrid (BX 1100) technical data sheet

Tensar

Tensar International Corporation
5883 Glenridge Drive, Suite 200
Atlanta, Georgia 30328-5363
Phone: 800-TENSAR-1
www.tensar-international.com

Product Specification - Biaxial Geogrid BX1100

Tensar International Corporation reserves the right to change its product specifications at any time. It is the responsibility of the specifier and purchaser to ensure that product specifications used for design and procurement purposes are current and consistent with the products used in each instance.

Product Type: Integrally Formed Biaxial Geogrid
Polymer: Polypropylene
Load Transfer Mechanism: Positive Mechanical Interlock
Primary Applications: Spectra System (Base Reinforcement, Subgrade Improvement)

Product Properties

Index Properties	Units	MD Values[1]	XMD Values[1]
• Aperture Dimensions[2]	mm (in)	25 (1.0)	33 (1.3)
• Minimum Rib Thickness[2]	mm (in)	0.76 (0.03)	0.76 (0.03)
• Tensile Strength @ 2% Strain[3]	kN/m (lb/ft)	4.1 (280)	6.6 (450)
• Tensile Strength @ 5% Strain[3]	kN/m (lb/ft)	8.5 (580)	13.4 (920)
• Ultimate Tensile Strength[3]	kN/m (lb/ft)	12.4 (850)	19.0 (1,300)
Structural Integrity			
• Junction Efficiency[4]	%	93	
• Flexural Stiffness[5]	mg-cm	250,000	
• Aperture Stability[6]	m-N/deg	0.32	
Durability			
• Resistance to Installation Damage[7]	%SC / %SW / %GP	95 / 93 / 90	
• Resistance to Long Term Degradation[8]	%	100	
• Resistance to UV Degradation[9]	%	100	

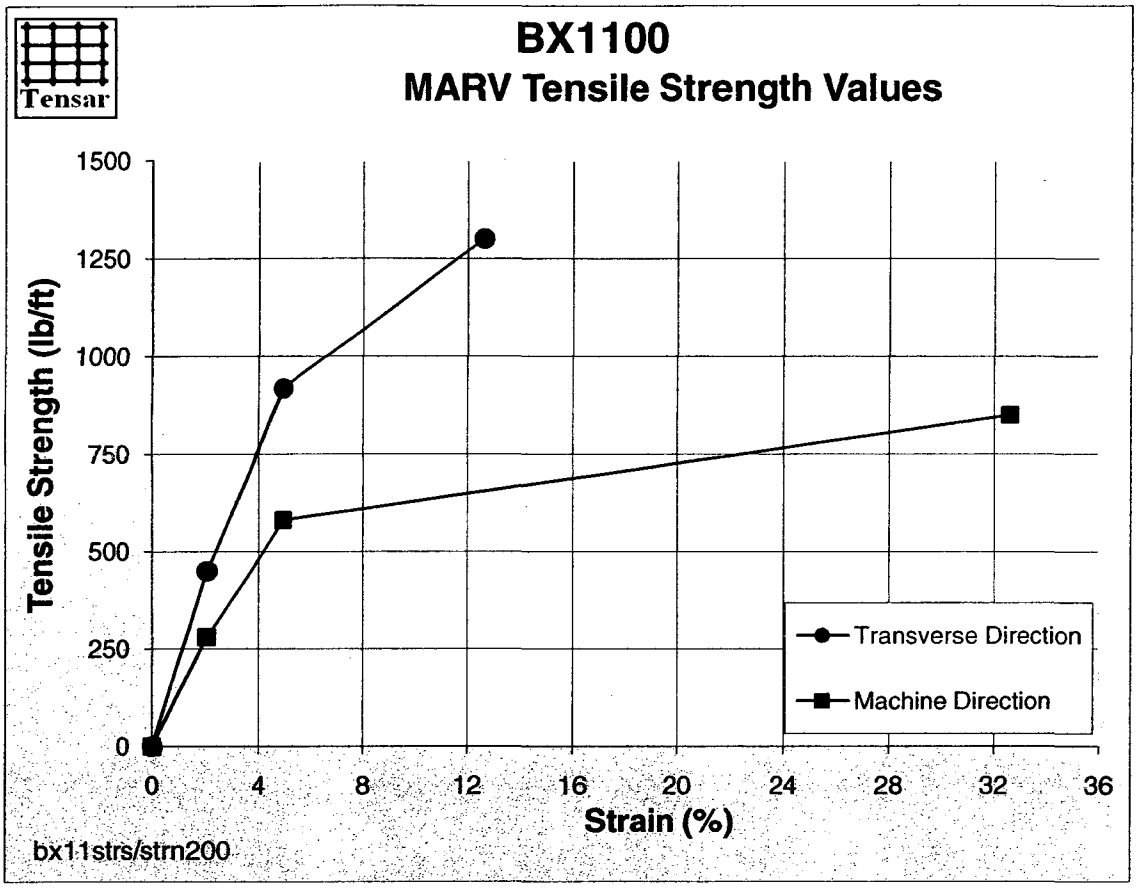

Figure (A-2): Stress-strain relationship for geogrid BX 1100